7-7-2020

Development of A Robust, Soft and Flexible Selfhealing Polymer Based on Dynamic Coordinate Metallig and Bonds

Julia Pignanelli
University of Windsor

DEVELOPMENT OF A ROBUST, SOFT AND FLEXIBLE SELF-HEALING POLYMER BASED ON DYNAMIC COORDINATE METAL-LIGAND BONDS

By

Julia Pignanelli

A Thesis

Submitted to the Faculty of Graduate Studies Through the Department of Chemistry and Biochemistry in Partial Fulfillment of the Requirements for the Degree of Master of Science

at the University of Windsor

Windsor, Ontario, Canada

2020

Development of a Robust, Soft and Flexible Self-Healing Polymer Based on Dynamic Coordinate Metal-Ligand Bonds

by

Julia Pignanelli

APPROVED BY:

_____

B. Balasingam,
Department of Electrical and Computer Engineering

_____

J. Trant
Department of Chemistry & Biochemistry

_____

J. Ahamed, Co-Advisor
Department of Mechanical, Automotive and Materials Engineering

_____

S. Rondeau Gagné, Co-Advisor
Department of Chemistry & Biochemistry

May 11, 2020

DECLARATION OF CO-AUTHORSHIP/PREVIOUS PUBLICATION

I. Co-Authorship

I hereby declare that this thesis incorporates material that is result of joint research, as follows:

Chapter 3 was co-authored with Blandine Billet, Matthew Straeten, Michaela Prado and Kory Schlingman under the supervision of Prof. Simon Rondeau-Gagné and Prof. Mohammed Jalal Ahamed. They main ideas, primary contributions, experimental designs, data analysis, interpretation, and writing were preformed by the author. The contribution of the co-authors was primarily through device and material characterization. Blandine Billet, Michaela Prado and Kory Schlingman contributed to the material characterization of the Iron-cross linked polymer system; Matthew Straeten contributed to the device characterization. All authors provided feedback and editions to the published manuscript. All authors have given approval to the final version of the manuscript. Chapter 3 was adapted with permission from Ref. 109 (Chapter 4) copyright 2019 The Royal Society of Chemistry.

Chapter 4 of this thesis was co-authored with Zhiyuan Qian, and Xiaodan Gu, under the supervision of Jalal Ahamed and Simon Rondeau-Gagné. The main ideas, contributions and writing were primarily done by the author. The co-authors contributed through a portion of the material characterization and data analysis. Zhiyuan Qian and Xiaodan Gu helped to study the viscoelasticity of the various metal-salt cross linked samples before and after healing using a rheometer to generate the storage and loss moduli of the materials. All authors provided editing and feedback to the submitted manuscript.

I am aware of the University of Windsor Senate Policy on authorship and I certify that I have properly acknowledged the contribution of the other researchers to my thesis and have obtained written permission from each of the co-author(s) to include the above material(s) in this thesis.

I certify that, with the above qualifications, this thesis, and the research it pertains refers to, is the product of my own work.

II. Previous Publications

This thesis includes one original paper that have been previously published in peer reviewed journal of Soft *Matter,* as follows:

Thesis Chapter	Publication title/full citation	Publication Status*
Chapter 3	**Pignanelli, J.; Billet, B.; Straeten, M.; Prado, M.; Schlingman, K.; Ahamed, M.; Rondeau-Gagné, S. Imine And Metal–Ligand Dynamic Bonds In Soft Polymers For Autonomous Self-Healing Capacitive-Based Pressure Sensors. *Soft Matter* 2019, *15* (38), 7654-7662.**	*Published*
Chapter 4	**Pignanelli, J.; Qian, Z.; Gu, X.; Ahamed, M.; Rondeau-Gagné, S. Modulating the Thermomechanical Properties and Self-Healing Efficiency of Siloxane-Based Soft Polymers Through Metal-Ligand Coordination,** 2020	*Published*

I certify that I have received a written permission from the copyright owner(s) to include the above published material(s) in my thesis. I certify that the above materials describe work completed during my registration as a graduate student at the University of Windsor.

III. General

I declare that, to the best of my knowledge, this thesis does not infringe upon anyone's copyright nor violate any proprietary rights and that any ideas, techniques, quotations, or any other material from the work of other people included in this thesis, published or otherwise, are fully acknowledged in accordance with the standard referencing practices. Furthermore, to the extent that I have included copyrighted material that surpasses the bounds of fair dealing within the meaning of the Canada Copyright Act, I certify that I have obtained a written permission from the copyright owner(s) to include such material(s) in my thesis.

I declare that this is a true copy of my thesis, including any final revisions, as approved by my thesis committee and the Graduate Studies office, and that this thesis has not been submitted for a higher degree to any other University or Institution.

ABSTRACT

Herein, an intrinsic autonomous self-healing polymer system has been developed and explored leading to new materials that are easily able to be fine-tuned both mechanically and chemically. Through an easy condensation reaction, the system explored incorporates dynamic and reversible bonds within polydimethylsiloxane monomer chains, namely dynamic imine and metal-coordinated bonds, to enable autonomous self-healing while also allowing for simple alteration of the system through manipulation of the metal salt used to coordinate the ligands of the monomer units. In addition to the autonomous self-healing of the system, controlled degradability at mild pH and ultra-high stretchability (up to 800% strain) are possible through alteration of the metal to ligand ratio and type of metal used in the coordination. Characterization of this dynamic system was performed through a variety of techniques such as tensile-pull strain testing, atomic force microscopy, UV-Vis spectroscopy, dynamic mechanical analysis, and shear rheology which showed that the highly dynamic imine bonds combined with the coordination with various transition metal salts allowed for the material to regenerate up to 88 % of its mechanical strength after physical damage while also being able to generate materials that ranged in their Young's modulus from approximately 0.2 MPa to 10 MPa through simply altering the bonds formed through the metal ligand coordination interaction. Results suggest the mechanical properties of the system under investigation is directly related to its ability to regenerate upon damage. The new soft polymer has also been used as a dielectric layer in a capacitive based pressure sensor that is able to regenerate its mechanical and electrical properties upon damage, proving the possibility of our self-healing polymer for use in the next generation of self-healing electronics.

DEDICATION

To anyone who has listen to me stress and complain over the last few years, I dedicate this one to you. We made it! Special shout out to my mom and dad who always keep me well fed and tolerate me at my worst. Also, for raising me with the confidence and courage pursue whatever it is I set my mind to, love you!

ACKNOWLEDGEMENTS

First, I would like to thank Dr. Ahamed for giving me the opportunity to begin my research career during my undergraduate degree despite my minimal knowledge and experience in any area of research, let alone one that was based in engineering! Becoming a part of his research team was my first step to transforming my university experience into a more meaningful one. Since joining his team, I have learned the value in stepping outside of my comfort zone and I am so grateful for the guidance, encouragement and confidence he has given me as a result.

I would of course also like to thank my other supervisor, Dr. Rondeau-Gagné who convinced me to pursue a graduate degree in the first place. I am grateful for his patience, guidance and encouragement that has allowed me to accomplish my goals to date. Not only has he been a staple in my academic growth, but his work ethic and passion for research has been a true inspiration and testament to the great leader he is. Every time the phrase "Don't give up" come about, SRG will come to mind.

Thank you to all the members of the Rondeau-Gagné Research group and the members of Dr. Ahamed's MicroNano Mechatronic Lab who have contributed to my graduate research experience. A special thank you to Kory Schlingman for his expertise and constant willingness to help out throughout my research work. I would also like to thank my internal reader of this thesis, Dr. John Trant, for taking the time to provide feedback to my work. Additionally, Dr. Bala Balasingham, my external reader from the Department of Electrical Department of Electrical and Computer Engineering for providing the comments on this thesis.

Last but not least, I would like to thank my family and friends for their constant support and friendship. Most of you won't read this so I will just save this speech for another time.

TABLE OF CONTENTS

LIST OF FIGURES

LIST OF TABLES

LIST OF ABREVIATIONS

AFM	Atomic Force Microscopy
AMLCD	Active-matrix liquid-crystal display
ARES	Advanced Rheometric Expansion System
CMOS	Complementary metal-oxide-semiconductor
DCPD	Dicyclopentadiene
HOMO	Highest occupied molecular orbital
LCD	Liquid-crystal display
LMCT	Ligand to metal charge transfer
LUMO	Lowest unoccupied molecular orbital
MIM	Metal-insulator-metal
M-L	Metal-ligand
MLTC	Metal to ligand charge transfer
MOSFET	Metal-oxide-semiconductor field effect transistor
OFET	Organic field-effect transistor
PA	Polyacrylate
PEG	Polyethylene glycol
PDMS	Polydimethylsiloxane
PS	Polystyrene
PU	Polyurea

ROMP	Ring-opening metathesis polymerization
SWCNTs	Single-walled carbon nanotubes
TFT	Thin film transistor
T_g	Glass transition temperature

CHAPTER 1. INTRODUCTION

1.1. The Revolutionary Field of Flexible Electronics

People of the 21st century have undoubtedly become dependent on technology as a result of the benefits it provides in many aspects of everyday life such as communication, navigation, education, film and media, health and wellness, to name a few. With the rapid advancement technology and the resulting interconnection between people and things, researchers are striving to build up devices with optimal durability and conformability in order to promote longer lasting, cost effective and lower power consuming devices. As a result, the field of flexible electronics is a hot topic for material scientist, chemists and engineers due to its wide variety of applications ranging from wearable, implantable electronics, flexible industrial and biosensing technologies to large area mass production of energy storage and harvesters (Figure 1.1).

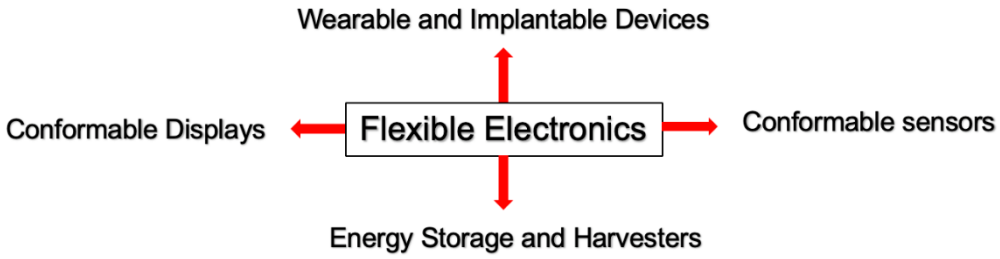

Figure 1.1 Possible avenues for the field of flexible electronics.

The term flexible can be defined by many qualities such as bendable, elastic, conformable, manufacturable or mass producible. With the rise in performance of flexible and conformable electronics, scientists are working towards development of novel materials and methods for fabrication of fully integrated, economically favorable electronic devices. Traditional materials for current state of the art electronics such as gold, crystalline silicon wafers, silver and carbon used in complementary metal oxide semiconductors (CMOS) are based on expensive substrates which limits their use from conformable and wearable devices.[1] CMOS technology that is used in the majority of our electronics today have evolved to have high performance yet are limited to their shapes and sizes due to the physical rigidity of the high performing silicon based technologies.[1] Organic materials prove to be promising candidates for these technologies as they possess the thermochemical properties and tunability required to produce robust technologies. Moreover, these materials have begun to show performance comparable to tradition Si-based electronics[2]

Therefore, researchers are moving towards optimizing the electromechanical properties of more organic electroactive components and elastomeric substrates to improve the flexibility and robustness of the next generation of electronics. The lightweight, foldable, stretchable devices promote great potential for smart technology such as e-skin, artificial intelligence, robotics, wearable and industrial technologies to further enhance and accommodate human lives.[1,3–6]

In the 1970's in response to the energy crisis, one of the first flexible electronic devices was made through thinning of single crystal silicon wafer cells that were used on a flexible plastic substrate to enhance solar cell array flexibility as well as cost effectiveness of photovoltaic electricity.[7] Flexible polymer substrates can be deposited with hydrogenated amorphous silicon as a result of the low deposition temperature to form the electrical contacts of the cells which allowed for the initial method of fabricating solar cells upon flexible substrates. Today solar cells are being made through roll-to-roll processes which allow for large scale, mass production of the photovoltaic energy sources. [8]

Thin film transistors (TFT) are also important components in the field of flexible electronics as they play a vital role in effective switches for pixel displays such as Liquid Chrystal Display (LCD) as well as medical imaging applications such as flexible digital detector for x-rays.[9] In 1968 Brody and colleagues reported one of the first flexible TFT's using matrices of the devices compose of tellurium on a strip of paper for display applications.[10] The group later applied this method using flexible substrates such as polyethylene and anodized aluminum warping foil and found that they were able to maintain device function upon bending at a 1/16' radius.10 Methods to further enhance production of efficient yet durable TFT's resulted in the active-matrix liquid-crystal display (AMLCD) which allows for large-area chemical deposition onto flexible substrates similarly to the method used for solar cell fabrication. Poly-Silicon TFT's later emerged on plastic substrates using laser-annealing to create switches for finger print detection sensors.[1]1 As the research in this area continues to grow, the application of electronics will also become enhanced.

In addition to the enhancement in the electronic signal processing speeds and displays, the benefits of conformable devices allow for 3-d data to be acquired similar to the human tactile sensation. Sensors that translate mechanical signals such as force or pressure into electronic signals are essential for creating new wearable electronics and electronic skin-like devices. All components of these flexible technologies must be able to withstand the conformability of the device including the power source, sensor, electrodes, communication and substrate aspects of the design. Pressure sensors in particular have gained interest in the field of flexible and wearable

electronics. For real monitoring of pressure it is crucial that the sensors are able to withstand bending, shear, torsion strain and vibration all while maintaining repeatable and sensitive output responses for a range of pressures applied (5-100 KPa).[12] There are four main sensing mechanisms for pressure detection including piezoresistive, piezoelectric, field-effect transistor and capacitive.[12] Among these mechanisms, field effect transistors are least suitable for flexible technologies despite their high sensitivity as a result of their mechanical rigidity for the metal-oxide-semiconductor field effect transistor (MOSFET)-based and complex nanostructure design required for the more conformable Organic Field effect transistor (OFET) design.[13] The most cost effective, large-area compatible and robust pressure sensing technologies for flexible electronic applications is capacitive based pressure sensing.[14–17] Capacitive pressure sensing is based on the relationship between capacitance and distance separating electrodes that form a capacitor (Equation 1).

$$C = k\frac{\varepsilon_0}{\Delta d} \qquad (1)$$

Applying a pressure to the top electrode results in a decrease in the distance between the electrodes and therefore an increased capacitance signal (Figure 1.2).

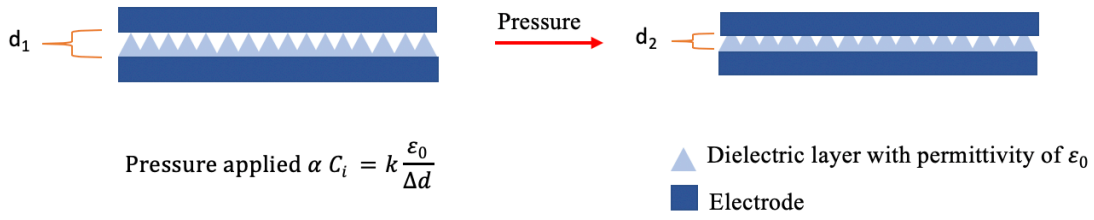

Figure 1.2. Schematic design of capacitive pressure sensors.

One of the benefits of this system includes the ability to use a wide range of flexible materials as the two components that form a parallel plate capacitor; the electrodes and dielectric material. For example, Lipomi and colleagues created a fully flexible capacitive pressure sensor made of an Ecoflex dielectric layer sandwiched between single-walled carbon nanotube (SWCNTs) coated polydimethylsiloxane (PDMS) electrodes.[18] To account for the viscoelastic properties of elastomers that result in lower pressure sensitivity and hysteresis, dielectric surface microstructures create voids that enable elastic and reversible deformation upon external pressure applied.[19] Bao and

colleagues created PDMS dielectric microstructures using a replica mold process to improve device sensitive from 0.02 KPa-1 to 0.55 KPa.[19] Figure 1.2 illustrates a schematic representing the structured dielectric layer of a capacitive pressure sensor and its response to pressure applied in relation to capacitance measured. Therefore, there is ample potential in the material science and chemistry research areas to create robust and tunable materials that can be used to further enhance the mechanical and electrical stability of the flexible pressure sensing technologies.

1.2. Soft Materials for Electronics

In order for the next generation of electronics to evolve it is essential that flexible, conformable materials to be optimized with the required electronic and mechanical properties to allow for the achievement of optimal and favorable performance and durability. Soft elastomeric materials are therefore critical to determining a rational design and development of materials needed in order to accelerate the fabrication of soft technologies to give material engineers an effective toolbox for the next generation of electronics.

For electronics to eventually become fully integrated into wearable technology, bendable, stretchable power sources and sensors, they must possess a wide variety of possible electronic and mechanical properties to account and provide for the robust nature of everyday life. In order to optimize material design to account for these properties, material chemists and engineers have discovered various methods to achieve flexible and stretchable materials through development of new structure architectures of conventional materials as well as the development of novel materials.[20] The materials that make up electronic devices include, a flexible insulating substrate, conducting, semiconducting, and dielectric materials.[21] The resulting devices are only as flexible as the most brittle component; therefore it is important that each piece of the system meets the desired robustness of the product. Foldable and stretchable circuits have been demonstrated by Rogers et al. using a wrinkled structure architecture of gold.[22] This method of producing a stretchable metal or conductor is based on the modification of the Au structure architecture, which allows for increased surface area of the electrodes to accommodate strain thus improvement of robustness of the material.[5] This method is known as strain engineering, where a rigid thin film semiconducting or conducting material is placed on a pre strained elastomer. Upon elastomer release, the rigid material conforms to a wavy-like structure. Fabrication of such electronics has been explored using a combination of robust and soft materials such as SWCNTs, ion-gels, nanosheets, poly(3-hexythiophene) fibers and rubber composites which has shown result in electronics able to withstand tensile strains up to 70% without failure.[21] Despite the advances in

improving the stretchability and robustness of soft materials for electronics, there is still more work required to enhance conventional material physical properties while maintaining its optimal electronic properties.

An approach to attaining flexible semiconducting materials involves entangled and covalently bonded hydrocarbon chains. The combination of covalently bonded and entangled hydrocarbon chains allows for robust and soft elastomers, however soft materials that possess a variety of material and electronics characteristics are required for the future of electronics. Elastomeric matrices can be dispersed with various compounds to alter the elastomers electronic properties while maintaining its elastic properties. For example, Selivanova and colleagues reported a blended system of semiconducting polymers with branched polyethylene elastomer in order to fine-tune the solid-state morphology of the semiconducting polymer, while also allowing for a semiconducting elastomer blend for future applications in OFETs.[23,24] Numerous other studies have focused on coating of SWCNTs films within silicon based rubbers to create transparent, conductive elastomers.[18,25–27] The SWCNTs form tangled aggregates that are able to reconfigure in response to strain in order to maintain a stable conductive path for charge transport with the ability to be printed onto flexible substrates.[28] Alternatively to this approach to modify the architecture of conventional materials, the synthesis of novel semi-conductive and conductive polymers is also a method to achieve soft, conformable materials for electronics through polymer backbone or side chain engineering.[29,30] Conjugated polymers with sp^2 hybridization allows for the electronic properties of conjugated polymers as a result of the delocalization of electrons throughout the polymer chain.[31] Alternatively, π-π-stacking of the polymer backbone can also create intermolecular charge transport in organic semiconducting polymer systems.[32] Figure 1.3 summarizes the methods used to achieve flexible semiconducting materials. Most recent advances in synthesis of organic semiconducting materials has focused on resolving the competition between electronic and mechanical properties as they relate to solid state morphology.[23,24,33,29]

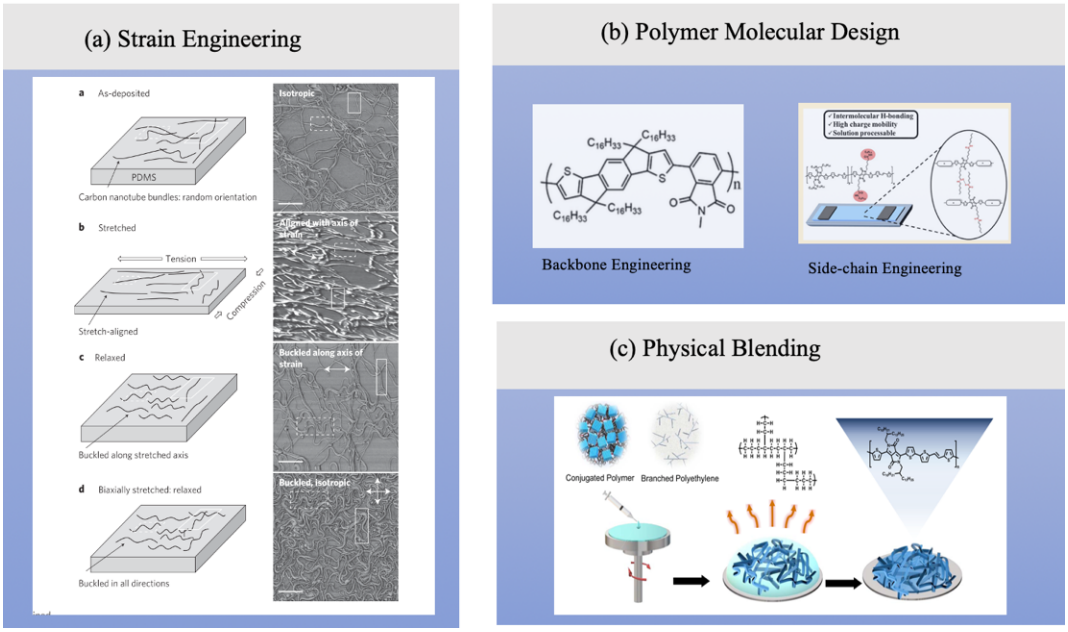

Figure 1.3. Summary of current methods used to achieve flexible semiconductive materials. (a) SWCNT Coating. Aadapted with permission from Ref. 18. Copyright 2011 Springer Nature. (b) Polymer Molecular Design. Adapted with permission from Ref. 33. Copyright 2015 American Chemical Society and from Ref. 29. Copyright 2019 American Chemical Society. (c) Physical Blending. Adapted with permission from Ref. 23. Copyright 2019 American Chemical Society.

In addition to the semiconducting materials for electronics, dielectric materials are also valuable in ensuring low power and safe electronics. Most modern electronic circuitry is based on thin film transistors to amplify or switch various device signals. Therefore, the material components of these electronics including the semiconductor, the dielectric, substrate and the conductor must possess the mechanical and electrical performances compatible with flexible and stretchable electronics.

While advances in enhancing the electronic capabilities of semiconducting and insulating materials has increased the potential for the future of flexible, stretchable electronics, another area of research that will further enhance the robustness of such materials is the field of self-healing materials. Considering the advances and progress in mechanically robust semiconducting materials for TFT's it is crucial to also integrate the dielectric material that allows for low voltage, flexible power sources required for these technologies.

1.3. Dielectric Materials

A dielectric material is an electrical insulator that is able to become polarized upon an applied voltage. Band theory is a theoretical model which describes conductivity of materials in their solid state based on the energy differences between the valence and conduction band. The smaller the energy gap, the easier it is for an electron to enter the higher energy conduction band. In comparison to conductive and semi-conductive materials, insulators have a high energy band gap between their lowest unoccupied molecular orbital (LUMO) or valence band and highest occupied molecular orbital (HOMO) or conduction band. Electrons in the valence band of semi-conductors can be promoted to the conduction band through application of an electric potential. The large difference between the conduction and valence band of insulating materials prevents electrons to flow when subjected to an electric potential. A comparison between the energy band gaps between insulators, semiconductors and conductors is illustrated in Figure 1.4.

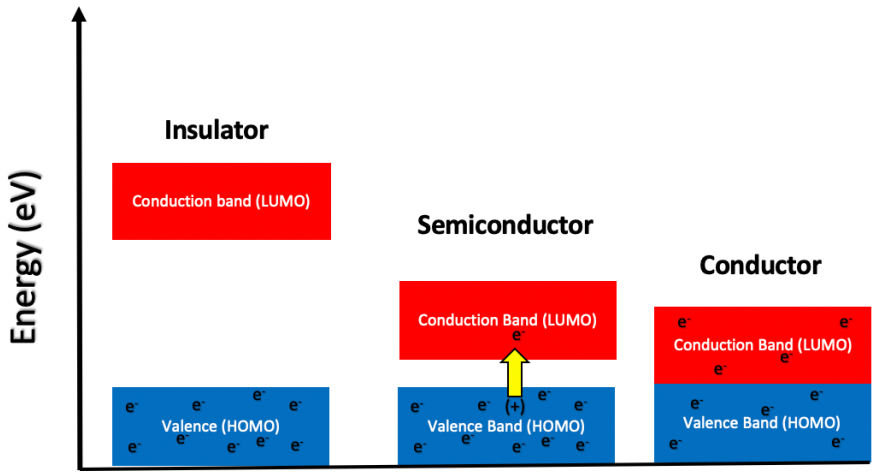

Figure 1.4 Band theory energy profile schematic comparing band gap energies of an insulator, semiconductor and conductor.

Dielectric polarization results from electrical charges shifting from their equilibrium position when placed in an electric field. Since charges repel one another, positive charges shift toward the electric field whereas the negative charges shift in the opposite direction of the field, as depicted in Figure 1.5. The electric field that is created within the dielectric material as a result decreases the overall field due to the countering vectors of the fields.[34]

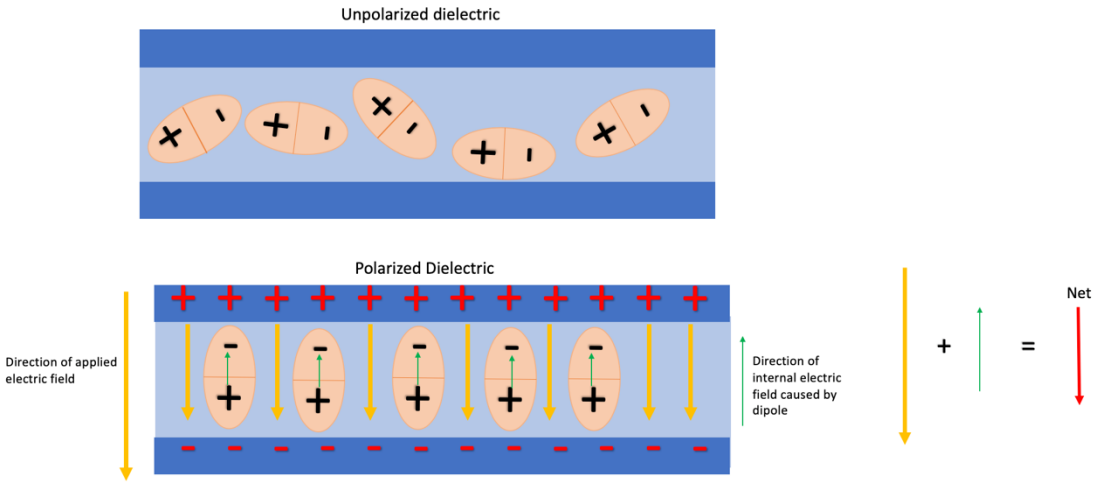

Figure 1.5. Schematic of the polarization of a dielectric through an applied electric field and the resulting decreased net electric field.

The dielectric constant (k) of a material is directly related to its ability to store electrical charge, known as capacitance at a given voltage when used in a parallel-plate metal-insulator-metal (MIM) capacitor. Rearrangement of Equation 1 for k represents this relationship, where d is the thickness of the dielectric material (Equation 2). High dielectric constant materials are important for the future of flexible electronics as higher storage of charge and therefore higher power is possible with lower operation voltage compared to lower dielectric constants with high operation voltages.

$$k = C\frac{\Delta d}{\varepsilon_0} \qquad (2)$$

Polarization density (**P**) of dielectric materials expresses the induced dipole moments of these materials where is the electric permittivity of vacuum (8. 854 × 10−12 F m−1), is the electrical susceptibility which is related to the materials dielectric constant (k). χ_e is the electrical susceptibility which is related to the materials dielectric constant (k). [35]

$$\chi_e = k - 1 \qquad (3)$$

$$P = \varepsilon_0 \chi_e \mathbf{E} \qquad (4)$$

Since the role of dielectric materials is to store electric potential energy, an important concept for TFT applications is for the material to be associated with a very low dielectric relaxation. Dielectric relaxation is defined as a delay in polarization in response to a changing electric field within the dielectric material. As a result there is an irreversible loss of energy or dielectric loss (tan δ) which

is a measure of dielectric relaxation, where k' and k represent imaginary and real dielectric constants. [34] The imaginary dielectric constant represents the energy absorbed by the material and the real dielectric constant represents the amount of energy stored. [36]

$$\tan \delta = \frac{k\prime}{k} \qquad (5)$$

Dielectric breakdown occurs when the dielectric material reaches a threshold energy storage that once surpassed, results in conduction or the flow of electrical current, defined as leakage current. Once the exponential increase of leakage occurs the dielectric insulating layer becomes partially conductive leading to physical damage of the dielectric material. Therefore, in practice it is important to have a dielectric film with a high breakdown strength in order to produce robust electronics. Typically, the breakdown voltage of the material should be 1.5 times greater than the operation voltage of the device.[37]

1.4. Overview and History of Self-Healing Materials

With the advancement of flexible and stretchable materials for electronic applications, the robustness of the materials is essential in order for function of the device to withstand the various forces it experiences in response to use in its flexible form. In terms of the semiconducting and conducting material components, the mechanical or physical structure of the films used to form circuits must be maintained in order to produce effective amplification or switching of the device. Not surprisingly, the dielectric insulating material must also maintain its shape and form in response to the various stresses experienced upon use in flexible devices in order to maintain its function of charge polarization effects. A common issue arises upon wear and tear of these advanced materials includes crack formation that results in device failure. Recently, scientists have begun to explore the field of advanced materials with the ability to self-repair upon damage; a promising characteristic for economical and safety, lifetime and use of the next generation of electronics.[26,38–41]

Living organisms possess interesting and useful features which allow for continuous self-healing ability after damage. One of the most evident examples is that of human skin that is able to heal from a wide variety of damage. The general guidelines of wound healing can be mimicked by synthetic systems to respond to damage. In the case of the case of skin, the injury signals an inflammatory response which triggers cell proliferation followed by matrix remodeling.[42] In synthetic systems a similar progression can be designed in order to initiate the material to regenerate

upon damage where actuation in response to damage triggers a kinetic chemical change that results in chemical repair (Figure1.6). Nature has inspired scientists to emulate these concepts to create the next generation of materials capable of regenerating their physical and functional properties upon damage.[39,43,44]

Figure 1.6. General Response to self-repair.

The concept of attempting to improve the durability and robustness of materials dates back to the Roman era. A primitive concept of self-healing was perhaps first created by the romans who established a concrete that has lasted and created impressive architecture to this day. The method in which this ancient concrete can self-heal upon cracking is based on use of a mortar that combines volcanic ash and lime to produce a "glue" to bind bricks together to form the concrete.[45] The lime becomes soluble when exposed to rain water and is able to be transported and redistributed through the concrete network. Once the water evaporates, the lime solidifies to fill in the gaps created from the cracks in the concrete which effectively reinforces the structure as a whole. As described previously with the example of nature's method of healing skin, the rainwater acts as a stimulus to actuate the healing process which transports to chemicals in the lime that become soluble in response to the water which later solidifies at the site of damage to repair the construct.

1.5. Categorization and Characterization of Self-Healing Materials

Applying these concepts to synthetic polymers that are used for flexible electronics applications, various works have introduced methods to achieve a wide variety of polymeric materials with the ability to self-heal.[39] Self-healing, can be described as the ability of a material to recover a portion or the entirety of its mechanical and or functional properties over time after damage. The two categories of self-healing include autonomous and non-autonomous healing.[38] Autonomous healing occurs without the need for external interventions, rather it occurs spontaneously in response to the damage. Non-autonomous healing involves an external intervention to create the required chemical response to the damage. As illustrated in Figure 1.7,

these two main categories of self-healing can be further divided into intrinsic or extrinsic self-healing. Intrinsic healing implies the polymer network contains all active components required to repair the network upon damage whereas extrinsic healing implies the polymer network requires additional components such as encapsulated healing agents to initiate the healing process.[46] An optimal self-healing system produces effective material and functional regeneration with minimal energy input and maximum repeatability of the healing process after repetitive damage. Therefore, intrinsic autonomous systems are preferred.

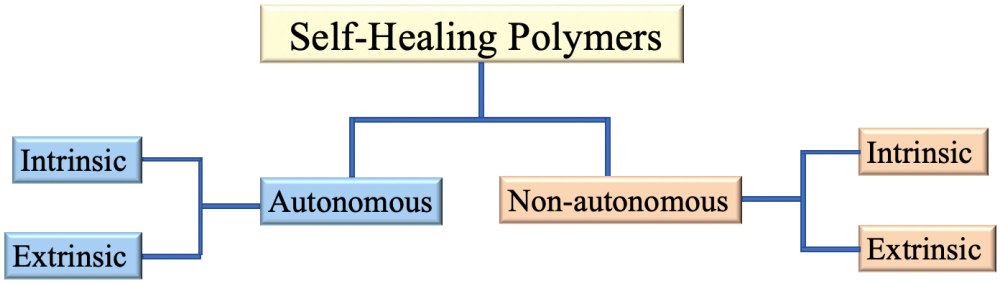

Figure 1.7. Types of self-healing polymers

Characterization of a materials self-healing efficiency (η), is done through comparison of the materials properties before damage and after healing. The healing efficiency is defined based on a specific function or property *(f)* that is restored which can be defined by equation 6:

$$\eta = \frac{\Delta f\ healed}{\Delta f\ native} \qquad (6)$$

Typically, the material property that is considered to calculate self-healing efficiency is the tensile strain percentage after healing over a certain period of time. Full recovery of a materials property after healing is challenging. A materials performance will continue to decline after successive damage-healing cycles as a result. Ideally, a system that is able to produce close to native performance upon damage to promote the maintenance of the material after failure and self-healing. Figure 1.8 illustrates the gradual decline in material performance in terms of percent strain in response to stress after successive healing cycles resulting in decreased self-healing efficiency as a function of repair cycles.

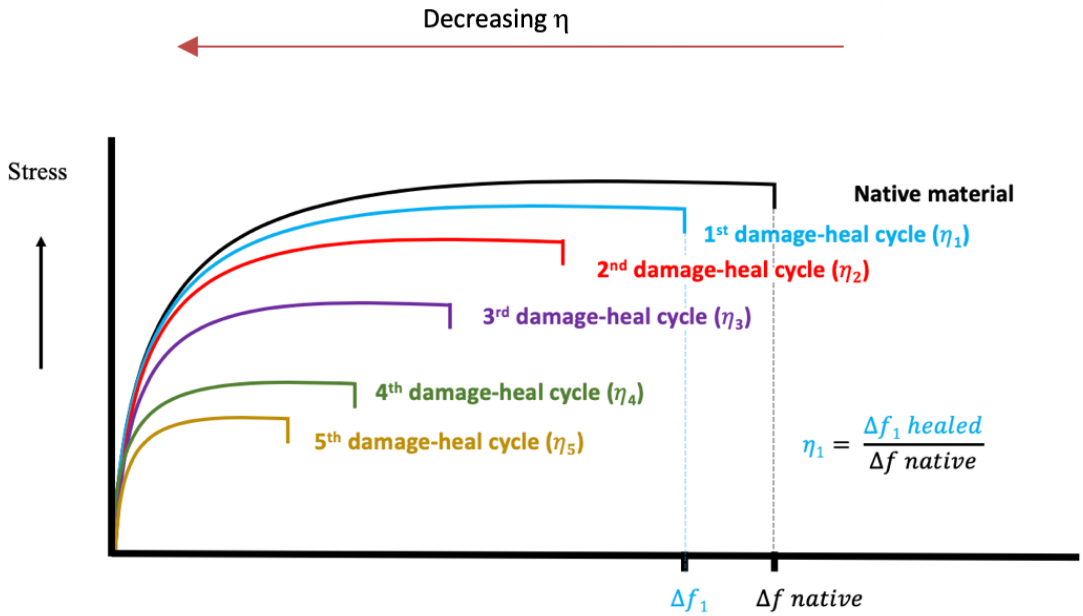

Figure 1.8. Material self-healing efficiency hysteresis after successive damage-heal cycles as a function of percent strain.

1.5.1. Extrinsic Encapsulated Healing Agents

One of the benefits of working with polymers to create self-healing material include its wide range of mechanical properties, ability to alter molecule functionality for fine tuning of the properties, high mobility and solubility. These factors have influenced researchers to incorporate encapsulated healing agents within the polymer matrix. The active agents contained within these capsules are released upon damage to produce an extrinsic autonomous healing reaction.[47] The concept is illustrated in Figure 1.9.[47]

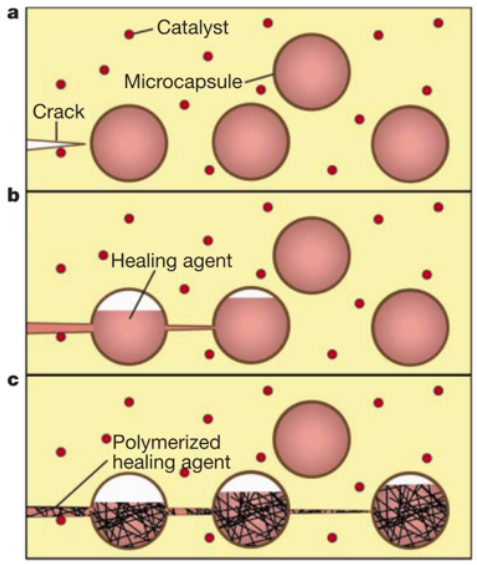

Figure 1.9. Autonomous self-healing via extrinsic encapsulation of healing agent.
Adapted with permission from Ref. [47]. Copyright 2001 Nature Publishing Group.

As illustrated in Figure 1.9 upon crack formation the inclusion containing monomers and or reagents is attracted toward the damage which results in their release. In addition to these heterogenic inclusions, a catalyst is also dispersed in the matrix in order to initiate the polymerization of the monomers in order to fill the crack site. Figure 1.10 demonstrates the efficient microencapsulated system for self-healing using encapsulated dicyclopentadiene (DCPD) monomers dispersed within an epoxy matrix with Grubb's catalyst, bis(tricyclohexylphosphine benzylidene ruthenium (IV) dichloride, used to trigger the ring-opening metathesis polymerization (ROMP).[47]

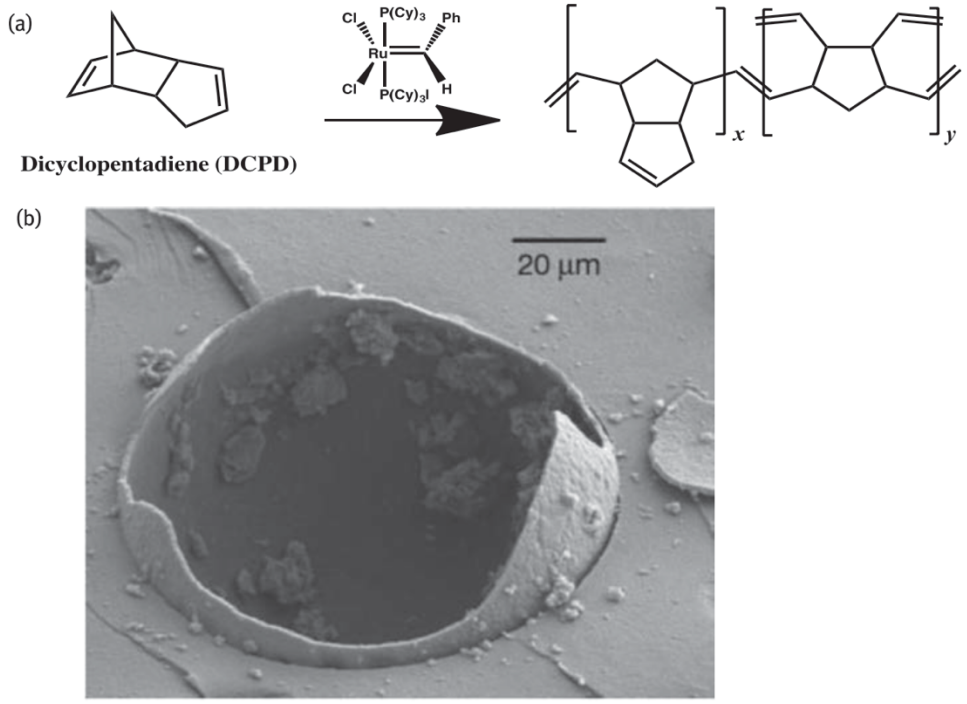

Figure 1.10 (a) Encapsulated monomer polymerization reaction that occurs upon capsule rupture of DCPD with Grub's catalyst. (b) SEM image of ruptured healing agent capsule. Adapted with permission from Ref. [47]. Copyright 2001 Nature Publishing Group.

The careful design of the system allowed for 75% recovery of its mechanical strength after damage. Various other cross-linking reactions have been explored to achieve extrinsic autonomous self-healing. For instance, PDMS polymerization triggered through release of a Pt catalyst, $CuBr_2$/2-methylimidazole complex reacted with epoxide as well as isocyanate with water have also shows promise for extrinsic self-healing of polymeric matrices.[48,49]

While these extrinsic, encapsulated healing agent systems have been effective for producing self-healing materials, it is important to recognize its various limitations. First, the system is not able to repeatedly self-heal. Once the reagents have been released and the polymerization at the site of damage is complete, there are no longer anymore for successive damage. Additionally, the reagents required for this method must be carefully selected. The membrane of the capsulated monomers or reagents must rupture upon damage. The size of the capsules and amount of released materials must be sufficient enough to substantially regenerate the damaged material. The bulk

properties of the material can be drastically affected by large capsules. Alternatively, smaller capsules minimally affect the bulk properties of the material however do not contain sufficient materials to fully repair the damage. In addition to these factors, the catalyst used to initiate polymerization must not drastically affect the mechanical properties of the polymer, work at moderate temperatures within a short amount of time, and the viscosity of the monomeric units must be low for effective mass transport to the site of damage.

1.5.2. Dynamic Bonding for Self-Healing

In order to generate intrinsic self-healing materials, polymers that are able to form and reform dynamic bonds in response to energy dissipation has provided a promising avenue for modern materials. Various dynamic bonds have been explored through inclusion of chemical motifs within coordination chemistry and supramolecular polymers with the ability to autonomously repair. Through careful chemical design, spontaneous polymer self-healing is feasible through bond reformation upon damage. Dynamic cross-linking most commonly occurs through reversible covalent bonding, hydrogen-bonding and metal ligand coordination. Due to the repeatability of the bond formation and reformation of dynamic bonds, these systems produce ideally behaving robust materials that are directly related to the binding energies of the dynamic bonding network.

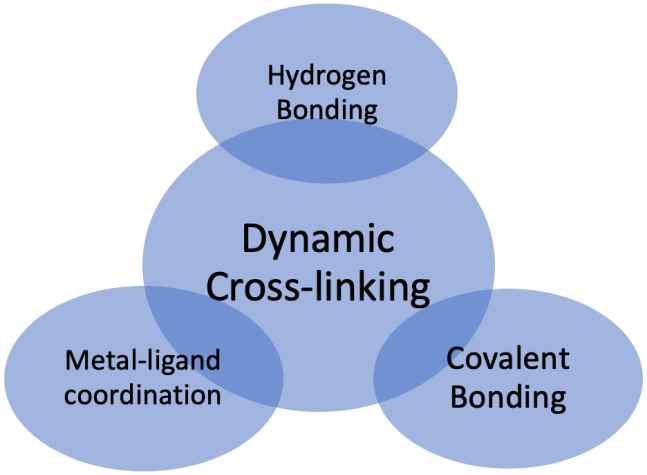

Figure 1.11. Most common methods for dynamic polymer cross-linking.

Generation of new chemical bonds as a method of self-healing is a popular approach to enable polymer self-healing properties at the intramolecular level. Covalent bonds have high binding energies and therefore are able to produce robust materials. Important factors to consider during chemical design of dynamic covalent bonds for self-healing polymers is the application and environment for the material use, the need for external triggers or reagents and the equilibrium energy barrier for the forward and reverse reaction. It is important to recognize the need for a system that is exchangeable at working conditions at the macroscopic level. Bond exchanged through heat or light for bulk self-healing has been explored which limits the possible use of these materials for a wide variety of applications.[50–54] Several chemical reactions have shown to be effective for self-healing at the macroscopic level. Diels-Alder chemistry based cycloaddition reactions has been studied to produce a self-healing thermoset polymer.[50] The temperature-controlled self-healing elastomeric material was created through siloxane chains functionalized with maleimidocarboxyphenyl groups cross linked with a furan-modified polyhedral oligomeric silsesquioxane to cross-link the siloxane chains through a Diels-Alder reaction. The carbon-carbon bonds formed from the cycloaddition reactions allow for stable and robust materials to be formed. The furan groups are used as reactive dienes to work with the maleimide derivative, which reacts at room temperature however requires higher temperatures in the reverse direction.[55] Functionalization of the diene, accessibility of the reactive groups and application of mechanical forces have been shown to facilitate the reverse reaction of the cycloaddition.[55,56] Additionally, the high activation energy required for the Diels-Alder reactions limits its compatibility with low glass transition (T_g) polymers.

Dynamic covalent exchange reactions are a promising approach towards autonomous self-healing. Imine bond formation generated from an acid-catalyzed condensation reaction of an aldehyde and amine has been studied.[57] This method composed of self-healing through imine cross-linkages allowed for a malleable, self-healing polymer network without the need for external catalyst as a result of residual unreacted primary amine chains within the low T_g network of polyethylene glycol (PEG) chains (Figure 1.13).[57]

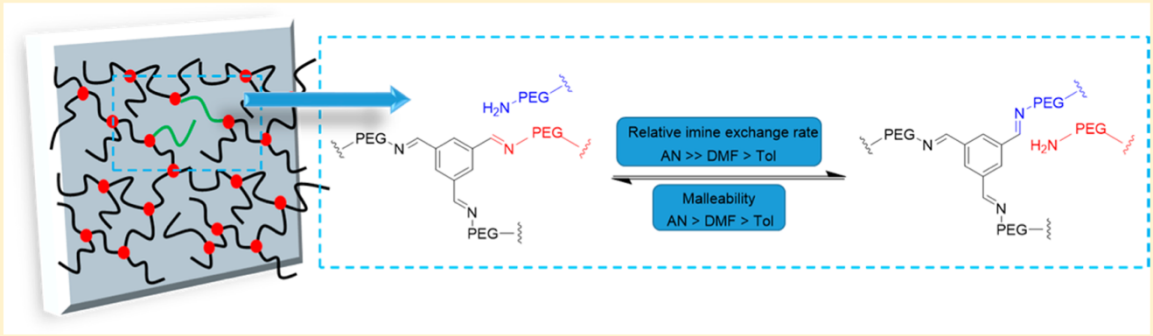

Figure 1.12. Self-healing covalent polymer based on imine bond exchange. Adapted with permission from Ref. [57]. Copyright 2016. American Chemical Society.

Additionally, the low energy barrier, spontaneous exchange of thiol and disulfide bonds has been exploited to produce spontaneously self-healing materials however, the exchange is pH dependent which again limits the possible applications.[58,59]

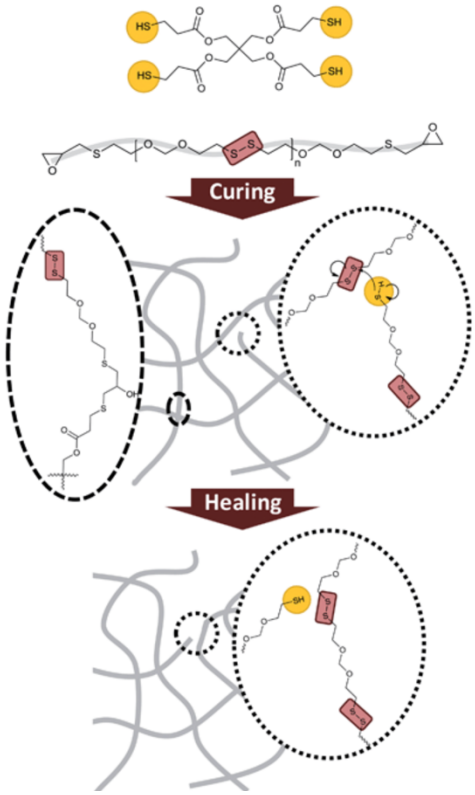

Figure 1.13. Self-healing covalent polymer based on spontaneous exchange of thiol and disulfide bonds. Adapted with permission from Ref. [58]. Copyright 2013. Royal Society of Chemistry.

Lastly, radical exchange has become a useful method for self-healing where covalent bond cleavage generates a dree radical that can be used in a radical exchange for self-repair. This type of cross linking can be done using the breakdown and generation of carbon free radicals from NO-C bonds using thiocarbonate, thiuram disulfide derivatives or alkoxyamine moieties have been used for this method of intermolecular crosslinking.[60,61] Figure 1.15 illustrates a polystyrene backbone functionalized with alkoxyamine moieties as intermolecular links for reversible cross linking.

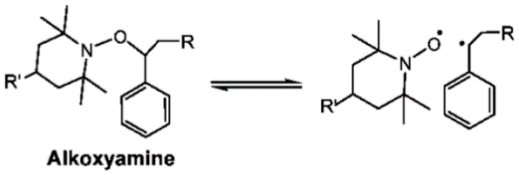

(a)

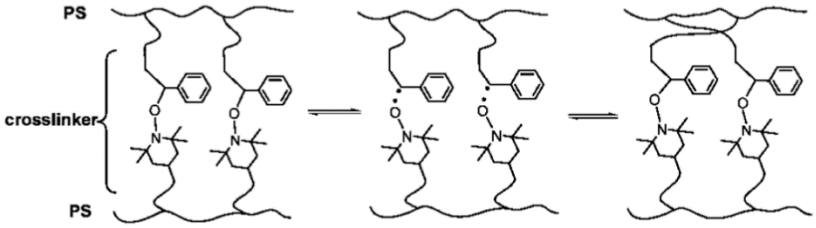

(b)

Figure 1.14. Reversible intermolecular cross-linking through nitroxide mediated polymerization. Adapted with permission from Ref. [61]. Copyright 2011. American Chemical Society.

Supramolecular bonding has also been investigated as a method of self-healing. Supramolecular chemistry refers to the chemical interactions between molecules, as oppose to within molecules. Hydrogen bonding is a supramolecular interaction that is used for dynamic non-covalent interactions and has been reported in numerous studies for its use for self-healing.[43,62–66] Hydrogen bonds are defined as weak, dipolar interactions of a hydrogen atom attached to an electronegative atom such as oxygen that interacts with a neighboring electronegative atom. The dynamic behavior of these bonds formed between polymer chains such as polyacrylate (PA) or polyurea (PU) allows for impressive mechanical and chemical resistant materials. Hydrogen bonded systems allows for fine tuning of the bonding strength through careful selection of the donor-acceptor pairs, with more complementarity creating more stable materials. For instance, Guan and colleagues developed a elastomer based on hydrogen bonding of brush polymers with polystyrene (PS) backbone and hydrogen bonding units of polyacrylate-amide brushes, assembled

into a hard-soft microphase-separated supramolecular system, allowing for enhanced stiffness of nanocomposites along with the self-healing characteristics of hydrogen bonding.[65] The design was able to regain 92% of its mechanical properties after 24 hours without the need to external influence or catalyst. Alteration of the brush lengths with the complimentary hydrogen bonding amide groups allowed for enhanced elastic modulus as a function of PA-amide brush repeat units (Figure 1.16). Additionally, the combination of a high and low T_g of this design allowed for phase separation at the bulk state with the polar phase containing the weak hydrogen bonds were ruptured as oppose to the stronger intermolecular bonds of the PS backbone. Ultimately this is explained to allow for the controlled self-healing process, where the low T_g of the PA amide matrix, the network mobility is high enough for the polymers to rearrange to reform the ruptured hydrogen bonds.[46] Although this method has proven effective for the design of versatile self-healing materials, it fails to work as effectively in bulk and large area applications as a result of their relative weak bonding nature limiting its environmental parameters and moisture sensitivity.

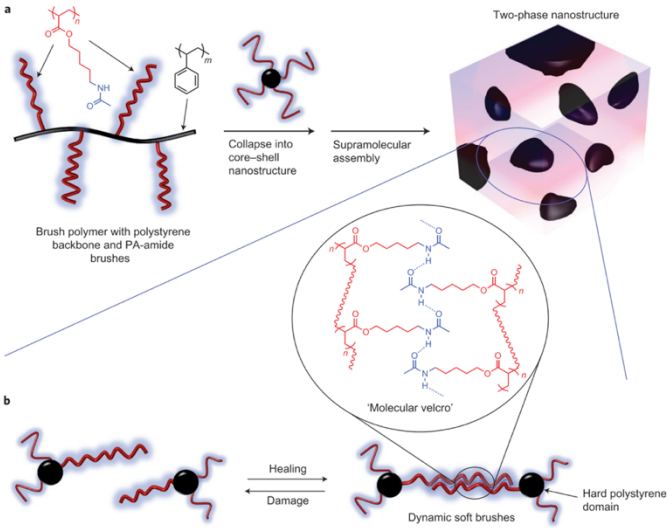

Figure 1.15. A hydrogen-bonding brush polymer design for self-healing supramolecular elastomers. Adapted with permission from Ref. [65]. Copyright 2012 Nature Publishing Group.

With similar dynamics as hydrogen bonded supramolecular polymers along with the possibility of forming stronger dynamic bonds as a method of cross linking, metal-ligand coordination has attracted interest as an approach for self-healing. The coordinate-covalent bonds formed are strong enough to produce robust materials while also possessing the proper ability to dissipate energy upon strain through bond formation/reformation. Through incorporation coordinating motifs to polymer chains which can then bind through affinity to metal centers, the possibilities and control over the mechanical and chemical characteristic of the self-healing material is possible. In this way, there are multiple degrees to which a polymer system can be tuned to embody desirable characteristics such as mechanical strength, versatility, stretchability and self-healing capabilities. The type of metal ion, counterion, ligand location within the polymer chain as well as metal-ligand affinity all allow for various degrees of mechanical and self-healing properties.[67–70] Coordination of Fe(III) by catechol units has been found in nature, where mussels' bysses thread posess stretchable and self-healing capabilities.[71] This has inspired a wide variety of investigations using various metals ligand interactions in order to create dynamic self-healing networks for modern materials. [67,68,70,72,73] As oppose to supramolecular cross-linking through hydrogen bonding, metal ligand interactions allow for stronger bonding and therefore more robust materials with larger avenues for tunability. Guan and colleagues designed a multiphasic system comparable to their study illustrated in Figure 1.16, however used metal-ligand coordination through imidazole containing brushes of PS backbones as a method of forming reversible crosslinks (Figure 1.17).

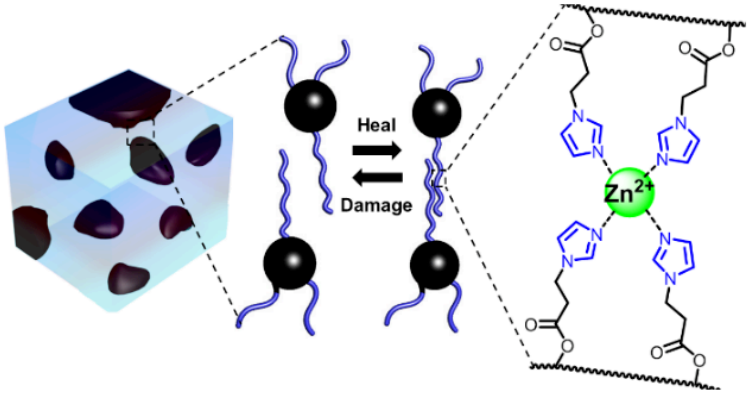

Figure 1.16. A hydrogen-bonding brush polymer design for self-healing supramolecular elastomers. Adapted with permission from Ref. [67]. Copyright 2014 American Chemical Society.

1.6. Coordination Chemistry for Self-Healing Polymers

The growth of crystal engineering and supramolecular chemistry has given rise to the development of coordination polymer research. Material properties are influenced by the way in which molecules are arranged. Crystal engineering focuses on understanding why molecules pack in certain ways in order to use to engineering molecules for new materials.[74] This understanding at the crystal level governs the way in which the constituent molecules are arranged and thus the material properties that result. It has been suggested that supramolecular chemistry is considered to be crystal engineering at the solid state since molecular interactions in coordination polymers determine their packing arrangements. [75]

Coordination polymers are a subset of supramolecular chemistry that use metal ions linked by coordinated ligands to form a polymer matrix. The molecular species are linked through coordination bonds which are defined as a bond in which both electrons originate from a single atom known as the ligand, whereas the metal acts as an electron acceptor. Main group and alkaline earth metals aren't typically used for coordination polymers since their bonding nature is more covalent and ionic, respectively. Therefore, the design of coordination polymers focuses on transition and lanthanoid metals to promote coordinate interactions that provide strength and lability of the bonds. The interactions of ligands with the metals are therefore reversible and thus a promising option for self-healing materials. The resulting polymer networks produce generally

predictable geometries around transition metal ions which provides a parameter of cross-linking density control.

Typical ligands used for metal-ligand coordinated polymers are illustrated in Figure 1.18. It is common for ligands to consist of two coordination sites, known as bidentate coordination. Pyridyl, imidazole, nitrile or carboxylate functional groups are common moieties used in coordination polymers as a result. While these are the most common ligands used for coordination polymers, it is important to highlight the point that any atom, molecule or ion can behave as a ligand as long as it contains a free lone pair of electrons. This is important to consider when selecting for the metal counterion used in the cross linking since a weaker coordinate bond can form with the anion of the metal, affecting the resulting polymer mechanics. Commonly used counterions used are halides, nitrate, perchlorate, tetrafluoroborate hexafluorophosphate and hexafluoro silicate or triflate salts. As for the typical transition metals used in the coordination, the first row of the transition metal elements in addition to Zn, Cs, Hg, Ag, Au, Pd and Pt. Such metals are selected due to their ready availability, stability and kinetic lability to participate in ligand coordination.

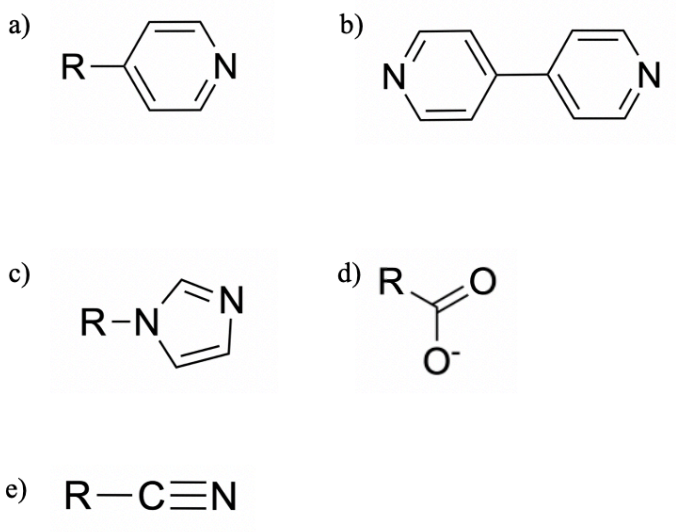

Figure 1.17. Common ligand functional groups used in M-L coordinated polymers. (a) pyridyl, (b) bipyridyl, (c) imidazole, (d) carboxylate and (e) nitrile.

Coordination spheres form to create cross linking sites where the metal is coordinate bonded to a few ligands. The crosslinking density is therefore dependent on the coordination number of the central metal ion, which is predicted based on crystal field theory crystallographic data. In addition

to the coordination number, the number of ligands that form the coordination sphere can be arranged in a monodentate or polydentate fashion, based on the number of atoms that are involved in the coordination on the ligand. Chelating ligands involved more than one donating atom on the ligand which creates a claw-like binding of the metal (Figure 1.19.). The coordination number of a metal is dependent on the metal and ligand size, metal ion charge and electronic configuration. The most common coordination geometries are illustrated in Figure 1.20.

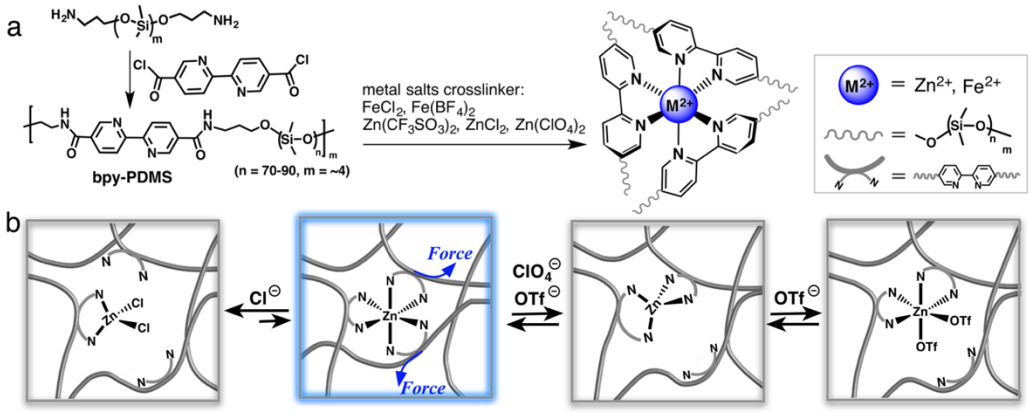

Figure 1.18. Example of a bidentate Metal-ligand coordination where one polymer chain contributes two coordination sites. Adapted with permission from Ref. [93]. Copyright 2016 American Chemical Society.

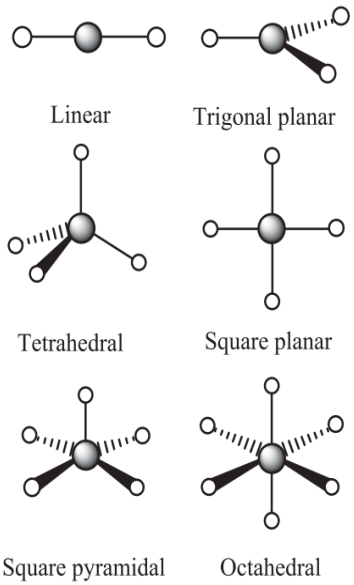

Figure 1.19.Common d-block metal coordination geometries.

The geometry of the metal-ligand (M-L) coordination in coordination polymers describes the cross-linking density. Based on the coordination number for transition metal complexes, the molecular geometries can be predicted. Crystal field theory explains the resulting geometries as the number of d-orbital electrons has an influence on the coordination geometry of the resulting material.[74] The negatively charged ligand overlaps the negatively charged electrons of the d-orbital transition metal electrons therefor influencing the d-orbital energy. Thus, the predicted geometries are based on the most stable arrangement resulting in metal d-orbital energies with minimal electron orbital overlap between the metal and ligand. It is important to mention that the coordination geometries can be distorted depending on the coordination environment which depends on the type of solvent and counterion used in the coordination reaction.[76] In addition to the predicted geometries of metal-ligand coordination, the bond strength of the metal-ligand interaction can be predicted based on crystallographic data which further influences the resulting properties of coordination polymers. The bond strength of the M-L bonds are directly related to the bond length, where the smaller the bond length the stronger the bond.[77] Therefor, in addition the geometry of the coordination effects cross linking density and resulting material properties, the M-L bond strength is another method to fine tune such systems.

1.7. Scope of thesis

In the past decade, there have been numerous studies and methods that have focused on the development of self-healing materials for flexible electronic applications.[50,78–81] Despite the impressive developments in this field, the combination of desired mechanical properties along with self-healing capabilities is still a challenge as a result of the indirect relationship between chemical design and self-healing efficiency.[82] Additionally, current methods require complex preparation or rely on external triggers for material regeneration. [47,83] Furthermore, the connection between self-healing efficiency and physical properties, such as the elastic modulus, is still not fully understood.

In this thesis a novel self-healing material is developed that is able to be chemically tuned to allow for a wide range of mechanical properties. The new materials will investigate metal-ligand coordination as a method of dynamic crosslinking using a PDMS based backbone.

The general strategy to access autonomously healable materials at room temperature has been done through incorporation of moieties able to generate weak supramolecular interactions that can dynamically crosslink polymer chains. [65,71,84] This system is particular efficient for low glass transition temperatures as the segmental chain mobility of these materials is high, allowing the chains to reform supramolecular interactions upon damage.[85,86] M-L supramolecular interactions are a particularly promising strategy toward robust, autonomous self-healing materials, however the importance of the methods to fine tune mechanical properties and self-healing capabilities of the materials is limited. Therefore, our work focuses of the simple preparation of a new self-healing material, based on end-capped PDMS-based oligomers with N-Ligands, and the rational fine-tuning of their self-healing efficiency and thermochemical properties through the variation and nature of the metal-ligand interactions used.

As a result of the new materials being based on PDMS, its use as a self-healing dielectric in a flexible, capacitive pressure sensor will also be explored. The system is investigated through UV-Vis spectroscopy, atomic force spectroscopy, tensile strain pull testing and shear rheology.

1.8. REFERENCES

1 A. M. Hussain and M. M. Hussain. CMOS-Technology-Enabled Flexible and Stretchable Electronics for Internet of Everything Applications, *Adv. Mater.*, 2016, **28**, 4219–4249.

2 Y. Yao, H. Dong and W. Hu. Charge Transport in Organic and Polymeric Semiconductors for Flexible and Stretchable Devices, *Adv. Mater.*, 2016, **28**, 4513–4523.

3 T. F. O 'connor, K. M. Rajan, A. D. Printz and D. J. Lipomi. Toward organic electronics with properties inspired by biological tissue, *J. Mater. Chem. B*, 2015, **3**, 4947–4952.

4 S. J. Benight, C. Wang, J. B. H. Tok and Z. Bao. Stretchable and self-healing polymers and devices for electronic skin, *Prog. Polym. Sci.*, 2013, **38**, 1961–1977.

5 M. Kaltenbrunner, T. Sekitani, J. Reeder, T. Yokota, K. Kuribara, T. Tokuhara, M. Drack, R. Schwödiauer, I. Graz, S. Bauer-Gogonea, S. Bauer and T. Someya. An ultra-lightweight design for imperceptible plastic electronics, *Nature*, 2013, **499**, 458–463.

6 Q. Hua, J. Sun, H. Liu, R. Bao, R. Yu, J. Zhai, C. Pan and Z. L. Wang. Skin-inspired highly stretchable and conformable matrix networks for multifunctional sensing, *Nat. Commun.*, 2018, **9**, 1–11.

7 K. A. Ray. Flexible Solar Cell reliable power source that can provide power at any KelWrd-, *IEEE Trans. Aerosp. Electron. Syst.*

8 D. Angmo, T. T. Larsen-Olsen, M. Jørgensen, R. R. Søndergaard and F. C. Krebs. Roll-to-roll inkjet printing and photonic sintering of electrodes for ITO free polymer solar cell modules and facile product integration, *Adv. Energy Mater.*, 2013, **3**, 172–175.

9 T.-T. Kuo, C.-M. Wu, H.-H. Lu, I. Chan, K. Wang and K.-C. Leou. Flexible x-ray imaging detector based on direct conversion in amorphous selenium, *J. Vac. Sci. Technol. A Vacuum, Surfaces, Film.*, 2014, **32**, 041507.

10 T. Peter Brody. The Thin Film Transistor—A Late Flowering Bloom, *IEEE Trans. Electron Devices*, 1984, **31**, 1614–1628.

11 N. D. Young, G. Harkin, R. M. Bunn, D. J. Mcculloch, R. W. Wilks and A. G. Knapp. Polysilicon TFT ' s on Glass and Polymer Substrates, 1997, **18**, 19–20.

12 C. Liu, N. Huang, F. Xu, J. Tong, Z. Chen, X. Gui, Y. Fu and C. Lao. 3D printing technologies for flexible tactile sensors toward wearable electronics and electronic skin, *Polymers (Basel).*, 2018, **10**, 1–31.

13 H. Bin Yao, J. Ge, C. F. Wang, X. Wang, W. Hu, Z. J. Zheng, Y. Ni and S. H. Yu. A

flexible and highly pressure-sensitive graphene-polyurethane sponge based on fractured microstructure design, *Adv. Mater.*, 2013, **25**, 6692–6698.

14 B. Zhuo, S. Chen, M. Zhao and X. Guo. High Sensitivity Flexible Capacitive Pressure Sensor Using Polydimethylsiloxane Elastomer Dielectric Layer Micro-Structured by 3-D Printed Mold, *IEEE J. Electron Devices Soc.*, 2017, **5**, 219–223.

15 D. J. Lipomi, J. A. Lee, M. Vosgueritchian, B. C. K. Tee, J. A. Bolander and Z. Bao. Electronic properties of transparent conductive films of PEDOT:PSS on stretchable substrates, *Chem. Mater.*, 2012, **24**, 373–382.

16 B. B. Narakathu, A. Eshkeiti, A. S. G. Reddy, M. Rebros, E. Rebrosova, M. K. Joyce, B. J. Bazuin and M. Z. Atashbar. A novel fully printed and flexible capacitive pressure sensor, *Proc. IEEE Sensors*, 2012, 26–29.

17 O. Atalay, A. Atalay, J. Gafford and C. Walsh. A Highly Sensitive Capacitive-Based Soft Pressure Sensor Based on a Conductive Fabric and a Microporous Dielectric Layer, *Adv. Mater. Technol.*, 2018, **3**, 1–8.

18 D. J. Lipomi, M. Vosgueritchian, B. C. K. Tee, S. L. Hellstrom, J. A. Lee, C. H. Fox and Z. Bao. Skin-like pressure and strain sensors based on transparent elastic films of carbon nanotubes, *Nat. Nanotechnol.*, 2011, **6**, 788–792.

19 S. C. B. Mannsfeld, B. C. K. Tee, R. M. Stoltenberg, C. V. H. H. Chen, S. Barman, B. V. O. Muir, A. N. Sokolov, C. Reese and Z. Bao. Highly sensitive flexible pressure sensors with microstructured rubber dielectric layers, *Nat. Mater.*, 2010, **9**, 859–864.

20 A. Sekiguchi, F. Tanaka, T. Saito, Y. Kuwahara, S. Sakurai, D. N. Futaba, T. Yamada and K. Hata. Robust and Soft Elastomeric Electronics Tolerant to Our Daily Lives, *Nano Lett.*, 2015, **15**, 5716–5723.

21 M. Shin, J. H. Song, G. H. Lim, B. Lim, J. J. Park and U. Jeong. Highly stretchable polymer transistors consisting entirely of stretchable device components, *Adv. Mater.*, 2014, **26**, 3706–3711.

22 A. D. Kim, J. Ahn, W. M. Choi, H. Kim, T. Kim, J. Song, Y. Y. Huang, Z. Liu, C. Lu and J. A. Rogers. Stretchable and Foldable Silicon Integrated Circuits, *Science (80-.).*, 2008, **320**, 507–511.

23 M. Selivanova, C. H. Chuang, B. Billet, A. Malik, P. Xiang, E. Landry, Y. C. Chiu and S. Rondeau-Gagné. Morphology and Electronic Properties of Semiconducting Polymer and

Branched Polyethylene Blends, *ACS Appl. Mater. Interfaces*, 2019, **11**, 12723–12732.

24 M. Selivanova, S. Zhang, B. Billet, A. Malik, N. Prine, E. Landry, X. Gu, P. Xiang and S. Rondeau-Gagné. Branched Polyethylene as a Plasticizing Additive to Modulate the Mechanical Properties of π-Conjugated Polymers, *Macromolecules*, 2019, **52**, 7870–7877.

25 Z. Huang, M. Gao, Z. Yan, T. Pan, S. A. Khan, Y. Zhang, H. Zhang and Y. Lin. Pyramid microstructure with single walled carbon nanotubes for flexible and transparent micro-pressure sensor with ultra-high sensitivity, *Sensors Actuators, A Phys.*, 2017, **266**, 345–351.

26 T. Sekitani, Y. Noguchi, K. Hata, T. Fukushima, T. Aida and T. Someya. A rubberlike stretchable active matrix using elastic conductors, *Science (80-.).*, 2008, **321**, 1468–1472.

27 D. J. Lipomi, M. Vosgueritchian, B. C. K. Tee, S. L. Hellstrom, J. A. Lee, C. H. Fox and Z. Bao. Skin-like pressure and strain sensors based on transparent elastic films of carbon nanotubes, *Nat. Nanotechnol.*, 2011, **6**, 788–792.

28 J. A. Rogers, T. Someya, Y. Huang, J. A. Rogers, T. Someya and Y. Huang. Materials and Mechanics for Stretchable Electronics Published by : American Association for the Advancement of Science Linked references are available on JSTOR for this article : Materials and Mechanics for Stretchable Electronics, 2010, **327**, 1603–1607.

29 M. U. Ocheje, B. P. Charron, Y. H. Cheng, C. H. Chuang, A. Soldera, Y. C. Chiu and S. Rondeau-Gagné. Amide-Containing Alkyl Chains in Conjugated Polymers: Effect on Self-Assembly and Electronic Properties, *Macromolecules*, 2018, **51**, 1336–1344.

30 Y. Li, W. K. Tatum, J. W. Onorato, S. D. Barajas, Y. Y. Yang, C. K. Luscombe and K. Christine. An indacenodithiophene-based semiconducting polymer with high ductility for stretchable organic electronics, *Polym. Chem.*, 2017, **8**, 5185–5193.

31 S. Braun. Studies of materials and interfaces for organic electronics, *Studies of materials and interfaces for organic electronics*, 2007.

32 N. Vogel. Springer Theses, *Springer Theses*, 2011.

33 J. S. Kim, J. H. Kim, W. Lee, H. Yu, H. J. Kim, I. Song, M. Shin, J. H. Oh, U. Jeong, T. S. Kim and B. J. Kim. Tuning Mechanical and Optoelectrical Properties of Poly(3-hexylthiophene) through Systematic Regioregularity Control, *Macromolecules*, 2015, **48**, 4339–4346.

34 B. Wang, D. Qin, G. Liang, A. Gu, L. Liu and L. Yuan. High-k materials with low

dielectric loss based on two superposed gradient carbon nanotube/cyanate ester composites, *J. Phys. Chem. C*, 2013, **117**, 15487–15495.

35 R. Ruppin. Electromagnetic energy density in a dispersive and absorptive material, *Phys. Lett. Sect. A Gen. At. Solid State Phys.*, 2002, **299**, 309–312.

36 B. Wang, G. Liang, Y. Jiao, A. Gu, L. Liu, L. Yuan and W. Zhang. Two-layer materials of polyethylene and a carbon nanotube/cyanate ester composite with high dielectric constant and extremely low dielectric loss, *Carbon N. Y.*, 2013, **54**, 224–233.

37 B. Wang, W. Huang, L. Chi, M. Al-Hashimi, T. J. Marks and A. Facchetti. High- k Gate Dielectrics for Emerging Flexible and Stretchable Electronics, *Chem. Rev.*, 2018, **118**, 5690–5754.

38 C. E. Diesendruck, N. R. Sottos, J. S. Moore and S. R. White. Biomimetic Self-Healing, *Angew. Chemie - Int. Ed.*, 2015, **54**, 10428–10447.

39 D. Y. Wu, S. Meure and D. Solomon. Self-healing polymeric materials: A review of recent developments, *Prog. Polym. Sci.*, 2008, **33**, 479–522.

40 Y. J. Tan, J. Wu, H. Li and B. C. K. Tee. Self-Healing Electronic Materials for a Smart and Sustainable Future, *ACS Appl. Mater. Interfaces*, 2018, **10**, 15331–15345.

41 F. W. Went. Cladistics Linked references are available on JSTOR for this article :, *Int. Assoc. Plant Taxon.*, 1971, **20**, 197–226.

42 B. Blaiszik, S. L. B. Kramer, J. S. Moore, N. R. Sottos, B. J. Blaiszik, S. L. B. Kramer, S. C. Olugebefola, J. S. Moore, N. R. Sottos and S. R. White. Self-Healing Polymers and Composites Second Sandia Fracture Challenge View project Shock Wave Energy Dissipation by Mechanochemically-active Materials View project Self-Healing Polymers and Composites, *Annu. Rev. Mater. Res*, 2010, **40**, 179–211.

43 F. Herbst, D. Döhler, P. Michael and W. H. Binder. Self-healing polymers via supramolecular forces, *Macromol. Rapid Commun.*, 2013, **34**, 203–220.

44 B. Zhang, Z. A. Digby, J. A. Flum, E. M. Foster, J. L. Sparks and D. Konkolewicz. Self-healing, malleable and creep limiting materials using both supramolecular and reversible covalent linkages, *Polym. Chem.*, 2015, **6**, 7368–7372.

45 C. De Nardi, S. Bullo, L. Ferrara, L. Ronchin and A. Vavasori. Effectiveness of crystalline admixtures and lime/cement coated granules in engineered self-healing capacity of lime mortars, *Mater. Struct. Constr.*, 2017, **50**, 1–12.

46 M. N. Tahir, M. U. Ocheje, K. Wojtkiewicz and S. Rondeau-gagné. 3 Self-Healing Materials : Design and Applications, .

47 S. R. White, N. R. Sottos, P. H. Geubelle, J. S. Moore, M. R. Kessler, S. R. Sriram, E. N. Brown and S. Viswanathan. Autonomic healing of polymer composites, *Nature*, 2001, **409**, 794–797.

48 J. Yang, M. W. Keller, J. S. Moore, S. R. White, N. R. Sottos, J. Yang, M. W. Keller, J. S. Moore, S. R. White and N. R. Sottos. Microencapsulation of Isocyanates for Self-Healing Polymers Microencapsulation of Isocyanates for Self-Healing Polymers, 2008, **41**, 9650–9655.

49 S. H. Cho, H. M. Andersson, S. R. White, N. R. Sottos and P. V. Braun. Polydiniethylsiloxane-based self-healing materials, *Adv. Mater.*, 2006, **18**, 997–1000.

50 A. Nasresfahani and P. M. Zelisko. Synthesis of a self-hea(1) Nasresfahani, A.; Zelisko, P. M. Synthesis of a Self-Healing Siloxane-Based Elastomer Cross-Linked via a Furan-Modified Polyhedral Oligomeric Silsesquioxane Investigation of a Thermally Reversible Silicon-Based Cross-Link. Polym, *Polym. Chem.*, 2017, **8**, 2942–2952.

51 C. C. Deng, W. L. A. Brooks, K. A. Abboud and B. S. Sumerlin. Boronic acid-based hydrogels undergo self-healing at neutral and acidic pH, *ACS Macro Lett.*, 2015, **4**, 220–224.

52 W. Li, C. Zhang, S. Qi, X. Deng, W. Wang, B. Yang, J. Liu and Z. Dong. Polymer Chemistry, .

53 B. D. Fairbanks, S. P. Singh, C. N. Bowman and K. S. Anseth. Photodegradable, photoadaptable hydrogels via radical-mediated disulfide fragmentation reaction, *Macromolecules*, 2011, **44**, 2444–2450.

54 G. Zhao, C. Yang, L. Guo, H. Sun, C. Chen and W. Xia. Visible light-induced oxidative coupling reaction: Easy access to Mannich-type products, *Chem. Commun.*, 2012, **48**, 2337–2339.

55 P. M. Imbesi, C. Fidge, J. E. Raymond, S. I. Cauët and K. L. Wooley. Model Diels-Alder studies for the creation of amphiphilic cross-linked networks as healable, antibiofouling coatings, *ACS Macro Lett.*, 2012, **1**, 473–477.

56 F. Yu, X. Cao, J. Du, G. Wang and X. Chen. Multifunctional Hydrogel with Good Structure Integrity, Self-Healing, and Tissue-Adhesive Property Formed by Combining

Diels-Alder Click Reaction and Acylhydrazone Bond, *ACS Appl. Mater. Interfaces*, 2015, **7**, 24023–24031.

57 A. Chao, I. Negulescu and D. Zhang. Dynamic Covalent Polymer Networks Based on Degenerative Imine Bond Exchange: Tuning the Malleability and Self-Healing Properties by Solvent, *Macromolecules*, 2016, **49**, 6277–6284.

58 M. Pepels, I. Filot, B. Klumperman and H. Goossens. Self-healing systems based on disulfide-thiol exchange reactions, *Polym. Chem.*, 2013, **4**, 4955–4965.

59 G. Deng, F. Li, H. Yu, F. Liu, C. Liu, W. Sun, H. Jiang and Y. Chen. Dynamic hydrogels with an environmental adaptive self-healing ability and dual responsive Sol-Gel transitions, *ACS Macro Lett.*, 2012, **1**, 275–279.

60 Z. P. Zhang, M. Z. Rong, M. Q. Zhang and C. Yuan. Alkoxyamine with reduced homolysis temperature and its application in repeated autonomous self-healing of stiff polymers, *Polym. Chem.*, 2013, **4**, 4648–4654.

61 C. Yuan, M. Z. Rong, M. Q. Zhang, Z. P. Zhang and Y. C. Yuan. Self-healing of polymers via synchronous covalent bond fission/radical recombination, *Chem. Mater.*, 2011, **23**, 5076–5081.

62 H. Li, R. Wang, H. Hu and W. Liu. Surface modification of self-healing poly(urea-formaldehyde) microcapsules using silane-coupling agent, *Appl. Surf. Sci.*, 2008, **255**, 1894–1900.

63 C. Wang, H. Wu, Z. Chen, M. T. Mcdowell, Y. Cui and Z. Bao. Self-healing chemistry enables the stable operation of silicon microparticle anodes for high-energy lithium-ion batteries, *Nat. Chem.*, 2013, **5**, 1042–1048.

64 C. Wang, N. Liu, R. Allen, J. B. H. Tok, Y. Wu, F. Zhang, Y. Chen and Z. Bao. A rapid and efficient self-healing thermo-reversible elastomer crosslinked with graphene oxide, *Adv. Mater.*, 2013, **25**, 5785–5790.

65 Y. Chen, A. M. Kushner, G. A. Williams and Z. Guan. Multiphase design of autonomic self-healing thermoplastic elastomers, *Nat. Chem.*, 2012, **4**, 467–472.

66 R. P. Sijbesma, F. H. Beijer, L. Brunsveld, B. J. B. Folmer, J. H. K. K. Hirschberg, R. F. M. Lange, J. K. L. Lowe and E. W. Meijer. Reversible polymers formed from self-complementary monomers using quadruple hydrogen bonding, *Science (80-.).*, 1997, **278**, 1601–1604.

67 D. Mozhdehi, S. Ayala, O. R. Cromwell and Z. Guan. Self-healing multiphase polymers via dynamic metal-ligand interactions, *J. Am. Chem. Soc.*, 2014, **136**, 16128–16131.

68 Z. Tang, J. Huang, B. Guo, L. Zhang and F. Liu. Bioinspired Engineering of Sacrificial Metal-Ligand Bonds into Elastomers with Supramechanical Performance and Adaptive Recovery, *Macromolecules*, 2016, **49**, 1781–1789.

69 C. H. Li, C. Wang, C. Keplinger, J. L. Zuo, L. Jin, Y. Sun, P. Zheng, Y. Cao, F. Lissel, C. Linder, X. Z. You and Z. Bao. A highly stretchable autonomous self-healing elastomer, *Nat. Chem.*, 2016, **8**, 618–624.

70 B. Sandmann, B. Happ, S. Kupfer, F. H. Schacher, M. D. Hager and U. S. Schubert. The self-healing potential of triazole-pyridine-based metallopolymers, *Macromol. Rapid Commun.*, 2015, **36**, 604–609.

71 N. et al. Holten-Andersen. Metal-coordination: using one of nature's tricks to control soft material mechanics., *J. Mater. Chem. B 2, 2467*, 2013, 5791–5797.

72 F. Dumitru, A. van der Lee and M. Barboiu. Chiral superstructures from homochiral Zn2+, Co2+, Fe2+-2,6-bis (aryl ethylimine)pyridine complexes, *Chirality*, 2019, **31**, 763–775.

73 S. Schmatloch, M. F. González and U. S. Schubert. Metallo-supramolecular diethylene glycol: Water-soluble reversible polymers, *Macromol. Rapid Commun.*, 2002, **23**, 957–961.

74 T. S. Thakur, R. Dubey and G. R. Desiraju. Crystal Structure and Prediction, *Annu. Rev. Phys. Chem.*, 2015, **66**, 21–42.

75 P. Blue, P. Blue and W. W. Ii. Coordination polymers design, analysis and application, in *Royal Society of Chemistry*, 2009, pp. 1–18Coordination polymers design, analysis and application.

76 M. L. Tong and X. M. Chen. Synthesis of Coordination Compounds and Coordination Polymers, *Synthesis of Coordination Compounds and Coordination Polymers*, Elsevier B.V., 2017.

77 W. Jacob and R. Mukherjee. Synthesis, structure, and properties of monomeric Fe(II), Co(II), and Ni(II) complexes of neutral N-(aryl)-2-pyridinecarboxamides, *Inorganica Chim. Acta*, 2006, **359**, 4565–4573.

78 Y. L. Rao, A. Chortos, R. Pfattner, F. Lissel, Y. C. Chiu, V. Feig, J. Xu, T. Kurosawa, X.

Gu, C. Wang, M. He, J. W. Chung and Z. Bao. Stretchable self-healing polymeric dielectrics cross-linked through metal-ligand coordination, *J. Am. Chem. Soc.*, 2016, **138**, 6020–6027.

79 Y. Cao, T. G. Morrissey, E. Acome, S. I. Allec, B. M. Wong, C. Keplinger and C. Wang. A Transparent, Self-Healing, Highly Stretchable Ionic Conductor, *Adv. Mater.*, 2017, **29**, 1–9.

80 J. 6b08220. pd. Ko, Y. J. Kim and Y. S. Kim. Self-Healing Polymer Dielectric for a High Capacitance Gate Insulator, *ACS Appl. Mater. Interfaces*, 2016, **8**, 23854–23861.

81 X. Y. Jia, J. F. Mei, J. C. Lai, C. H. Li and X. Z. You. A Highly Stretchable Polymer that Can Be Thermally Healed at Mild Temperature, *Macromol. Rapid Commun.*, 2016, **37**, 952–956.

82 W. H. Binder. The Past 40 Years of Macromolecular Sciences: Reflections on Challenges in Synthetic Polymer and Material Science, *Macromol. Rapid Commun.*, 2019, **40**, 1–7.

83 I. L. Hia, V. Vahedi and P. Pasbakhsh. Self-Healing Polymer Composites: Prospects, Challenges, and Applications, *Polym. Rev.*, 2016, **56**, 225–261.

84 K. Imato, M. Nishihara, T. Kanehara, Y. Amamoto, A. Takahara and H. Otsuka. Self-healing of chemical gels cross-linked by diarylbibenzofuranone-based trigger-free dynamic covalent bonds at room temperature, *Angew. Chemie - Int. Ed.*, 2012, **51**, 1138–1142.

85 Y. Yang, X. Ding and M. W. Urban. Chemical and physical aspects of self-healing materials, *Prog. Polym. Sci.*, 2015, **49**–**50**, 34–59.

86 S.-M. Kim, H. Jeon, S.-H. Shin, S.-A. Park, J. Jegal, S. Y. Hwang, D. X. Oh and J. Park. Self-Healing Materials: Superior Toughness and Fast Self-Healing at Room Temperature Engineered by Transparent Elastomers (Adv. Mater. 1/2018), *Adv. Mater.*, 2018, **30**, 1870001.

87 R. R. L. De, D. A. C. Albuquerque, T. G. S. Cruz, F. M. Yamaji and F. L. Leite. Measurement of the Nanoscale Roughness by Atomic Force Microscopy: Basic Principles and Applications, *At. Force Microsc. - Imaging, Meas. Manip. Surfaces At. Scale*, , DOI:10.5772/37583.

88 Y. Yang and M. W. Urban. Self-healing polymeric materials, *Chem. Soc. Rev.*, 2013, **42**, 7446–7467.

89 T. Aida, E. W. Meijer and S. I. Stupp. Functional Supramolecular Polymers, *Science (80-.).*, 2012, **335**, 813–817.

90 A. B. W. Brochu, S. L. Craig and W. M. Reichert. Self-healing biomaterials, *J. Biomed. Mater. Res. - Part A*, 2011, **96 A**, 492–506.

91 J. Y. Oh, S. Rondeau-Gagné, Y. C. Chiu, A. Chortos, F. Lissel, G. J. N. Wang, B. C. Schroeder, T. Kurosawa, J. Lopez, T. Katsumata, J. Xu, C. Zhu, X. Gu, W. G. Bae, Y. Kim, L. Jin, J. W. Chung, J. B. H. Tok and Z. Bao. Intrinsically stretchable and healable semiconducting polymer for organic transistors, *Nature*, 2016, **539**, 411–415.

92 S. Zhang and F. Cicoira. Water-Enabled Healing of Conducting Polymer Films, *Adv. Mater.*, 2017, 29, 1703098.

93 Y. L. Rao, A. Chortos, R. Pfattner, F. Lissel, Y. C. Chiu, V. Feig, J. Xu, T. Kurosawa, X. Gu, C. Wang, M. He, J. W. Chung and Z. Bao. Stretchable self-healing polymeric dielectrics cross-linked through metal-ligand coordination, *J. Am. Chem. Soc.*, 2016, **138**, 6020–6027.

94 M. L. Hammock, A. Chortos, B. C. K. Tee, J. B. H. Tok and Z. Bao. 25th anniversary article: The evolution of electronic skin (E-Skin): A brief history, design considerations, and recent progress, *Adv. Mater.*, 2013, **25**, 5997–6038.

95 W. H. Binder. The Past 40 Years of Macromolecular Sciences: Reflections on Challenges in Synthetic Polymer and Material Science, *Macromol. Rapid Commun.*, 2019, **40**, 1–7.

96 R. P. Wool. Self-healing materials: A review, *Soft Matter*, 2008, **4**, 400–418.

97 J. A. Syrett, C. R. Becer and D. M. Haddleton. Self-healing and self-mendable polymers, *Polym. Chem.*, 2010, **1**, 978–987.

98 N. Holten-Andersen, A. Jaishankar, M. J. Harrington, D. E. Fullenkamp, G. DiMarco, L. He, G. H. McKinley, P. B. Messersmith and K. Y. C. Lee. Metal-coordination: using one of nature's tricks to control soft material mechanics, *J. Mater. Chem. B*, 2014, **2**, 2467.

99 H. Ying, Y. Zhang and J. Cheng. Dynamic urea bond for the design of reversible and self-healing polymers, *Nat. Commun.*, 2014, **5**, 1–9.

100 S. M. Kim, H. Jeon, S. H. Shin, S. A. Park, J. Jegal, S. Y. Hwang, D. X. Oh and J. Park. Superior Toughness and Fast Self-Healing at Room Temperature Engineered by Transparent Elastomers, *Adv. Mater.*, 2018, **30**, 1–8.

101 Z. Xu. Mechanics of metal-catecholate complexes: The roles of coordination state and

metal types, *Sci. Rep.*, 2013, **3**, 7–9.

102 J. Zhao, R. Xu, G. Luo, J. Wu and H. Xia. Self-healing poly(siloxane-urethane) elastomers with remoldability, shape memory and biocompatibility, *Polym. Chem.*, 2016, **7**, 7278–7286.

103 B. S. Cash, J. J.; Kubo, T.; Bapat, A. P.; Sumerlin. Room-Temperature Self-Healing Polymers Based on Dynamic- Covalent Boronic Esters, *Macromolecules*, 2015, 2098.

104 Y. Zhao, W. Zhang, L. P. Liao, H. M. Wang and W. J. Li. The self-healing composite anticorrosion coating, *Phys. Procedia*, 2011, **18**, 216–221.

105 Y. L. Liu and T. W. Chuo. Self-healing polymers based on thermally reversible Diels-Alder chemistry, *Polym. Chem.*, 2013, **4**, 2194–2205.

106 R. Hoogenboom. Hard autonomous self-healing supramolecular materials-A contradiction in terms?, *Angew. Chemie - Int. Ed.*, 2012, **51**, 11942–11944.

107 D. Y. Zhu, M. Z. Rong and M. Q. Zhang. Self-healing polymeric materials based on microencapsulated healing agents: From design to preparation, *Prog. Polym. Sci.*, 2015, **49**–**50**, 175–220.

108 J. A. Syrett, G. Mantovani, W. R. S. Barton, D. Price and D. M. Haddleton. Self-healing polymers prepared via living radical polymerisation, *Polym. Chem.*, 2010, **1**, 102–106.

109 J. Pignanelli, B. Billet, M. Straeten, M. Prado, K. Schlingman, M. J. Ahamed and S. Rondeau-Gagné. Imine and metal–ligand dynamic bonds in soft polymers for autonomous self-healing capacitive-based pressure sensors, *Soft Matter*, 2019, **15**, 7654–7662.

110 Y. L. Rao, V. Feig, X. Gu, G. J. Nathan Wang and Z. Bao. The effects of counter anions on the dynamic mechanical response in polymer networks crosslinked by metal–ligand coordination, *J. Polym. Sci. Part A Polym. Chem.*, 2017, **55**, 3110–3116.

111 S. Bode, M. Enke, R. K. Bose, F. H. Schacher, S. J. Garcia, S. van der Zwaag, M. D. Hager and U. S. Schubert. Correlation between scratch healing and rheological behavior for terpyridine complex based metallopolymers, *J. Mater. Chem. A*, 2015, **3**, 22145–22153.

112 J. M. Sirrine, S. A. Schexnayder, J. M. Dennis and T. E. Long. Urea as a monomer for isocyanate-free synthesis of segmented poly(dimethyl siloxane) polyureas, *Polymer (Guildf).*, 2018, **154**, 225–232.

113 D. D. Zhang, Y. B. Ruan, B. Q. Zhang, X. Qiao, G. Deng, Y. Chen and C. Y. Liu. A self-

healing PDMS elastomer based on acylhydrazone groups and the role of hydrogen bonds, *Polymer (Guildf).*, 2017, **120**, 189–196.

114 B. Zhang, P. Zhang, H. Zhang, C. Yan, Z. Zheng, B. Wu and Y. Yu. A Transparent, Highly Stretchable, Autonomous Self-Healing Poly(dimethyl siloxane) Elastomer, *Macromol. Rapid Commun.*, 2017, **38**, 1–9.

115 L. Liu, S. Liang, Y. Huang, C. Hu and J. Yang. A stretchable polysiloxane elastomer with self-healing capacity at room temperature and solvatochromic properties, *Chem. Commun.*, 2017, **53**, 12088–12091.

116 F. García, J. Pelss, H. Zuilhof and M. M. J. Smulders. Multi-responsive coordination polymers utilising metal-stabilised, dynamic covalent imine bonds, *Chem. Commun.*, 2016, **52**, 9059–9062.

117 H. Liu, H. Zhang, H. Wang, X. Huang, G. Huang and J. Wu. Weldable, malleable and programmable epoxy vitrimers with high mechanical properties and water insensitivity, *Chem. Eng. J.*, 2019, **368**, 61–70.

118 A. F. Wells. Structural Inorganic Chemistry, 5th Edition, Clarendon Press, Oxford, 1984, p. 1288Structural Inorganic Chemistry, 5th Edition.

119 R. D. Shannon. Revised Effective Ionic Radii and Systematic Studies of Interatomie Distances in Halides and Chalcogenides, *Acta Crystallogr.*, 1976, **A32**, 751–767.

120 J. Cui, F. M. Nie, J. X. Yang, L. Pan, Z. Ma and Y. S. Li. Novel imidazolium-based poly(ionic liquid)s with different counterions for self-healing, *J. Mater. Chem. A*, 2017, **5**, 25220–25229.

121 J. Pignanelli, K. Schlingman, T. B. Carmichael, S. Rondeau-Gagné and M. J. Ahamed. A Comparative Analysis of Capacitive-Based Flexible PDMS Pressure Sensors, *Sensors Actuators A. Phys.*, 2019, **285**, 427–436.

122 Y. Wang, J. He, S. Aktas, S. A. Sukhishvili and D. M. Kalyon. Rheological behavior and self-healing of hydrogen-bonded complexes of a triblock Pluronic® copolymer with a weak polyacid, *J. Rheol. (N. Y. N. Y).*, 2017, **61**, 1103–1119.

123 E. Archives. Engineering Archives, Engineering Archives, http://www.engineeringarchives.com/img/les_mom_necking_1.png.

124 Malvern Instruments Worldwide. Malvern Instruments White Paper - A Basic Introduction to Rheology Shear Flow, 2016, 1–20.

CHAPTER 2. Experimental Procedure and Characterization Methods

2.1 Materials

Commercial reactants were used without further purification unless stated otherwise. All the solvents used in these reactions were distilled prior to use. Aminopropyl-terminated polydimethylsiloxane with molecular weight of 1000 Da, and dispersity of 1.33 was purchased from Gelest (Pennsylvania, USA). Pyridine-2-carboxaldehyde and Iron (II) tetrafluoroborate hexahydrate, Cobalt (II) tetrafluoroborate hexahydrate, Zinc tetrafluoroborate hydrate, Zinc trifluoromethanesulfonate and Zinc perchlorate hexahydrate were purchased from Sigma-Aldrich and used as received.

2.2 Experimental Procedure

Pre-polymer 1. A round bottom flask equipped with a magnetic stir bar was charged with aminopropyl-terminated PDMS (20 g, 0.020 mol), pyrimidine-2-carboxaldehyde (4.28 g, 0.042 mol) and $CHCl_3$ (20 mL). The reaction was left stirring for 48 hours at room temperature and CH_3Cl was removed under reduced pressure. The resulting materials was diluted in hexanes and was extracted with MeCN to remove unreacted monomer and dried under vacuum to afford pre-polymer 1 (P1) as a viscous thick oil. ^{1}H NMR (300MHz, $CDCl_3$, 298 K): 8.62 (d, J= 4.2 Hz, 2H), 8.35 (s, 2H), 7.98 (dd, 7.8 Hz, 2H), 7.72 (t, 2H), 7.29 (t, J= 15.3 , 2H), 3.67 (t, J= 14.1, 4H), 2.29 (m, 12H), 1.79 (m, 4H), 0.584 (t, 7.5 Hz, 4H) is reported in Figure A1. Molecular weight estimated from high temperature GPC (1,2,4-trichlorobenzene, 200°C): M_n = 839 Da, M_w = 2286 Da, PDI = 2.737.

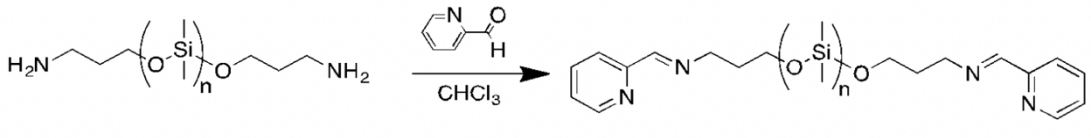

Pre-polymer 1, n = 20,30

Figure 2. 1. Synthetic scheme of pre-polymer 1.

Metal-Ligand Cross linking. In order to prepare crossed liked samples, pre-polymer (P1) was solubilized in dichloromethane, filtered on 0.45 μm filter, crosslinked with either $Fe(BF_4)_2$, $Co(BF_4)_2$, $Zn(BF_4)_2$, $Zn(ClO_4)_2$ or $Zn(OTf)_2$ salts dissolved in a minimal amount of methanol.

Solutions were left stiring for 30 minutes at room temperature prior to sample preparation.

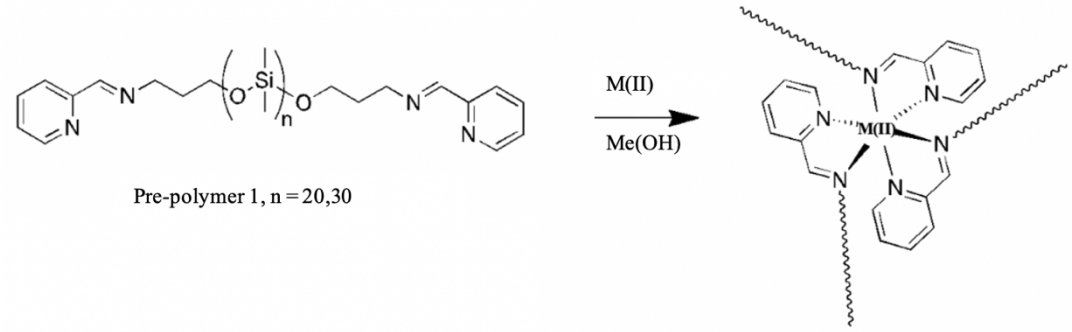

Figure 2. 2. Synthetic scheme for chemical cross linking of P1 where M(II) is either Fe(II), Co(II) or Zn(II) metal salts.

2.3 Sample Preparation

2.3.1 Self-healing dielectric for a self-healing capacitive pressure sensor

Once the pre-polymer was solubilized in dichloromethane, filtered on a 0.45 µm filter and crosslinked with Fe(II), it was casted into 3-cavities PTFE mold with cavity dimensions of 37.6mm L x 13.8mm W x 3mm D (Ted Pella). Once a gel was formed, the samples were placed in a vacuum oven at 50 °C and left to dry for 48 hours. Structuring of the dielectrics was performed by using an inverse PDMS-based mold prepared from commercially-available safety tape ribbons following a previously reported procedure.[1,2] The mold was cured with UV-ozone for 5 minutes and was used as a stamp to produce the nanostructure on the desired materials. The polymer was then left for 24 hours in vacuum at 50 °C to dry. Once dried, the sample was slowly peeled off and directly used for the fabrication of the devices.

2.3.2 Preparation of model imine compounds

The synthesis of the (*E*)-*N*-butyl-1-(pyridin-2-yl)methanimine has been performed according to a previously reported procedure.[3] Following its preparation, the compound (1 eq.) was reacted with 6-aminohexan-1-ol (1.2 eq.) in tetrahydrofuran (2 M). The reaction mixture was stirred for 72 h at 30 °C. The product was used without any further purification for LC-MS analysis.

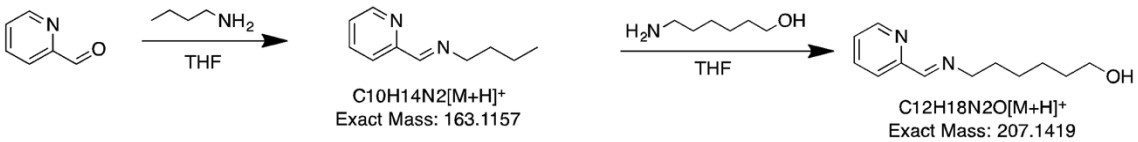

2.3.3. Sample preparation for comparison of various metal salts as cross-linking agents

Pre-polymer **P1** was solubilized in dichloromethane, filtered on 0.45 μm filter, crosslinked with either $Fe(BF_4)_2$, $Co(BF_4)_2$, $Zn(BF_4)_2$, $Zn(ClO_4)_2$ or $Zn(OTf)_2$. The resulting materials was casted into custom-made dog-bone shaped PTFE mold with dimensions in accordance to the ASTM standard for thermoplastic elastomers (ASTM D412). Once a gel was formed, the samples were placed in a vacuum oven at 50 °C and left to dry for 48 hours. Once dried, the sample was slowly peeled off and used directly for further characterizations.

2.4 Measurements and Characterization

Nuclear magnetic resonance (NMR) spectra were recorded on a Bruker 300 MHz spectrometer. The viscous oil of pre-polymer 1 (P1) was dissolved in deuterated chloroform ($CDCl_3$) at room temperature. Chemical shifts are given in parts per million (ppm). Number average molecular weight (M_n), weight average molecular weight (M_w) and polydispersity index (PDI) were evaluated by high temperature size exclusion chromatography (SEC) using 1,2,4-trichlorobenzene. UV-Visible spectroscopy was performed on a Varian UV/Visible Cary 50 spectrophotometer. The surface structure of polymer film was obtained using a Multimode atomic force microscope (AFM, Digital Instruments) operated in the tapping mode at room temperature. Images were collected using Nanoscope 6 software and processed using WSxM 5.0 Develop 8.0 software. FTIR spectroscopy was performed on a Bruker ALPHA FTIR Spectrometer using a Platinum ATR sampling module. Calorimetric studies were conducted on a TA instruments DSC2500 and thermal gravimetric analysis was performed on a TA instruments TGA5500. Nitrogen (99.999%) was used to purge the systems at a flow rate of 60 mL/min. All samples were run in aluminum crucibles. TGA samples were held at 25 °C for 30 min before heated to 500 °C at a rate of 10 °C/min. An Agilent E4980A 2MHz Precision LCR meter was used for capacitance measurements.

2.4.1 Evans method for determining effective magnetic moment

A previously reported procedure was followed.[4] Briefly, samples of known concentration (0.9 mM) were prepared. An NMR tube made of concentric tubes was filled with pure solvent ($CDCl_3$, inner tube) and sample (outer tube). The magnetic susceptibility ($\chi mass$) was determined by using the formula $\chi mass = 3\Delta f/4\pi fm + \chi 0 + \chi 0(d0- ds)/m$, where $\chi mass$ is mass susceptibility (cm^3g^{-1}), Δf is the observed frequency difference (Hz), f is spectrometer frequency (Hz), m is the mass of paramagnetic substance ($g \cdot cm^{-3}$), χ_0 is the mass susceptibility of solvent (cm^3g^{-1}), d_0 is the density of solvent ($g \cdot cm^{-3}$), and d_s is the density of solution ($g \cdot cm^{-3}$). The magnetic susceptibility

was further converted to the effective magnetic moment (μ_{eff}) following a previously reported procedure. [4]

2.4.2. Evaluation of self-healing properties for capacitive pressure sensor dielectric layer

Self-healing was evaluated by tensile strain analysis as well as by device signal sensitivity before and after healing. For the tensile strain analysis, a flat molded sample was simply cut in half with a blade, pressed back together and left to heal for 24 or 48 hours before being characterized. Tensile-strain analysis was performed on an Instron Tensile Strain instrument with a test rate of 100 mm/min. Self-healing ability of the pressure sensing devices was characterized by testing the device before and after a healing period of 48 hours. For evaluation of the self-healing properties by atomic force microscopy, a sample was frozen in liquid nitrogen and carefully cut with a scalpel. The films analyzed were spin coated on a cleaned glass substrate, at 2000 rpm for 1 min. It is important to mention that several attempts were required to make a cut small enough to properly self-heal, but large enough that the full capability of the material is demonstrated. The cut sample was then left on the AFM stage on day 0 and measured after 24, 48 and 72 hours.

2.4.3. Evaluation of self-healing properties for comparison of samples cross-liked with different metal salts

Self-healing was evaluated by using a flat molded sample which was cut in half with a blade, pressed back together and left to heal for 2 hours before being characterized. Tensile-strain analysis was performed on an Instron Tensile Strain instrument with a test rate of 5 mm/min.

2.4.4. Evaluation of degradability

A small piece of the self-healing material was characterized in terms of degradability by placing a solid piece of the polymer in solution with ~ 1 M acetic acid and left to stir until fully dissolved (2 days). The resulting solution was then directly characterized without further treatments.

2.4.5. Capacitive Pressure Sensor Device Fabrication and Characterization

The structured dielectric used as the middle layer of the capacitive devices was prepared from the P1 polymer cross linked with $Fe(BF_4)_2$ in DCM solution through a previously reported method.[2] Capacitive Pressure Sensor Devices were fabricated by lamination of the structured dielectrics (self-healing polymer) with copper tape. Note that an overhanging end was left to be connected and

tested using Agilent E4980A 2MHz Precision LCR meter for capacitance measurements. Sensors were tested using Agilent E4980A 2MHz Precision LCR meter for capacitance measurements. Sensitivity upon pressure was evaluated using a home-made force linear actuator and force sensor connected to the device. The range of pressure evaluated was from 0 to 32 kPa. The devices were tested at various pressures within this range in order to construct a sensitivity curve. Stretched samples were subjected to 30% strain for 100 cycles using a custom-built stretching station. Healed samples were cut in half with a blade and pressed back together for intrinsic self-healing before being used as a dielectric.

2.4.5 Atomic Force Microscopy

Atomic Force Microscopy (AFM) has become a valuable tool in materials chemistry due to its high resolution at the nanometer scale allowing for the characterization of material topography.[5] (AFM nanoindentation to determine Young's modulus for different EPDM elastomers) AFM works by using a sharp cantilever tip that scans over a sample mounted on a piezo Chrystal. Changes that result in the Z direction (height) are due to the interaction of the tip with the substrate allowing for a topographical image to be formulated. The forces between the tip and surface allows for a 3D profile to be formed. The various modes used for AFM are dependent on the tips motion which is monitored using a laser beam which reflects off the cantilever tip and collected by a photodetector for image formation (Figure 2.1). [87]

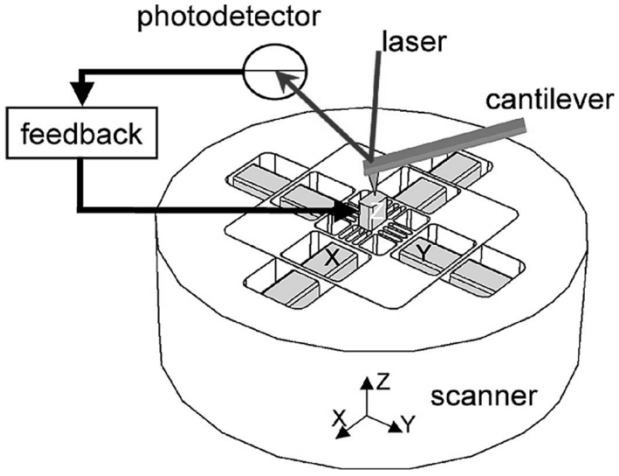

Figure 2.3. AFM Scanner Set up. [87]

2.4.6. UV-Vis spectroscopy

Ultraviolet-visible spectroscopy is a powerful tool used for quantitative, analytical chemistry to determine presence of various transition metal ions, conjugation of organic molecules and

biological molecules within assays. In principle, UV-Vis works by exciting the bonding and non-bonding electrons with a source wavelength and comparing the intensity of light before and after collecting the sample to determine the absorbance at a particular wavelength of energy.

The absorbance of a particular wavelength is dependent on the bonding and non-bonding electrons present in the molecule of interest. The lower the energy gap between the high energy occupied molecular orbital (HOMO) and lower energy unoccupied molecular orbital (LUMO) energy bands, the easier it is to excite these electrons at lower energy or longer wavelengths. The possible transitions from lowest energy to highest energy gap includes: n–π*, π–π*, n–σ*and σ–σ* The absorbance of a solution is directly related to the concentration of the of the absorbing molecule according to the Beer-Labert law. Therefore, a UV-Vis spectrophotometer is useful to determine molecular interactions as well as a quantitative tool for determining concentration of a particular molecule of interest.

In particular, metal-ligand interactions are often characterized through UV-Vis spectroscopy. [6,7] When a metal-ligand complex is formed, the electronic transitions that result from the interaction leads to a unique spectrum that illustrates the various transitions present in the system. Transition metals form stable ions with incompletely filled d orbitals which create a repelling force when bounded to the electrons of a ligand. As a result, there is an increase in the energy of the d orbitals with a splitting between the 5 d orbitals. The energy absorbed is equal to the energy gap between the splitting of the 5 d orbitals. This energy varies based on the transition metal complexed as well as the nature of the ligands used. The charge transfer process also absorbs energy as a result of the electron transfer from the Highest Occupied Molecular Orbital (HOMO) of one species to the Lowest Unoccupied Molecular Orbital (LUMO) of another. From this information, Ligand to Metal Charge Transfer (LMCT) and Metal to Ligand Charge (MLTC) bands are created in the UV-Vis spectrum. As a result, upon titration of a transition metal to a ligand solution, characteristic charge transfer bands allow for identification of the chemical interactions present.[6,7] Therefore, UV-vis is a powerful tool used to characterize the presence of metal ligand coordination.

2.4.7. Tensile Strain Analysis

Tensile testing works by applying an increasing load to a test sample until the point of failure. An extensometer measures the displacement of the sample in response to the strain rate applied throughout the tensile test. As a result a stress/strain curve is created allowing for the mechanical characterization of a material to be determined. The sample is loaded onto top and bottom grips attached to the universal testing machine, which are moved apart at a constant rate to create a strain, or elongation of the sample. The force on the sample and the resulting displacement of the grips are continuously collected as a function of time which allows for the construction of a stress-strain curve until the point of failure. After these data are collected, the tensile strength or Young's modulus, yield strength and ductility can be determined. The tensile strength is calculated by the slope of the linear region of the stress-strain curve to the point of maximum stress. The yield strength corresponds to the stress at which the material reaches permanent deformation, or no longer behaves elastically. The ductility is determined as the strain at which the material failure occurs. [8]

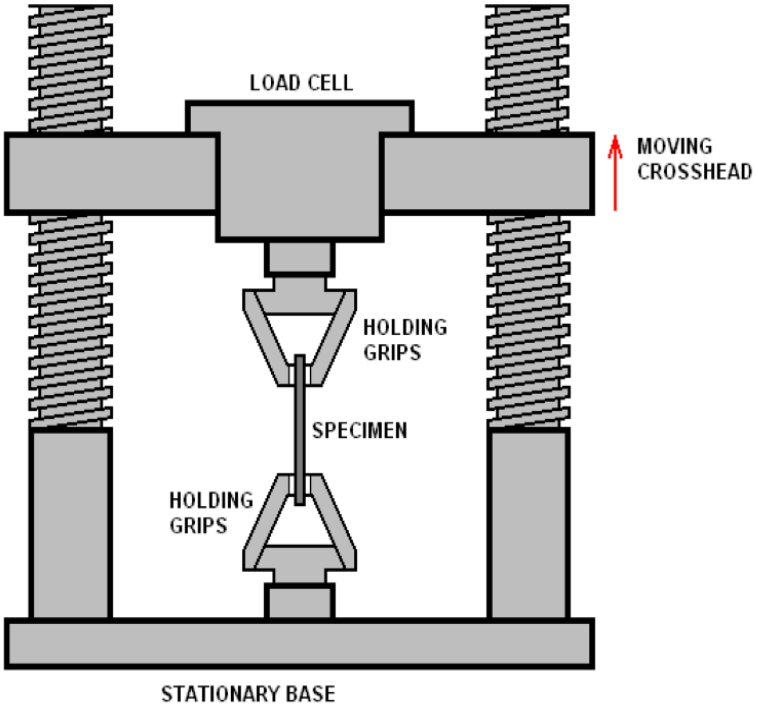

Figure 2.4. Schematic of a tensile strain test. [123]

2.4.8. Shear Rheology

Shear rheology is an experimental technique used to examine the flow and deformation of materials upon subjection to a shear force. Rheometers are used to create a shear force, where a sample is subjected to a torque and the resulting rotational speed is collected to maintain the force or vice versa. A schematic of a single head rotational rheometer measuring system is illustrated in Figure 2.3.

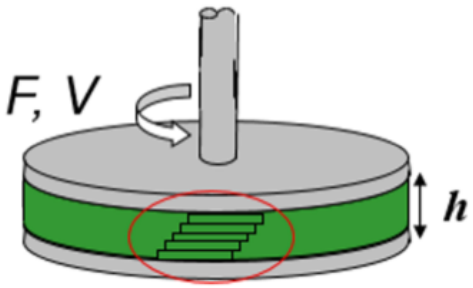

Figure 2.5. Illustration of a parallel plate rheometer. [124]

Advanced Rheometric Expansion System (ARES) is a strain-controlled instrument where the stress is measured on a sample as strain is applied. The shear strain applied through a motor to the top plate in a sinusoidal or constant frequency, and then the torque that is experienced by the sample of interest is measured by a transducer. The amplitude and frequency of the strain applied by the motor are controlled by the operator, and the sample deformation or torque, is determined by the motor and transducer displacement with a known height (h) between plates. Oscillatory time sweeps provide information about a materials ability to change in response to applied strain which results in macro or microstructural rearrangements in response to shear strain. The ratio of applied strain to the measured stress gives a quantitative measure of a materials stiffness based on its resistance to deformation. From this information, an oscillatory time sweep allows for determination of the viscoelasticity of a material. Pure elastic materials reach maximum stress directly in phase with the maximum strain. Viscous materials experience maximum stress when the strain is out of phase by 90 degrees at a maximum. Therefore, a viscoelastic material will have a phase difference between stress and strain in between being in and out of phase. The phase angel is used as a relative measure of the materials viscous and elastic characteristics. The elastic contribution (G') is the storage modulus, where energy is stored and the viscous contribution (G")

is the loss modulus, which represents energy lost by the system upon shear strain applied to the sample. Together the G' and G" sum to represent the material stiffness (G*).

2.5. REFERENCES

1 B. Grzybowski, D. Qin, R. Haag and G. M. Whitesides. Elastomeric optical elements with deformable surface topographies: Applications to force measurements, tunable light transmission and light focusing, *Sensors Actuators, A Phys.*, 2000, **86**, 81–85.

2 J. Pignanelli, K. Schlingman, T. B. Carmichael, S. Rondeau-Gagné and M. J. Ahamed. A Comparative Analysis of Capacitive-Based Flexible PDMS Pressure Sensors, *Sensors Actuators A. Phys.*, 2019, **285**, 427–436.

3 M. Zeng, L. Li and S. B. Herzon. A highly active and air-stable ruthenium complex for the ambient temperature anti-markovnikov reductive hydration of terminal alkynes, *J. Am. Chem. Soc.*, 2014, **136**, 7058–7067.

4 D. F. Evans. The Determination of the Paramagnetic Susceptibility of Substances in Solution by Nuclear Magnetic Resonance, *J. Chem. Soc.*, 1959, 2003–2005.

5 R. Ferencz, J. Sanchez, B. Blümich and W. Herrmann. AFM nanoindentation to determine Young's modulus for different EPDM elastomers, *Polym. Test.*, 2012, **31**, 425–432.

6 S. Schmatloch, M. F. González and U. S. Schubert. Metallo-supramolecular diethylene glycol: Water-soluble reversible polymers, *Macromol. Rapid Commun.*, 2002, **23**, 957–961.

7 Y. L. Rao, A. Chortos, R. Pfattner, F. Lissel, Y. C. Chiu, V. Feig, J. Xu, T. Kurosawa, X. Gu, C. Wang, M. He, J. W. Chung and Z. Bao. Stretchable self-healing polymeric dielectrics cross-linked through metal-ligand coordination, *J. Am. Chem. Soc.*, 2016, **138**, 6020–6027.

8 J. Pelleg. Mechanical properties of materials, *Mechanical properties of materials*, 2013, vol. 190.

9 E. Archives. Engineering Archives, Engineering Archives, http://www.engineeringarchives.com/img/les_mom_necking_1.png.

10 Malvern Instruments Worldwide. Malvern Instruments White Paper - A Basic Introduction to Rheology Shear Flow, 2016, 1–20.

CHAPTER 3. IMINE AND METAL-LIGAND DYNAMIC BONDS IN SOFT POLYMERS FOR AUTONOMOUS SELF-HEALING CAPACITIVE-BASED PRESSURE SENSORS

3.1 Introduction

Self-healing is an interesting property, inspired from the natural healing in living organisms, that can be synthetically enabled in a wide variety of materials.[1,2] Best described as the ability of a specific material to regenerate itself upon damage (mechanical, thermal or chemical), self-healing can occur through different strategies/mechanisms and with/without the need for an external trigger.[3,4] Self-healing has shown important promise for enhancing the durability and robustness of materials for various applications including healthcare, structural and biomedical engineering, advanced manufacturing and electronics.[5–7] Therefore, research in self-healing materials has significantly intensified in the last decade with the design and preparation of a wide variety of new materials capable of regenerating themselves upon damage.[8–10]

In recent years, a wide variety of strategies have been designed and used to enable self-healing in materials. Among others, the use of healing agents uniformly dispersed in an elastomeric matrix is one of the most common and efficient method to trigger self-healing upon mechanical stress.[11,12] Another promising strategy relies on the rational design of self-healing materials through the use of chemical bonds capable of fission/recombination upon damage.[13] This strategy, based on the dynamic crosslinking of polymers, has the advantage of being intrinsic, i.e. no external agent required for the regeneration.[14] However, depending on the chemistry used, an external trigger (photoirradiation, thermal annealing, solvent annealing, etc.) can be necessary.[15,16] For example, to point out only a few, the use of dynamic imine bonds,[17] metal coordination with ligand moieties,[18–20] hydrogen bonds,[21,22] and disulfide bonds have been shown to lead to an efficient self-healing.[23] In the field of electronics, the application of self-healing materials through dynamic bonds has led to the fabrication of multiple devices, including pressure sensors,[24] strain sensors,[25,26] and thin-film transistors.[27,28] A variety of self-healable conductors,[29,30] semiconductors,[31,32] and dielectrics materials have also been developed to access self-healing electronics.[33,34] However, despite the promises of self-healing materials, their large-scale use and application is still challenging. First, the need for an external trigger to enable the self-healing can limit the application of the materials and can be a significant drawback.[35] Moreover, with the current environmental crisis created by non-degradable plastics, the application of materials that can regenerate themselves and be more robust might not help to reduce the environmental burden.[36] Finally, the large-scale preparation of the materials can be costly, especially when expensive reactant or healing agents are required.

Therefore, the development of inexpensive, degradable and autonomous self-healing materials is critical.

Herein, we report the facile synthesis of novel silicone-based materials specifically designed to include a unique combination of dynamic imine and metal-coordination bonds. Through an easy condensation reaction, imine bonds are generated at the end-termini of a short siloxane chain. The resulting end-capped materials was chemically crosslinked with different ratios of a Fe(II)-based salt to achieve a dynamically crosslinked network. By controlling the ratio of metal crosslinker utilized, the dynamic materials and new crosslinking system were shown to be highly tunable, leading to materials with ultra-high stretchability (800% strain elongation), autonomous self-healing (24 hours at room temperature), and degradability in mild acidic conditions. The new materials have been characterized chemically and mechanically before and after healing, and after degradation through a combination of techniques, including UV-Vis and infrared spectroscopy (FTIR), nuclear magnetic resonance (NMR), size-exclusion chromatography (SEC), and tensile-pull strain testing. Furthermore, the resulting self-healing polymer has been utilized to fabricate highly sensitive and self-healable capacitive pressure sensors, capable of regenerating electrical and mechanical properties after damage. The method and results presented in this work open new opportunities for the large-scale synthesis of autonomous self-healing materials in a cost-effective manner, without requiring expensive or external healing agents as well as without impacting the long-term environmental sustainability.

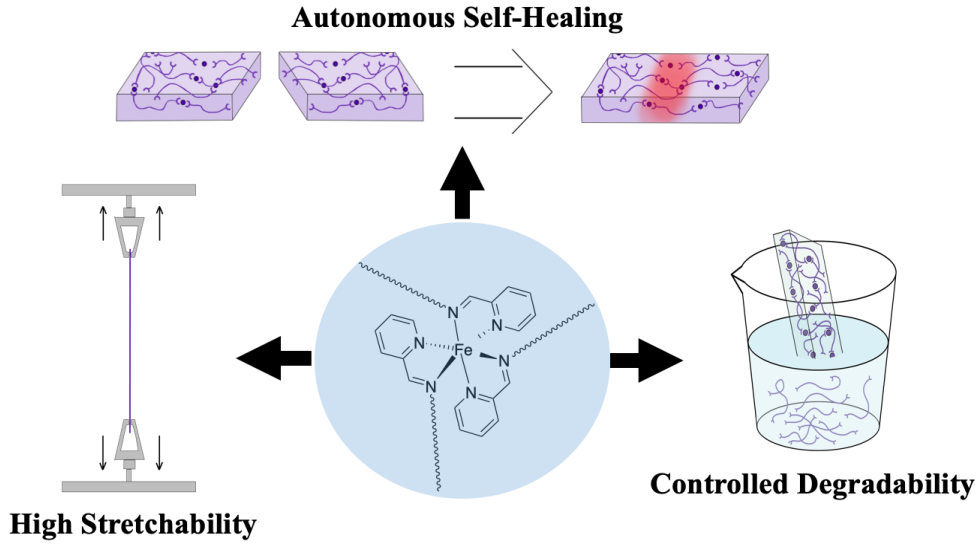

Figure 3.1. General approach to stretchable, self-healing and degradable materials through a combination of imine and metal-coordinating bonds.

3.2 Results and Discussion

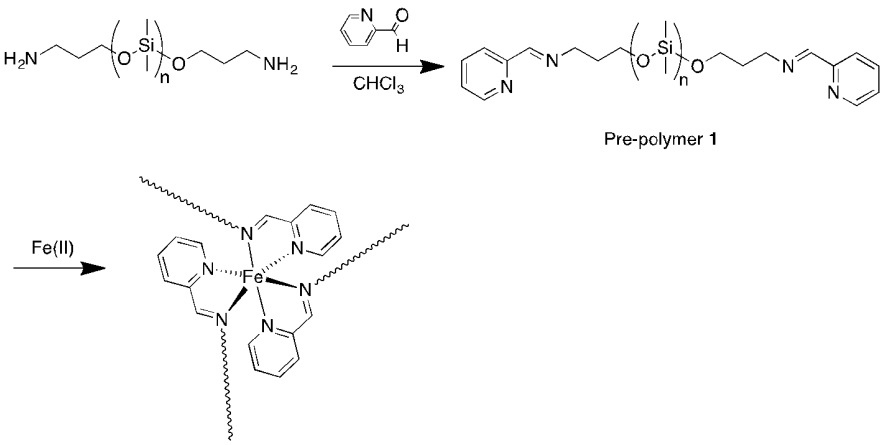

Scheme 3.1. Synthesis of pre-polymer 1 followed by chemical crosslinking with Fe(II)-based salts.

The synthesis of the new self-healing polymer is depicted in Scheme 1. Starting from commercially-available aminopropyl-terminated polydimethylsiloxane, a condensation reaction is performed with 2-pyridinecarboxaldehyde to generate pre-polymer 1. Pre-polymer 1 (1000 Da) was directly used without further purification in a crosslinking reaction with a Fe(II)-based salt. In this study, Fe(II) tetrafluoroborate was used. Interestingly, as soon as the salt is added, the pre-polymer immediately gelified and turned purple, which is typical for the formation of a Fe(II) coordination complex.[39–41] To confirm the presence of Fe(II) in the materials, the materials' effective magnetic moment (μeff) was determined by nuclear magnetic resonance (NMR) in solution, using Evans method (see Supporting Information).[42,43] The crosslinked materials was found to have a μeff = 3.08 μb, which is a value that can be assigned to a high-spin Fe(II) complex.[44]

From a design point of view, a system combining dynamic imine and metal-ligand bonds has been selected for multiple reasons. First, the generation of the pre-polymer does not require any heating or catalyst, and all the initial precursors are commercially available (cost below $0.5 per gram). Furthermore, both imine and metal-coordinating bonds have been shown to be highly dynamic, and typically lead to good self-healing properties in elastomeric materials.[45–47] Therefore, the combination of both types of bonds can enable the formation of a very dynamic system, ideal for self-healing and stretchability. Finally, imine bonds are known to undergo reverse condensation in mild conditions, which is particularly interesting to trigger a controlled degradation of the materials.[48]

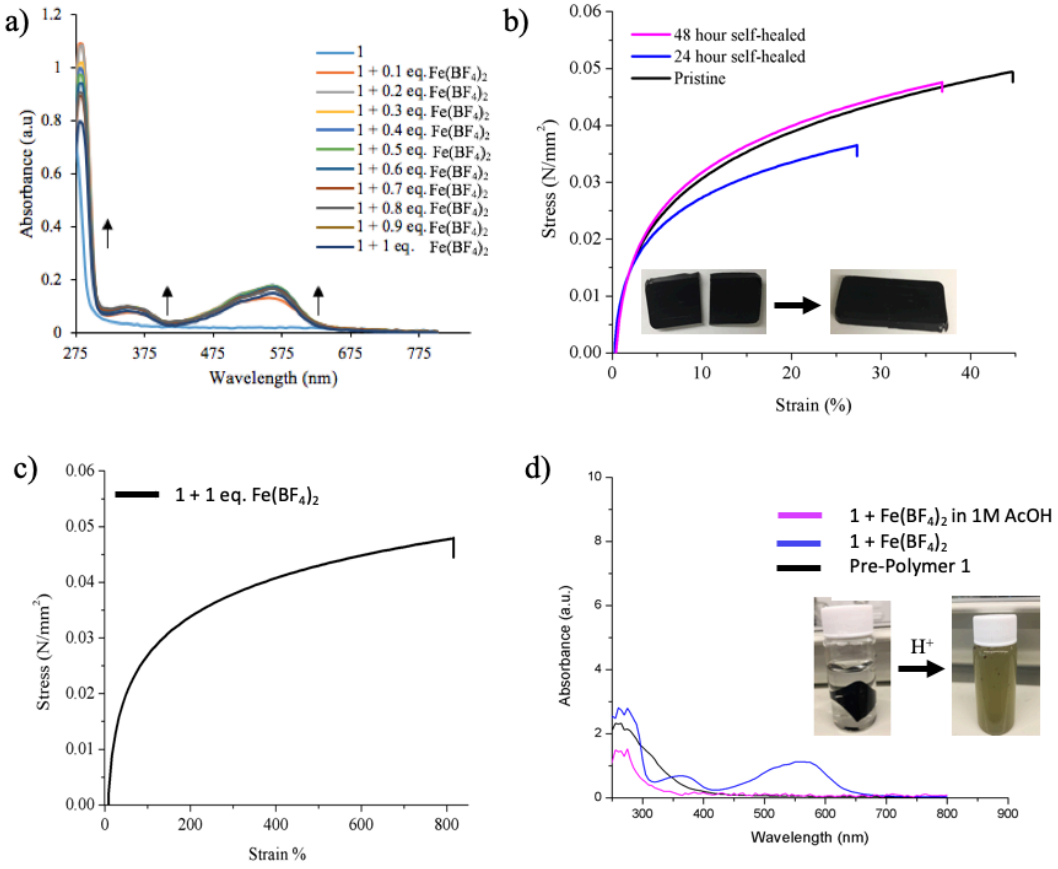

Figure 3.2. a) UV-vis absorption spectra of pre-polymer 1 in $CHCl_3$ upon titration with 0.1 equivalent increments of $Fe(BF_4)_2$ per polymer chain ; b) stress-strain curves of pre-polymer 1 crosslinked with 0.25 equivalent of $Fe(BF_4)_2$ before and after self-healing for 2.

To optically probe for the formation of a metal-coordination complex between the N-ligand generated after condensation reaction and Fe(II), UV-vis spectroscopy was utilized and the results are summarized in Figure 2a. To confirm the formation of the complex, a solution of pre-polymer 1 was prepared and increments of 0.1 equivalent of a stock solution of Fe(BF4)2 were added up to two equivalents to ensure saturation of the coordination sites. As typically observed for Fe complexes with other N-ligands (bipyridine, triazoles, etc.), strong absorption bands appeared progressively at 350, 575 and 650 nm.[49] These bands can be directly attributed to the formation of the Fe coordination complex in the materials, which is crosslinking the short oligomeric chains into a rigid polymer network.[39,50,51] Further characterization of the crosslinked materials by Fourier-Transform IR spectroscopy (FTIR) (Figure S1) and solution NMR showed very minor differences in the system before and after coordination, which can be attributed to the relatively low signal from the metal-ligand complex compared to the siloxane-based polymeric backbone. Interestingly,

^{19}F NMR analysis performed on the crosslinked materials shown the presence of only one signal (singlet) associated to fluorine (Supporting Information). This result potentially indicates that the tetrafluoroborate counter-ion remained close to the coordination complex. As shown on Figure 2a, the pre-polymer 1 almost immediately form a dense gel upon the addition of the metal salt, and completely becomes solid after 24 hours under a vacuum oven at 50 °C. As detailed in Figure S2 and S3, energy-dispersive x-ray spectroscopy (EDX) and atomic force microscopy (AFM) images recorded on the crosslinked materials shown a uniform morphology, without metallic cluster or aggregate. It is also important to mention that no glass transition temperature was observed by dynamic scanning calorimetry (DSC) below -50°C, which can be observed for other PDMS-based materials.[34]

Elastic modulus and tensile resistance are two critical parameters that can be used to assess the mechanical properties of soft materials. Therefore, tensile-pull testing was performed on free-standing films of crosslinked polymers before and after healing. Results are summarized in Figure 2b. First, the bulk mechanical properties were investigated for pre-polymer 1 crosslinked with 0.25 equivalents of Fe, in order to excess the stoichiometric amount of ligand for the formation of an octahedral complex. Despite not being required to ensure a saturation of the thermomechanical properties, which should occur upon formation of the octahedral complexes, an excess of ligand was used to ensure a complete coordination of the Fe salt and avoid the presence of metallic cluster embedded in the materials, potentially negatively affecting the bulk stretchability and self-healing efficiency. Interestingly, the materials showed decent mechanical properties, with a maximum elongation before fracture at around 58 ±12 % (averaged on three samples). The difference in maximum elongation compared to other PDMS-based system can be attributed to a strong crosslinking between the short polymer chains upon adding Fe. A Young's modulus of 1.53 MPa was also measured directly from the tensile-pull testing results. The crosslinked materials was then cut in half with a blade and self-healed (room temperature) for 24 and 48 hours. Interestingly, the resulting self-healed materials were shown to regain 48 ± 3 % and 88 ± 7 % of their maximum elongation before fracture, after respectively 24 and 48 hours (averaged on three samples). As shown in Supporting Information, it is important to mention that no external stimuli or trigger was used to enable that self-healing. Moreover, a similar stretchability and self-healing properties were observed for pre-polymer 1 crosslinked with 0.33 equivalents of Fe (Figure S4). These results strongly suggest that the pyridine ligands of the PDMS backbone can dynamically re-coordinate with the Fe and therefore reform the mechanical nature of the material as the crosslinking density is able to regenerate autonomously as a function of time. To demonstrate the versatility of the new

dynamic crosslinking system, pre-polymer 1 was also crosslinked with 1 equivalent of Fe^{2+} to allow for a lower crosslinking density. As demonstrated in Figure 2c, the polymer crosslinked with 1 equivalent of metal shown ultra-high stretchability, and a more viscoelastic behavior, ultimately capable to be elongated up to 800% of its initial length without fracturing. The modulus of the resulting crosslinked materials was found to be 0.06 MPa, which is considerably lower than the crosslinked materials with higher amount of Fe ions. This result demonstrates that the crosslinking can be completely tuned by controlling the metal to ligand ratio, thus enabling the preparation of materials with a wide range of mechanical properties and elasticity.

AFM was also used to investigate the self-healing behaviour of the new crosslinked materials in thin films, and results are summarized on Figure S5. The films analyzed were spin coated on a cleaned glass substrate, frozen in liquid nitrogen and carefully cut with a scalpel to damage the surface. The cut samples were then left on the AFM stage on day 0 and measured after 24, 48 and 72 hours of self-healing. Since self-healing can only occur when the polymer chains are getting back in close proximity to regenerate the initial dynamic crosslinks, the amount of materials is critical. If the materials is too thin or the cut too large, one can expect that the self-healing will not be optimal given the absence of enough materials to fill the gap and regenerate the initial morphology. Interestingly, the nanoscale crack started to heal after 24 hours and was shown to be almost disappeared after 72 hours, which confirm the efficiency of the self-healing in thin films, even when the quantity of materials to fill up the damaged region is minimal and that the segmental polymer chain mobility is reduced.

As previously observed with other self-healing materials, both imine and metal-ligand bonds are known to be highly dynamic.[17,52–54] In order to get insight into the contribution of both dynamic bonds for the self-healing of the current materials, further analysis on a model compound was performed. Specifically, model compound (E)-N-butyl-1-(pyridin-2-yl)methanimine) was synthesized using previously reported procedure.[55] The compound was then reacted with 6-aminohexan-1-ol in order to probe through mass spectrometry for the formation of an exchange product through transimination. As shown in Figure S6, a characteristic peak associated to the formation of an exchange product was observed, which confirms the dynamic behavior of the imine bond through bond exchange.

With the ongoing environmental burden caused by the accumulation of non-degradable plastics and e-wastes, there is a growing interest in the design and synthesis of degradable functional materials to address the surge in demand for flexible electronics and sensors.[56,57] As

previously demonstrated in other types of materials, the incorporation of dynamic bonds to chemically crosslink shorter units is a very promising strategy to control and trigger the degradation of materials into shorter sub-units, non-damageable for the environment.[58,59] Since pre-polymer **1** was shown to efficiently crosslink upon adding metal salts and to generate a dynamic crosslinked network, the investigation of the degradability of the materials was performed in order to determine if the resulting materials could be broken down into smaller siloxane-based units through the hydrolysis of the imine dynamic bonds. Toward that objective, the crosslinked materials (0.33 equivalent of $Fe(BF_4)_2$) were submerged into an acidic aqueous solution (1M acetic acid) and the degradation reaction was probed by UV-Vis spectroscopy. Results are summarized in Figure 2d. It is important to mention that the mild acidic conditions were selected to match previous reports on the fabrication of transient electronics.[60,61] As previously observed, the formation of a metal-ligand coordination complex with Fe ions results in the appearance of two strong absorption bands centered at 360 and 545 nm. Upon stirring the materials in 1 M acetic acid aqueous solutions for 24 hours, the solid materials completely lost its characteristic purple color (typically associated with the formation of Fe complexes) and was slowly degraded until complete disappearance and formation of a resulting brown solutions (Figure 2d). This phenomenon was directly observed by UV-Vis, which showed the disappearance of the absorption bands attributed to the Fe complex and the return to the pre-polymer state. In order to probe for the degradability of the new materials under different conditions, a similar experiment was also performed in aqueous hydrochloric acid solutions with pH ranging from 1 to 6 (Figures S7 and S8). Similar to the results obtained with acetic acid, the self-healing polymer was completely degraded after 24 hours for pH= 1 to 3, confirmed by UV-Vis spectroscopy. For pH= 4 to 7, complete degradation of the crosslinked materials into smaller monomeric units was also observed after 72 hours. Upon degradation at each pH, an oil residue suspended in the aqueous solution was observed, which was further confirmed to be starting siloxane-based precursors. This simple experiment confirmed the possibility to control and activate the degradation of the new materials, thus enabling new opportunities for the design of degradable, yet robust, technologies. This property is particularly promising for the development of transient electronic materials and the possibility to completely degrade electronic devices.[60]

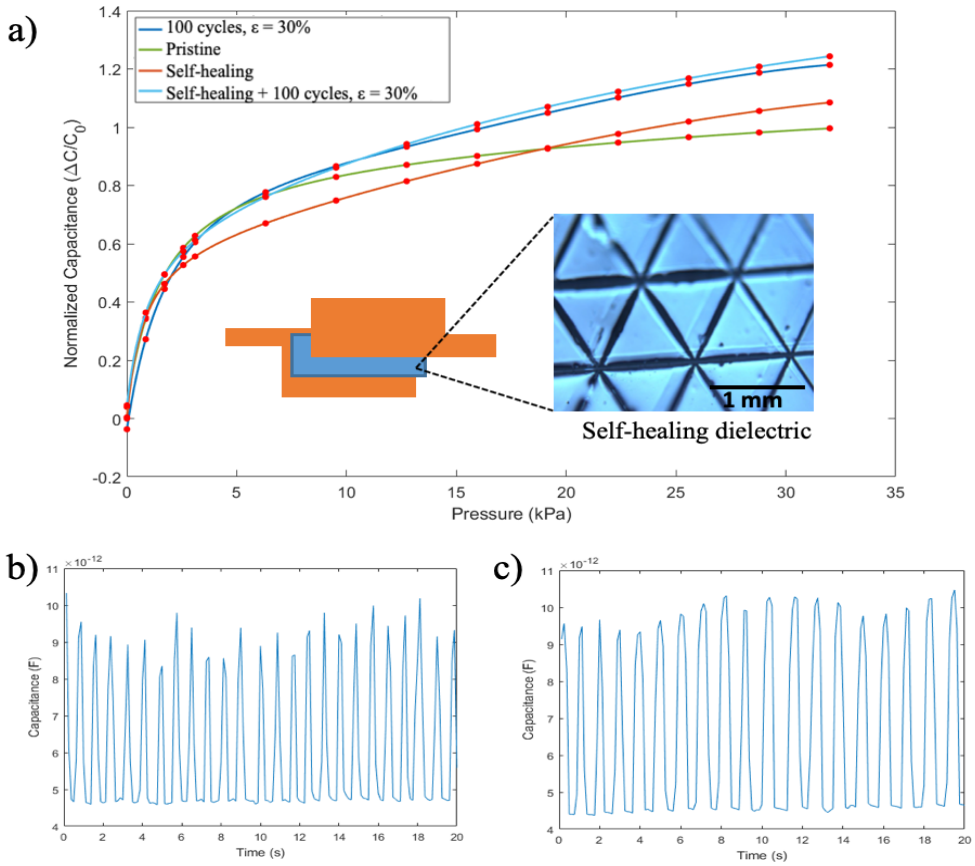

Figure 3.3. Normalized sensitivity curves for capacitance-based pressure sensor using self-healing polymer as dielectric layer. Sensors varied in terms of the conditions of dielectric materials; pristine, healed and stretched to 30% strain for 100 cycles. Optical microscope image shows the dielectric structuring and device design; dynamic sensor response of b) pristine and c) healed sensor, when subjected to simple repetitive finger tapping for a time range of 20 seconds

In order to demonstrate the application of the new autonomous self-healing of the siloxane-based materials, flexible and self-healable pressure sensors were fabricated, and results are summarized in Figure 3a. In order to determine the sensitivity of the capacitance-based pressure sensor, a force actuator was connected to a force meter to apply a range of pressures ranging from 0 to 32 kPa. Results were measured and averaged from three pressure sensor devices. Since device sensitivity to small variation of pressure relies on the deformation of the dielectric materials upon pressure, microstructuring of the dielectric self-healing materials (0.33 equivalent of $Fe(BF_4)_2$) was performed by following a method previously described (Figure S9).[37] These microstructures are important in increasing device sensitivity since they provide for multiple points along the device able to elastically respond to pressures applied.[38] Additionally, these structures provide for air gaps

that can be replaced by the dielectric material once compressed from pressure applied which in turn, increases the dielectric constant and capacitance signal recorded according to the following equation $C = \varepsilon_o\varepsilon_r S/\delta$ where is capacitance which is governed by the free-space permittivity ε_0, ε_r the relative permittivity and S and , the area of the conducting planes and the distance between them, respectively. In order to reassure that these materials are able to regenerate after fracture, each device was cut into half after initial pressure sensitivity measurements and allowed to heal over a 48-hour period in order to be retested. According to our results, the device maintained its mechanical and electrical properties to give approximately the same sensitivity (0.33 kPa^{-1}) over four trials where the samples were either pristine, strained 30% for 100 cycles, self-healed and self-healed followed by 30% strain for 100 cycles. The fact that the capacitive devices were able to maintain a good sensitivity after healing and 30% strain for 100 cycles confirmed the strong potential of the new tunable system for the design of wearable electronics human skin is typically known to experience a 30% strain elongation.[62,63] It is important to highlight the fact that these devices can self-heal after simply pressing the two halves back together and let rest at room temperature without any other external factors, which most previous works require. An average change in capacitance change versus average pressure applied curve was constructed in order to demonstrate the small standard deviation between the 4 devices with different test conditions (Figure S10). Dynamic sensor data was also collected to show the response ability of the sensor before versus after healing of the dielectric layer (Figure 3 b and c, respectively). A consistent finger tapping pressure was applied to the device for a 20-second interval. Data was collected every 100 ms. Interestingly, the sensor maintained a relatively constant response before and after healing, with the base capacitance varying from 4.5 to 5 pF and reaching 9.5 to 10 pF once the weight was placed. As shown in Table 1, the capacitive pressure sensors fabricated from the new self-healing polymeric system have a sensitivity comparable to devices prepared from more common elastomer and dielectric. However, the new system is entirely tunable, thus leading to a wide variety of properties, including self-healing, degradability and ultra-high stretchability. Moreover, the complexity of the system is reduced, as well as the cost of preparation, which is undoubtedly an important advantage for large-scale applications.

Table 3.1. Performance comparison of the new self-healing pressure sensors with previously reported devices.

Materials	Sensitivity	Healability	Degradability/ Stretchability	Ref.

Fe-crosslinked siloxane oligomers (this work)	0.33 kPa^{-1}	Autonomous	1M AcOH, ε = 800 %	-
Calcium carbonate, polyacrylic acid and alginate	0.17 kPa^{-1}	Autonomous	ε = 55 %	64
PDMS	1.0 kPa^{-1}	No	-	65
PDMS	0.28 kPa^{-1}	No	-	66
Polyurethane	1.9 kPa^{-1}	Non-autonomous	-	67

3.3. Conclusion

A new approach towards autonomously self-healing was developed through rational design of siloxane-based oligomers with imine and metal-coordination moieties. This unique combination of dynamic bonds was achieved by preparing soft polymers by a facile condensation reaction between amino-terminated siloxanes and pyridine carboxaldehyde. The resulting materials were crosslinked with Fe(II) salts, crosslinking that can be easily tuned by controlling the amount of metal used. Interestingly, the new polymer was shown to be ultra-highly stretchable when a 1:1 Fe/polymer ratio was used, reaching a maximum tensile strain before fracture of 800%. The samples prepared with 0.33 equivalents of Fe2+ showed autonomous intrinsic self-healing and were able to regenerate 88% of their initial mechanical properties after 48 hours without aid from any external stimuli. The materials were also shown to be entirely degraded into small oligomeric species in acidic conditions, thus opening the way for a controlled degradability. Since the new materials are particularly interesting as a component for self-healable electronics, the new polymer was used as a dielectric in self-healable capacitive-based pressure sensors. The dielectric was structured at the microscale to enhance device sensitivity in a pressure range of 0-32 kPa. The device was completely characterized before and after self-healing, and after multiple cycles of 30% strain conditions to investigate the performance of the self-healing dielectric. Our results demonstrate no significant deviation in terms of device sensitivity of the lower range of pressure applied (0-5 kPa), with a sensitivity of ~ 0.33 kPa-1. Additionally, the dynamic testing of our sensor

showed good response time and accuracy. Based on their low cost, high tunability and simple preparation, we believe this new dynamic polymer system will provide new opportunities for the creation of next-generation stretchable electronics that require improved material robustness, degradability, conformability and durability to improve lifespan and performance of electronics

3.4. REFERENCES

1 C. E. Diesendruck, N. R. Sottos, J. S. Moore and S. R. White, *Angew. Chem. Int. Ed.*, 2015, **54**, 2–22.

2 B. M. D. Hager, P. Greil, C. Leyens, S. Van Der Zwaag and U. S. Schubert, *Adv. Mater.*, 2010, 5424–5430.

3 D. Y. Wu, S. Meure and D. Solomon, *Prog. Polym. Sci.*, 2008, **33**, 479–522.

4 R. P. Wool, *Soft Matter*, 2008, **4**, 400.

5 J. Zhao, R. Xu, G. Luo, J. Wu and H. Xia, *Polym. Chem.*, 2016, **7**, 7278–7286.

6 Y. Zhao, W. Zhang, L. P. Liao, H. M. Wang and W. J. Li, *Phys. Procedia*, 2011, **18**, 216–221.

7 A. B. W. Brochu, S. L. Craig and W. M. Reichert, *J. Biomed. Mater. Res. - Part A*, 2011, **96**, 492–506.

8 K. Imato, M. Nishihara, T. Kanehara, Y. Amamoto, A. Takahara and H. Otsuka, *Angew. Chem. Int. Ed.*, 2012, **51**, 1138–1142.

9 T. F. O 'Connor, K. M. Rajan, A. D. Printz and D. J. Lipomi, *J. Mater. Chem. B*, 2015, **3**, 4947–4952.

10 Y. Yang and M. W. Urban, *Chem. Soc. Rev.*, 2013, **42**, 7446–67.

11 S. R. White, N. R. Sottos, P. H. Geubelle, J. S. Moore, M. R. Kessler, S. R. Sriram, E. N. Brown and S. Viswanathan, *Nature*, 2001, **409**, 794–797.

12 J. Yang, M. W. Keller, J. S. Moore, S. R. White, N. R. Sottos, J. Yang, M. W. Keller, J. S. Moore, S. R. White and N. R. Sottos, *Macromolecules*, 2008, **41**, 9650–9655.

13 F. Herbst, D. Döhler, P. Michael and W. H. Binder, *Macromol. Rapid Commun.*, 2013, **34**, 203–220.

14 Y. Heo, M. H. Malakooti and H. A. Sodano, *J. Mater. Chem. A*, 2016, **4**, 17403–17411.

15 D. Habault, H. Zhang and Y. Zhao, *Chem. Soc. Rev.*, 2013, **42**, 7244–7256.

16 A. Nasresfahani and P. M. Zelisko, *Polym. Chem.*, 2017, **8**, 2942–2952.

17 A. Chao, I. Negulescu and D. Zhang, *Macromolecules*, 2016, **49**, 6277–6284.

18 Z. Tang, J. Huang, B. Guo, L. Zhang and F. Liu, *Macromolecules*, 2016, **49**, 1781–1789.

19 N. Holten-Andersen, A. Jaishankar, M. J. Harrington, D. E. Fullenkamp, G. DiMarco, L. He, G. H. McKinley, P. B. Messersmith and K. Y. C. Lee, *J. Mater. Chem. B*, 2014, **2**, 2467.

20 J.-C. Lai, X.-Y. Jia, D.-P. Wang, Y.-B. Deng, P. Zheng, C.-H. Li, J.-L. Zuo and Z. Bao, *Nat. Commun.*, 1164–1173.

21 Y. Chen, A. M. Kushner, G. a. Williams and Z. Guan, *Nat. Chem.*, 2012, **4**, 467–472.

22 C. Wang, N. Liu, R. Allen, J. B. H. Tok, Y. Wu, F. Zhang, Y. Chen and Z. Bao, *Adv. Mater.*, 2013, **25**, 5785–5790.

23 M. Pepels, I. Filot, B. Klumperman and H. Goossens, *Polym. Chem.*, 2013, **4**, 4955.

24 J. Liu, C. S. Y. Tan, Z. Yu, N. Li, C. Abell and O. A. Scherman, *Adv. Mater.*, 2017, **29**, 1605325.

25 G. Cai, J. Wang, K. Qian, J. Chen, S. Li and P. S. Lee, *Adv. Sci.*, 2017, **4**, 1600190.

26 X. Liu, C. Lu, X. Wu and X. Zhang, *J. Mater. Chem. A*, 2017, **5**, 9824–9832.

27 W. Huang, K. Besar, Y. Zhang, S. Yang, G. Wiedman, Y. Liu, W. Guo, J. Song, K. Hemker, K. Hristova, I. J. Kymissis and H. E. Katz, *Adv. Funct. Mater.*, 2015, **25**, 3745–3755.

28 Y. J. Tan, J. Wu, H. Li and B. C. K. Tee, *ACS Appl. Mater. Interfaces*, 2018, **10**, 15331–15345.

29 S. Zhang and F. Cicoira, *Adv. Mater.*, 2017, 29, 1703098.

30 E. T. Thostenson and T. W. Chou, *Adv. Mater.*, 2006, **18**, 2837–2841.

31 M. U. Ocheje, M. Selivanova, S. Zhang, T. H. Van Nguyen, B. P. Charron, C.-H. Chuang, Y.-H. Cheng, B. Billet, S. Noori, Y.-C. Chiu, X. Gu and S. Rondeau-Gagné, *Polym. Chem.*, 2018, **9**, 5531.

32 J. Y. Oh, S. Rondeau-Gagné, Y.-C. Chiu, A. Chortos, F. Lissel, G.-J. N. Wang, B. C. Schroeder, T. Kurosawa, J. Lopez, T. Katsumata, J. Xu, C. Zhu, X. Gu, W.-G. Bae, Y. Kim, L. Jin, J. W. Chung, J. B.-H. Tok and Z. Bao, *Nature*, 2016, **539**, 411–415.

33 J. Ko, Y. J. Kim and Y. S. Kim, *ACS Appl. Mater. Interfaces*, 2016, **8**, 23854–23861.

34 Y. L. Rao, A. Chortos, R. Pfattner, F. Lissel, Y. C. Chiu, V. Feig, J. Xu, T. Kurosawa, X. Gu, C. Wang, M. He, J. W. Chung and Z. Bao, *J. Am. Chem. Soc.*, 2016, **138**, 6020–6027.

35 W. H. Binder, *Macromol. Rapid Commun.*, 2019, **40**, 1–7.

36 T. P. Haider, C. Völker, J. Kramm, K. Landfester and F. R. Wurm, *Angew. Chem. Int. Ed.*, 2019, **58**, 50–62.

37 B. Grzybowski, D. Qin, R. Haag and G. M. Whitesides, *Sensors Actuators B. Chem.*, 2000, 81–85.

38 J. Pignanelli, K. Schlingman, T. B. Carmichael, S. Rondeau-Gagné and M. J. Ahamed, *Sensors Actuators A. Phys.*, 2019, **285**, 427–436.

39 W. Jacob and R. Mukherjee, *Inorganica Chim. Acta*, 2006, **359**, 4565–4573.

40 P. Mal, D. Schultz, K. Beyeh, K. Rissanen and J. R. Nitschke, *Angew. Chem. Int. Ed.*, 2008, **47**, 8297–8301.

41 A. Rajput and R. Mukherjee, *Coord. Chem. Rev.*, 2013, **257**, 350–368.

42 D. F. Evans, *J. Chem. Soc.*, 1959, 2003–2005.

43 B. Weber and F. A. Walker, *Inorg. Chem.*, 2007, **46**, 6794–6803.

44 L. Zheng, X. Fang, K. Lii, H. Song, X. Xin, H.-K. Fun, K. Chinnakali and I. Abdul Razak, *J. Chem. Soc., Dalt. Trans.*, 1999, **3**, 2311–2316.

45 C.-H. Li, C. Wang, C. Keplinger, J.-L. Zuo, L. Jin, Y. Sun, P. Zheng, Y. Cao, F. Lissel, C.

Linder, X.-Z. You and Z. Bao, *Nat. Chem.*, 2016, **8**, 618–624.

46 Z. H. Williams, E. D. Burwell, A. E. Chiomento, K. J. Demsko, J. T. Pawlik, S. O. Harris, M. R. Yarolimek, M. B. Whitney, M. Hambourger and A. D. Schwab, *Soft Matter*, 2017, **13**, 6542–6554.

47 F. García, J. Pelss, H. Zuilhof and M. M. J. Smulders, *Chem. Commun.*, 2016, **52**, 9059–9062.

48 C. D. Meyer, C. S. Joiner and J. F. Stoddart, *Chem. Soc. Rev.*, 2007, **36**, 1705–1723.

49 E. C. Constable, G. Baum, E. Bill, R. Dyson, R. Van Eldik, D. Fenske, S. Kaderli, D. Morris, A. Neubrand, M. Neuburger, D. R. Smith, K. Wieghardt, M. Zehnder and A. D. Zuberbühler, *Chem. Eur. J.*, 1999, **5**, 498–508.

50 J. Wang, B. Djukic, J. Cao, A. Alberola, F. S. Razavi and M. Pilkington, *Inorg. Chem.*, 2007, **46**, 8560–8568.

51 B. Sandmann, B. Happ, S. Kupfer, F. H. Schacher, M. D. Hager and U. S. Schubert, *Macromol. Rapid Commun.*, 2014, **36**, 604–609.

52 D. Mozhdehi, S. Ayala, O. R. Cromwell, Z. Guan, D. Mozhdehi, S. Ayala, O. R. Cromwell and Z. Guan, *J. Am. Chem. Soc.*, 2014, **136**, 16128–16131.

53 M. Ciaccia, R. Cacciapaglia, P. Mencarelli, L. Mandolini and S. Di Stefano, *Chem. Sci.*, 2013, **4**, 2253–2261.

54 P. Kovaříček and J. M. Lehn, *J. Am. Chem. Soc.*, 2012, **134**, 9446–9455.

55 M. Zeng, L. Li and S. B. Herzon, *J. Am. Chem. Soc.*, 2014, **136**, 7058–7067.

56 P. B. Shah, S. Bandopadhyay and J. R. Bellare, *Polym. Degrad. Stab.*, 1995, **47**, 165–173.

57 M. Irimia-Vladu, E. D. Głowacki, G. Voss, S. Bauer and N. S. Sariciftci, *Mater. Today*, 2012, **15**, 340–346.

58 C. M. Boutry, A. Nguyen, Q. O. Lawal, A. Chortos, S. Rondeau-Gagné and Z. Bao, *Adv. Mater.*, 2015, 27, 6954–6961.

59 H. Ying, Y. Zhang and J. Cheng, *Nat. Commun.*, 2014, **5**, 1–9.

60 T. Lei, M. Guan, J. Liu, H.-C. Lin, R. Pfattner, L. Shaw, A. F. McGuire, T.-C. Huang, L. Shao, K.-T. Cheng, J. B.-H. Tok and Z. Bao, *Proc. Natl. Acad. Sci.*, 2017, **114**, 5107–5112.

61 T. Lei, X. Chen, G. Pitner, H. S. P. Wong and Z. Bao, *J. Am. Chem. Soc.*, 2016, **138**, 802–805.

62 C. Edwards and R. Marks, *Clin. Dermatol.*, 1995, **13**, 375–380.

63 M. L. Hammock, A. Chortos, B. C.-K. Tee, J. B.-H. Tok and Z. Bao, *Adv. Mater.*, 2013, **25**, 5997–6038.

64 Z. Lei, Q. Wang, S. Sun, W. Zhu and P. Wu, *Adv. Mater.*, 2017, **29**, 1700321.

65 H. Kim, G. Kim, T. Kim, S. Lee, D. Kang, M. S. Hwang, Y. Chae, S. Kang, H. Lee, H. G. Park and W. Shim, *Small*, 2018, **14**, 1–10.

66 A. Chhetry, H. Yoon and J. Y. Park, *J. Mater. Chem. C*, 2017, **5**, 10068–10076.

67 X. Liang, T. Zhao, D. Zhu, F. Han, J. Li, G. Zhang, L. Ling, R. Sun, D. Ho, S. Zhao, C.-P. Wong and F. Liu, *Chem. Eur. J.*, 2018, **24**, 16823–16832.

CHAPTER 4. MODULATING THE THERMOMECHANICAL PROPERTIES AND SELF-HEALING EFFICIENCY OF SILOXANE-BASED SOFT POLYMERS THROUGH METAL-LIGAND COORDINATION

4.1 Introduction

Self-healing, defined as the capacity of a materials to regenerate spontaneously and autonomously, and restore completely (or partially) its initial properties after suffering from damages (strain, puncture, cracks, etc.), is a phenomenon attracting a lot of attention in materials science and engineering.[38,40,88–90] Particularly promising for the development of advanced electronics and biotechnology, there has been a constant effort to develop novel strategies and materials designs to enable rapid and autonomous self-healing, without the use of external triggers or complex methodology.[3,91–93] Among other, self-healing materials hold tremendous potential for applications in wearable and skin-inspired (bio)electronics, as devices need to emulate the properties of human skin, with the ability to autonomously regenerate its mechanical properties, while maintaining good electrical properties upon damage to preserve their initial function.[4,6,94] Despite important developments in this field, the combination of self-healing capabilities along with desired mechanical properties remains a challenge as the relationship between chemical design and self-healing efficiency is not always direct.[95] Moreover, complex preparation or utilization of external trigger is still often required to activate materials regeneration.[47,83] Furthermore, the relationship between self-healing efficiency and other physical properties, such as the elastic modulus, is still not fully unveiled. Therefore, a completely tunable approach to access a library of self-healing materials is highly desirable.

In recent years, various chemical strategies have been explored to enable self-healing in soft materials.[96,97] A general strategy to access autonomously healable materials at room temperature has been developed through the incorporation of moieties capable of generating weak supramolecular interactions that dynamically crosslink the polymer chains.[65,84,98,99] This strategy is particularly efficient for materials with low glass transition temperatures as the segmental chain mobility of these materials is high, thus enabling the chains to reconnect and regenerate the supramolecular bonds upon damage.[85,100] Among other recent examples, Xu *et al.* reported a detailed investigation on the mechanical properties of metal-catecholate complexes.[101] In addition to the role of coordination states on the mechanical properties, the authors also highlighted the importance of metal types for tunability. Self-healing capabilities have also been enabled through other strategies, such as metal-catalyzed reactions, reversible Diels-Alder reactions, and

encapsulation of regenerating agents.[102–105] It is important to mention that most of these systems require external stimuli such as heat or light, or require particular catalysts, solvents or plasticizers.[106–108]

Recently, our group reported the design and preparation of new self-healing materials, based on polydimethylsiloxane (PDMS) oligomers end-capped with imine and metal-coordinating moieties.[109] Interestingly, by using a Fe(II) source, metal-ligand coordination occurs, thus supramolecular crosslinking the oligomers and generating a dynamic network. The new system was shown to be ultra-stretchable (ε = 800%) at room temperature. Moreover, depending on the amount of metal crosslinker used, the materials was also shown to be autonomously self-healing by regenerating 88% of its initial mechanical properties after 48 hours without aid from any external stimuli. Despite achieving good self-healing behavior and tunability, this system was limited Fe(II) source, and a complete rational evaluation of the influence of the metal source onto the self-healing efficiency and mechanical properties is required to design a large library of efficient self-healing materials.

Herein, we report the preparation of new self-healing materials, based on end-capped PDMS-based oligomers with N-ligands, and the rational fine-tuning of their self-healing efficiency and thermomechanical properties through the variation of the nature of the metal-ligand interactions used (Figure 1). More specifically, pre-polymer P1 (Scheme S1) was coordinated with different metal sources, including $Fe(BF_4)_2$, $Co(BF_4)_2$, $Zn(BF_4)_2$, $Zn(OTf)_2$ and $Zn(ClO_4)_2$. These were carefully selected to probe for the effect of coordination geometry and bonds strengths on the thermomechanical properties. Moreover, through this evaluation, the important effect of the counter-ion on the self-healing properties was also accessed, which is sometimes overlooked in the literature.[110,111] The results obtained through this investigation revealed a strong correlation between coordination bond strength and geometry and self-healing properties of the materials. A fine-tuning of the materials self-healing efficiency was achieved, ranging from 60% to 80% after only 2 hours for cobalt and zinc-crosslinked materials respectively. Furthermore, the Young's modulus was also fine-tuned, reaching a minimal value of 0.23 MPa, by varying the nature of the counter-ion used in complexation. This new and completely tunable approach to self-healing materials highlights the importance of dynamic metal-ligand crosslinking toward robust, self-healing soft polymers. Furthermore, this system provides for a simple, low-cost yet effective method for obtaining a wide range of self-healing materials that can be used for various applications.

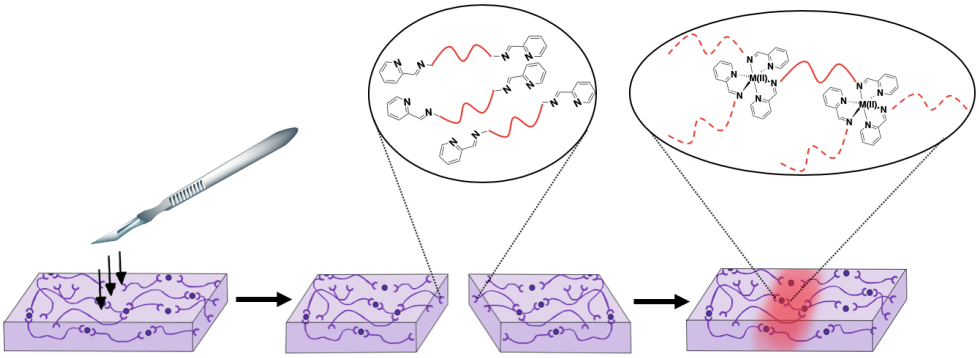

Figure 4.1. Self-healing of siloxane-based soft polymers (before and after physical cutting) through metal coordination.

4.2. Results and Discussion

The synthesis of pre-polymer P1, used toward the self-healing materials, is depicted in Scheme S1. The materials were prepared through a simple condensation between aminopropyl-terminated polydimethylsiloxane (1000 Da) with pyridine-2-carboxaldehyde to generate N-ligands from pyridine and imine functional groups as end-groups. Materials were used without further purification, and the complete synthetic procedure, characterization by thermogravimetric analysis (TGA) and differential scanning calorimetry (DSC) are detailed in Experimental Section and Supporting Information. Thermogravimetric analysis (TGA) confirmed that all materials, independently of the metal salt used for crosslinking, are stable at temperature up to 150°C (Figures S1 to S5). As expected, DSC experiments confirmed that all materials have a T_g well below room temperature, typical for PDMS-like materials.[112] In fact, for all materials, independently of the metal used, no T_g has been observed, indicating that the metal used for crosslinking does not have enough influence to significantly affect this parameter (Figures S6 to S10). This phenomenon has been previously reported with other self-healing materials.[113,114]

To compare the metal-ligand coordination effect on the thermomechanical properties of the system, $Co(BF_4)_2$, $Fe(BF_4)_2$ and $Zn(BF_4)_2$ metal salts where used. The effect of the counter-ion was probed by utilizing $Zn(ClO_4)_2$, $Zn(OTf)_2$ and $Zn(BF_4)_2$ salts. For all samples, 0.33 equivalents of the metal salt were used in solution to generate the metal-coordinated polymer. Metal-ligand interactions were selected as dynamic crosslinking strategy as their reversibility is well known, which has been confirmed by multiple techniques such as single molecule force spectroscopy.[69] Upon stress, the metal-ligand interactions are able to dissipate energy through rupture of the coordinate bond. However, due to the kinetic lability of the bonds, the supramolecular interaction

can reform upon release from strain. In general, the weaker the metal-ligand interaction (more kinetically labile chain and better ability to dissipate energy), the faster the bonds are able to reform. This dynamic reversibility has been observed with various ligands and metal centers including with cobalt, iron, and zinc, which are utilized in this work.[93,115] It is also important to mention that the imine bonds are also known to be dynamically reversible, and are also playing a role on the self-healing ability of this system.[57,109,116,117]

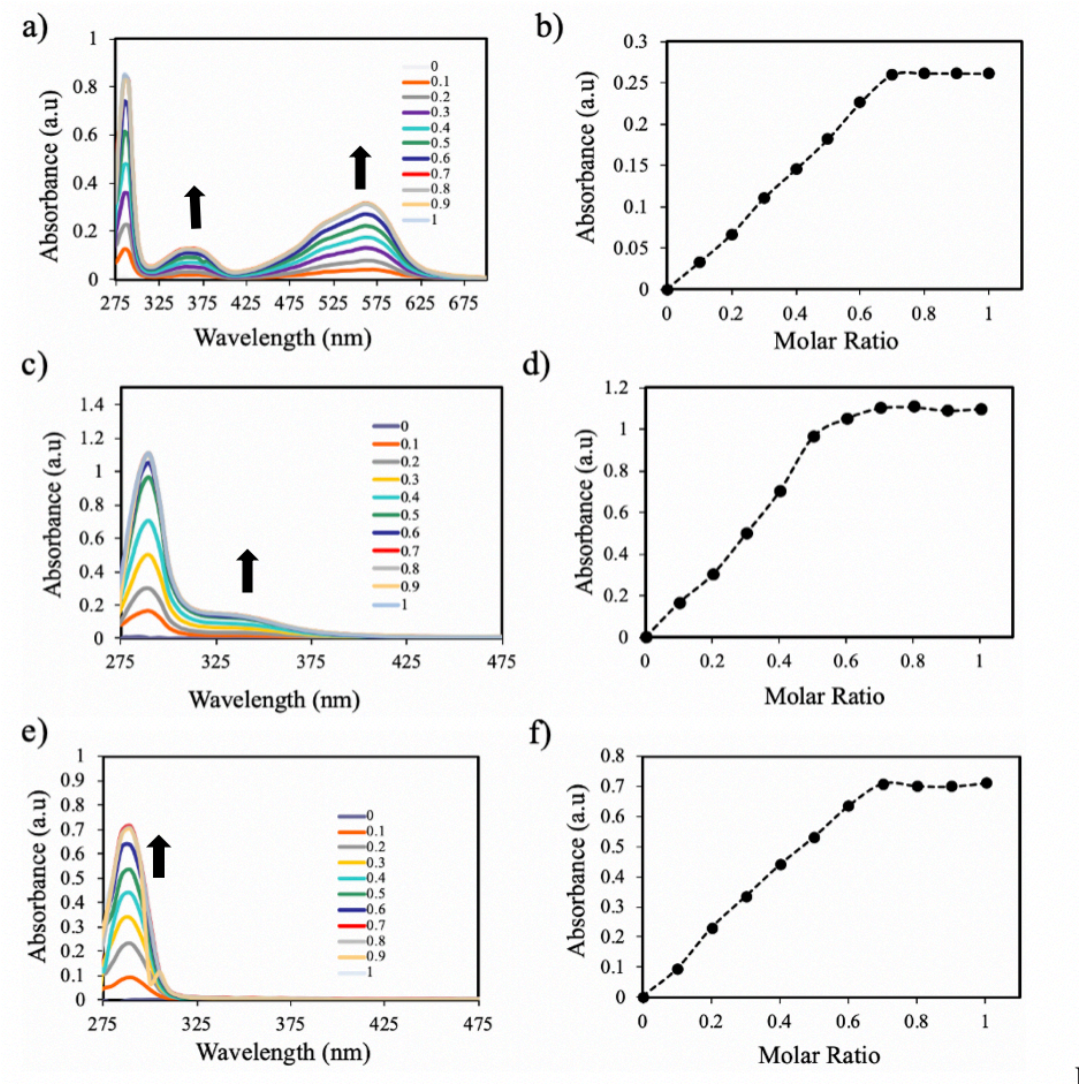

Figure 4. 2. a) UV-vis absorption spectra of P1 in CH_2Cl_2 with $Fe(BF_4)_2$; b) molar ratio of $Fe(BF_4)_2$ versus absorbance at 530 nm; c) UV-vis absorption spectra of P1 in CH_2Cl_2 with $Co(BF_4)_2$; d) molar ratio of $Co(BF_4)_2$ versus absorbance at 290 nm; e) UV-vis absorption spectra of P1 in CH_2Cl_2 with $Zn(BF_4)_2$, and f) molar ratio of $Zn(BF_4)_2$ versus absorbance at 290 nm. Each titration included

0.1 molar equivalents of the respective metal salt (4.4 x 10^{-5} mM) per N-ligand in P1 (7.2 x 10^{-7} mM).

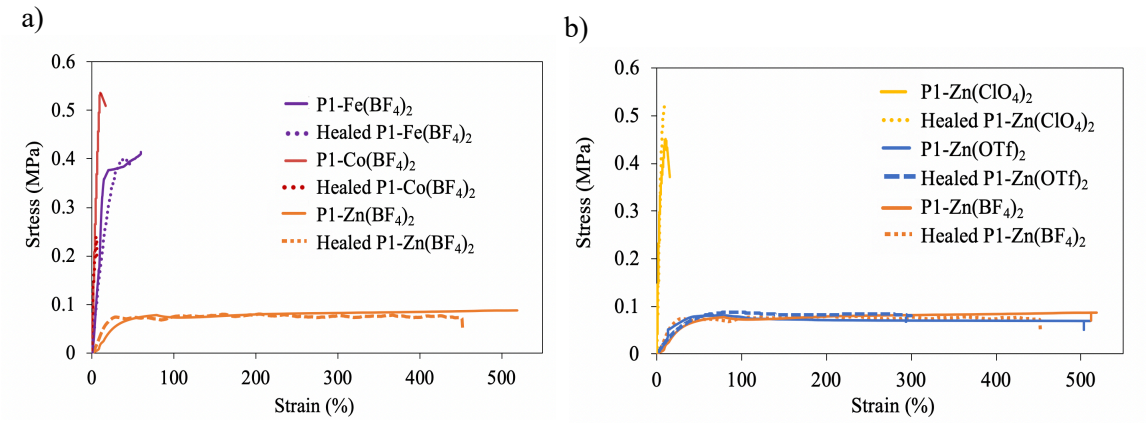

Figure 4.3. a) Stress-strain curve of pre-polymer P1 crosslinked with 0.33 eq. of Fe(II), Zn(II) or Co(II) before self-healing. BF_4^- has been selected as counter-anion; b) Stress-strain curve of pre-polymer P1 crosslinked with 0.33 eq. Zn(II) with BF_4^-, ClO_4^- and $CF_3SO_3^-$ (OTf^-) as counter-anions, before self-healing; c) Stress-strain curve of pre-polymer P1 crosslinked with 0.33 eq. of Fe(II), Zn(II) or Co(II) after self-healing at room temperature for 2 hours. BF_4^- has been selected as counter-anion, and d) Stress-strain curve of pre-polymer P1 crosslinked with 0.33 eq. Zn(II) with BF_4^-, ClO_4^- and $CF_3SO_3^-$ (OTf^-) as counter-anions, after self-healing at room temperature for 2 hours.

After confirming the coordination of metals and the geometry of the resulting complexes, a detailed investigation on the mechanical properties was performed in order to unveil the effect of coordination motif on self-healing. To perform this investigation, samples of **P1** crosslinked with either $Fe(BF_4)_2$, $Co(BF_4)_2$ and $Zn(BF_4)_2$ were prepared in solution and casted into a PTFE mold. The resulting materials was dried at room temperature for 24 hours to remove any solvent residue. First, tensile-strain pull tests were performed on the soft crosslinked materials with different metals (Fe, Co and Zn) to get insight onto the maximal fracture strain, and the results are shown in Figure 3a. Interestingly, despite showing similar coordination geometry for the metal-ligand complexes, the metal center selected was shown to have a significant effect on the maximal elongation before fracture. Samples prepared from Zn(II), Fe(II) and Co(II) demonstrated a maximum strain before fracture of respectively of 525%, 75% and 25%. This significant difference between the materials can directly be explained by the difference in M-L bond strengths. A direct relationship can be suggested between the bond length or strength of the M-L interactions where the smaller the bond

length, the stronger the association and thus the more brittle the material. Based on previous reports, bond lengths of Fe^{2+}, Co^{2+} and Zn^{2+} coordinated to bipyridine-based ligands are 1.852, 1.848 and 2.002 Å, which can be directly related to bond strength.[118] Therefore, despite also having an octahedral geometry, coordination of Zn(II) is much weaker than Co(II) and Fe(II), which can explain the more brittle nature of the cobalt and iron-based polymers.

A similar investigation was also performed by varying the counter-ion using $Zn(BF_4)_2$, $Zn(ClO_4)$ and $Zn(OTf)_2$ for the preparation of the materials. These specific counter-ions were selected for various reasons. First, tetrafluoroborate, perchlorate and triflate are non-coordinating counter-ions which promote the octahedral coordination geometry of the polymer ligands with the metal center, as confirmed by UV-Vis spectroscopy. Moreover, their size and stability differ, which can have an influence on the resulting supramolecular network and thermomechanical properties.[119] As shown in Figure 3b, materials prepared from tetrafluoroborate and triflate counter-ions showed similar maximum strain before fracture, around 515%. The sample prepared from zinc perchlorate showed a significantly reduced robustness, with a maximum fracture strain around 15%. This important counter-ion effect can be attributed to various factors, including size, coordinating ability and strength, and ion aggregation.[120] Self-healing could be explained by the rearrangement of ion aggregation and the interdiffusion of polymer chains over the surface of the crack. Strong cation–anion interaction and intensive ion aggregation for the counterion can restrict the mobility of the surrounding polymer chain, thus improving the mechanical strength but reducing self-healing ability. The three selected counter-ions are weakly coordinating, but OTf^- and BF_4^- are slightly bigger than ClO_4^- with weak coordinating abilities, which ultimately can result in a plasticizing effect. This impact of counter-ion on the mechanical properties and crystallization processes have been observed in various systems, including in self-healing PDMS-based polymers using nitrate and triflate-containing metal crosslinkers and in silver-thiadiazol complexes which strongly suggests this direct trend on metal-ligand coordination dynamics and counter anion size.[76,110]

To evaluate the self-healing efficiency of the materials, free-standing films of the different crosslinked materials were cut in two pieces and were slowly put back in physical contact. The resulting materials were left on the benchtop at room temperature for 2 hours and the healed film were evaluated by tensile-strain pull testing. It is important to mention that no additional trigger (thermal annealing, light exposure, etc.) were used in order to ensure an autonomous self-healing mechanism. The resulting self-healed materials were then analyzed by tensile-strain pull testing and the results are summarized in Figure 3c-d. The self-healing efficiency was determined by comparing the maximum elongation before damage and after a 2-hour healing period. As observed

with the pristine samples, the healed materials showed a similar trends in terms of maximum fracture strain, with the Zn(II)-crosslinked materials showing a maximum elongation of 450% after self-healing (2 hours), corresponding to a self-healing efficiency of 87% (Table 1). This trend can be directly explained by the coordination of Zn(II), weaker but more dynamic than Co(II) and Fe(II), which can allow for a fast regeneration of the coordination complex when the polymer chains are put back in contact. Nonetheless, despite the stronger coordination, the Co(II) and Fe(II)-containing self-healing polymers showed self-healing efficiencies of 61% and 71% respectively. For the effect of the counter-ion on the maximum strain at fracture after self-healing, a similar trend was also observed with the non-coordination large counter-ion having an increase plasticizing effect than the smaller ones. For the materials prepared from $Zn(BF_4)_2$ and $Zn(ClO_4)_2$, self-healing efficiency were relatively good after 2 hours (88 and 75% respectively).

Table 4. 1. Elastic moduli and self-healing efficiencies of pre-polymer P1 crosslinked with various metal (II) sources.

Metal Salt	Elastic Modulus (MPa)	Self-Healing Efficiency[a] (%)
$Co(BF_4)_2$	8.10 ± 2.80	61
$Fe(BF_4)_2$	1.80 ± 0.15	71
$Zn(BF_4)_2$	0.26 ± 0.09	88
$Zn(ClO_4)_2$	10.2 ± 1.40	75
$Zn(CF_3SO_3)_2$	0.23 ± 0.04	73

[a] Defined as the difference between the maximum elongation before damage and after a 2-hour

The metal center and type of counter-ion used in this system are not only have an important effect on the maximal strain before fracture and self-healing efficiency, but also directly influencing the thermomechanical properties of the soft materials. Therefore, to unveil the impact of the crosslinker used to prepare the materials on the soft materials, a complete evaluation of the thermomechanical properties, including Young's moduli and maximum strain at fracture was performed using tensile-strain pull testing. First, the Young's modulus for all systems was evaluated by tensile-strain pull testing, and the results are summarized in Table 1. Similar to the trend observed for the maximum strain at fracture, the selection of the metal used for coordination has a direct effect on the elastic modulus of the resulting crosslinked materials. Zn(II), with the weaker interaction, led to a polymer

with a modulus of 0.26 MPa, which is one order of magnitude lower than commonly used PDMS.[121] When Fe(II) was used, this modulus increased to 1.8 MPa. Finally, when Co(II) was used, the resulting materials was more brittle, and its Young's modulus increase to 8.1 MPa. This result can be directly correlated to the coordination bonds strength. The elastic moduli of Zn(II)-based materials with different counter-ions was then evaluated. Interestingly, when the counter-ion used is large and non-coordinating (tetrafluoroborate and triflate), the moduli remained fairly low, with a value of 0.26 and 0.23 MPa respectively. However, when perchlorate was used, the resulting materials became brittle with an elastic modulus of 10.2 MPa, which is considerably higher than commonly used PDMS-based elastomer. Nonetheless, in the current system, the Young's modulus was showed to have a limited correlation with self-healing, as illustrated in Table 1.

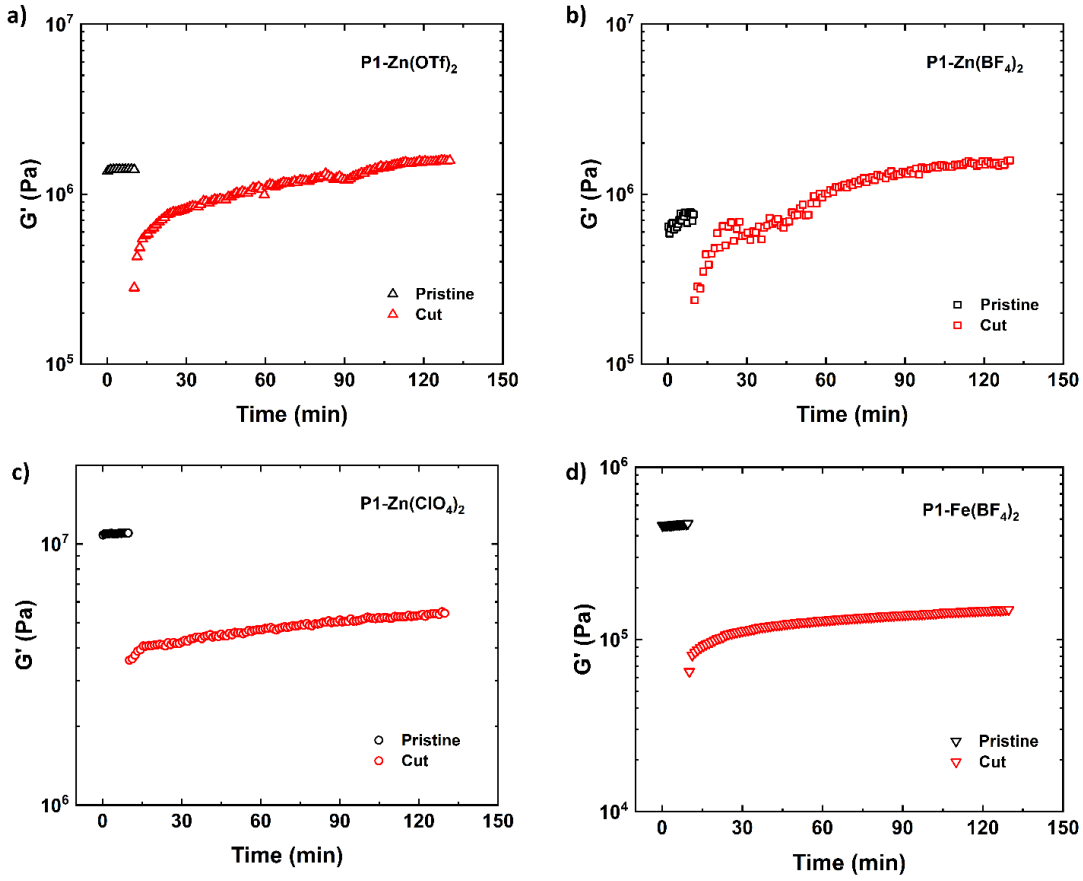

Figure 4.4. Storage modulus (G') as a function of time during self-healing (a). P1-Zn(OTf)2, (b). P1-Zn(BF4)2, (c). P1-Zn(ClO4)2, and (d). P1-Fe(BF4)2. Both the modulus for sample before (black curve) and after (red) self-healing are plotted.

The self-healing efficiency of the materials was also evaluated with shear rheometry using a method previously reported in the literature for similar soft materials.[122] Briefly, a disk-shape (8-mm diameter and approximately 1.5 mm thickness) pristine sample was first measured with a time sweep for 10 minutes using 8-mm parallel plates to establish the benchmark performance; then the sample, while sit between two plates, was split into two halves horizontally and brought into contact with a normal force of 0.5 N. Finally, another time sweep was immediately performed on the cut sample for 2 hours. Figure 4 plots storage modulus (G') as a function of time for P1 crosslinked with $Zn(OTf)_2$, $Zn(BF_4)_2$, $Zn(ClO_4)_2$, and $Fe(BF_4)_2$. It is important to mention that the samples crosslinked with $Co(BF_4)_2$ were shown to be too brittle for being characterized through this technique. Interestingly, it was observed that for the pristine materials, G' (approximately equals to one third of elastic modulus for elastomer) is higher than the value derived from tensile strain analysis for $Zn(OTf)_2$, $Zn(BF_4)_2$ and $Zn(ClO_4)_2$, while remains comparable for $Fe(BF_4)_2$. This can be attributed to the weaker coordination of Zn(II) than Fe(II). In addition, Figure 4 shows distinct self-healing behavior among these four samples: within 2 hours timeframe, G' of $Zn(OTf)_2$ and $Zn(BF_4)_2$ gets fully recovered or even shows higher G' compared to the pristine sample, whereas $Zn(ClO_4)_2$, and $Fe(BF_4)_2$ only exhibits partial recovery of 49% and 32%. The trend is qualitatively consistent with the results from tensile-strain pull test. However, the efficiency of $Zn(ClO_4)_2$, and $Fe(BF_4)_2$ was found to be much smaller than the results obtained from tensile-strain pull test. This can be attributed to the difference in the cross-section area of the cut in the measurements, i.e., the cut for rheology measurements introduces a larger cross-section for self-healing. Yet, a full recovery of G' is observed for $Zn(OTf)_2$ and $Zn(BF_4)_2$. In addition, during recovery, $Zn(OTf)_2$ and $Zn(BF_4)_2$ even shows a higher G' than the pristine sample. This is presumably due to the high mobility of polymer chain crosslinked with $Zn(OTf)_2$ and $Zn(BF_4)_2$ possessing weaker coordination. During the self-healing process, crosslinker migrates to the interface and potentially increases the crosslinking density and results in a higher G'. Similar behavior has been observed for a hydrogen-bonded polymer complex by Wang et al.[122] In terms of counterion effect, since ClO_4^- shows slightly stronger coordination ability than OTf^- and BF_4^-, a lower self-healing efficiency was observed.

4.3. Conclusion

In summary, a novel approach to fine-tune the thermomechanical properties of soft, siloxane-based elastomers has been developed through the use dynamic metal-ligand interactions. Specifically, a new imine-based siloxane-based polymer has been crosslinked with various metal centers, including with Fe(II), Zn(II) and Co (II). Interestingly, the resulting polymers were shown to undergo rapid self-healing at room temperature (two hours) without the use of any external trigger. By tuning the strength of the metal-ligand interactions, a fine-tuning of the thermomechanical properties was effectuated. Samples prepared from Zn(II), Fe(II) and Co(II) demonstrated a maximum strain before fracture of 525%, 75% and 25%, and a self-healing efficiency of 88%, 71% and 61% respectively. This can be directly attribute to the difference in bond lengths (strength of the M-L interactions) where the smaller the bond length, the stronger the association and thus the more brittle the material. In addition to the effect of the metal center, an evaluation of the effect of the counter-ion on the self-healing efficiency and thermomechanical properties was also performed. Interestingly, an important effect of the counter-ion on the maximum strain at fracture after self-healing was observed and can be attributed to the large counter-ions having an increase plasticizing effect than the smaller ones. For the materials prepared from Zn(BF4)2 and Zn(ClO4)2, self-healing efficiency of 88 and 75 % respectively were observed after 2 hours. Furthermore, materials prepared from tetrafluoroborate and triflate counter-ions showed an almost similar maximum strain before fracture, around 515%. Finally, the fine-tuning of the metal-ligand interaction in the soft polymer allowed for the preparation of a wide variety of self-healing polymers with Young's moduli ranging from 0.23 to 10.2 MPa. This new strategy to fine-tune the thermomechanical properties and self-healing of soft, siloxane-based polymers is highly versatile and the preparation of the materials is relatively simple. Therefore, this approach is particularly promising for many applications, including for soft electronics, advanced coatings and manufacturing and healthcare.

4.4. REFERENCES

1 A. M. Hussain and M. M. Hussain. CMOS-Technology-Enabled Flexible and Stretchable Electronics for Internet of Everything Applications, *Adv. Mater.*, 2016, **28**, 4219–4249.

2 Y. Yao, H. Dong and W. Hu. Charge Transport in Organic and Polymeric Semiconductors for Flexible and Stretchable Devices, *Adv. Mater.*, 2016, **28**, 4513–4523.

3 T. F. O 'connor, K. M. Rajan, A. D. Printz and D. J. Lipomi. Toward organic electronics with properties inspired by biological tissue, *J. Mater. Chem. B*, 2015, **3**, 4947–4952.

4 S. J. Benight, C. Wang, J. B. H. Tok and Z. Bao. Stretchable and self-healing polymers and devices for electronic skin, *Prog. Polym. Sci.*, 2013, **38**, 1961–1977.

5 M. Kaltenbrunner, T. Sekitani, J. Reeder, T. Yokota, K. Kuribara, T. Tokuhara, M. Drack, R. Schwödiauer, I. Graz, S. Bauer-Gogonea, S. Bauer and T. Someya. An ultra-lightweight design for imperceptible plastic electronics, *Nature*, 2013, **499**, 458–463.

6 Q. Hua, J. Sun, H. Liu, R. Bao, R. Yu, J. Zhai, C. Pan and Z. L. Wang. Skin-inspired highly stretchable and conformable matrix networks for multifunctional sensing, *Nat. Commun.*, 2018, **9**, 1–11.

7 K. A. Ray. Flexible Solar Cell reliable power source that can provide power at any KelWrd-, *IEEE Trans. Aerosp. Electron. Syst.*

8 D. Angmo, T. T. Larsen-Olsen, M. Jørgensen, R. R. Søndergaard and F. C. Krebs. Roll-to-roll inkjet printing and photonic sintering of electrodes for ITO free polymer solar cell modules and facile product integration, *Adv. Energy Mater.*, 2013, **3**, 172–175.

9 T.-T. Kuo, C.-M. Wu, H.-H. Lu, I. Chan, K. Wang and K.-C. Leou. Flexible x-ray imaging detector based on direct conversion in amorphous selenium, *J. Vac. Sci. Technol. A Vacuum, Surfaces, Film.*, 2014, **32**, 041507.

10 T. Peter Brody. The Thin Film Transistor—A Late Flowering Bloom, *IEEE Trans. Electron Devices*, 1984, **31**, 1614–1628.

11 N. D. Young, G. Harkin, R. M. Bunn, D. J. Mcculloch, R. W. Wilks and A. G. Knapp. Polysilicon TFT ' s on Glass and Polymer Substrates, 1997, **18**, 19–20.

12 C. Liu, N. Huang, F. Xu, J. Tong, Z. Chen, X. Gui, Y. Fu and C. Lao. 3D printing technologies for flexible tactile sensors toward wearable electronics and electronic skin, *Polymers (Basel).*, 2018, **10**, 1–31.

13 H. Bin Yao, J. Ge, C. F. Wang, X. Wang, W. Hu, Z. J. Zheng, Y. Ni and S. H. Yu. A

flexible and highly pressure-sensitive graphene-polyurethane sponge based on fractured microstructure design, *Adv. Mater.*, 2013, **25**, 6692–6698.

14 B. Zhuo, S. Chen, M. Zhao and X. Guo. High Sensitivity Flexible Capacitive Pressure Sensor Using Polydimethylsiloxane Elastomer Dielectric Layer Micro-Structured by 3-D Printed Mold, *IEEE J. Electron Devices Soc.*, 2017, **5**, 219–223.

15 D. J. Lipomi, J. A. Lee, M. Vosgueritchian, B. C. K. Tee, J. A. Bolander and Z. Bao. Electronic properties of transparent conductive films of PEDOT:PSS on stretchable substrates, *Chem. Mater.*, 2012, **24**, 373–382.

16 B. B. Narakathu, A. Eshkeiti, A. S. G. Reddy, M. Rebros, E. Rebrosova, M. K. Joyce, B. J. Bazuin and M. Z. Atashbar. A novel fully printed and flexible capacitive pressure sensor, *Proc. IEEE Sensors*, 2012, 26–29.

17 O. Atalay, A. Atalay, J. Gafford and C. Walsh. A Highly Sensitive Capacitive-Based Soft Pressure Sensor Based on a Conductive Fabric and a Microporous Dielectric Layer, *Adv. Mater. Technol.*, 2018, **3**, 1–8.

18 D. J. Lipomi, M. Vosgueritchian, B. C. K. Tee, S. L. Hellstrom, J. A. Lee, C. H. Fox and Z. Bao. Skin-like pressure and strain sensors based on transparent elastic films of carbon nanotubes, *Nat. Nanotechnol.*, 2011, **6**, 788–792.

19 S. C. B. Mannsfeld, B. C. K. Tee, R. M. Stoltenberg, C. V. H. H. Chen, S. Barman, B. V. O. Muir, A. N. Sokolov, C. Reese and Z. Bao. Highly sensitive flexible pressure sensors with microstructured rubber dielectric layers, *Nat. Mater.*, 2010, **9**, 859–864.

20 A. Sekiguchi, F. Tanaka, T. Saito, Y. Kuwahara, S. Sakurai, D. N. Futaba, T. Yamada and K. Hata. Robust and Soft Elastomeric Electronics Tolerant to Our Daily Lives, *Nano Lett.*, 2015, **15**, 5716–5723.

21 M. Shin, J. H. Song, G. H. Lim, B. Lim, J. J. Park and U. Jeong. Highly stretchable polymer transistors consisting entirely of stretchable device components, *Adv. Mater.*, 2014, **26**, 3706–3711.

22 A. D. Kim, J. Ahn, W. M. Choi, H. Kim, T. Kim, J. Song, Y. Y. Huang, Z. Liu, C. Lu and J. A. Rogers. Stretchable and Foldable Silicon Integrated Circuits, *Science (80-.).*, 2008, **320**, 507–511.

23 M. Selivanova, C. H. Chuang, B. Billet, A. Malik, P. Xiang, E. Landry, Y. C. Chiu and S. Rondeau-Gagné. Morphology and Electronic Properties of Semiconducting Polymer and

Branched Polyethylene Blends, *ACS Appl. Mater. Interfaces*, 2019, **11**, 12723–12732.

24 M. Selivanova, S. Zhang, B. Billet, A. Malik, N. Prine, E. Landry, X. Gu, P. Xiang and S. Rondeau-Gagné. Branched Polyethylene as a Plasticizing Additive to Modulate the Mechanical Properties of π-Conjugated Polymers, *Macromolecules*, 2019, **52**, 7870–7877.

25 Z. Huang, M. Gao, Z. Yan, T. Pan, S. A. Khan, Y. Zhang, H. Zhang and Y. Lin. Pyramid microstructure with single walled carbon nanotubes for flexible and transparent micro-pressure sensor with ultra-high sensitivity, *Sensors Actuators, A Phys.*, 2017, **266**, 345–351.

26 T. Sekitani, Y. Noguchi, K. Hata, T. Fukushima, T. Aida and T. Someya. A rubberlike stretchable active matrix using elastic conductors, *Science (80-.).*, 2008, **321**, 1468–1472.

27 D. J. Lipomi, M. Vosgueritchian, B. C. K. Tee, S. L. Hellstrom, J. A. Lee, C. H. Fox and Z. Bao. Skin-like pressure and strain sensors based on transparent elastic films of carbon nanotubes, *Nat. Nanotechnol.*, 2011, **6**, 788–792.

28 J. A. Rogers, T. Someya, Y. Huang, J. A. Rogers, T. Someya and Y. Huang. Materials and Mechanics for Stretchable Electronics Published by : American Association for the Advancement of Science Linked references are available on JSTOR for this article : Materials and Mechanics for Stretchable Electronics, 2010, **327**, 1603–1607.

29 M. U. Ocheje, B. P. Charron, Y. H. Cheng, C. H. Chuang, A. Soldera, Y. C. Chiu and S. Rondeau-Gagné. Amide-Containing Alkyl Chains in Conjugated Polymers: Effect on Self-Assembly and Electronic Properties, *Macromolecules*, 2018, **51**, 1336–1344.

30 Y. Li, W. K. Tatum, J. W. Onorato, S. D. Barajas, Y. Y. Yang, C. K. Luscombe and K. Christine. An indacenodithiophene-based semiconducting polymer with high ductility for stretchable organic electronics, *Polym. Chem.*, 2017, **8**, 5185–5193.

31 S. Braun. Studies of materials and interfaces for organic electronics, *Studies of materials and interfaces for organic electronics*, 2007.

32 N. Vogel. Springer Theses, *Springer Theses*, 2011.

33 J. S. Kim, J. H. Kim, W. Lee, H. Yu, H. J. Kim, I. Song, M. Shin, J. H. Oh, U. Jeong, T. S. Kim and B. J. Kim. Tuning Mechanical and Optoelectrical Properties of Poly(3-hexylthiophene) through Systematic Regioregularity Control, *Macromolecules*, 2015, **48**, 4339–4346.

34 B. Wang, D. Qin, G. Liang, A. Gu, L. Liu and L. Yuan. High-k materials with low

dielectric loss based on two superposed gradient carbon nanotube/cyanate ester composites, *J. Phys. Chem. C*, 2013, **117**, 15487–15495.

35 R. Ruppin. Electromagnetic energy density in a dispersive and absorptive material, *Phys. Lett. Sect. A Gen. At. Solid State Phys.*, 2002, **299**, 309–312.

36 B. Wang, G. Liang, Y. Jiao, A. Gu, L. Liu, L. Yuan and W. Zhang. Two-layer materials of polyethylene and a carbon nanotube/cyanate ester composite with high dielectric constant and extremely low dielectric loss, *Carbon N. Y.*, 2013, **54**, 224–233.

37 B. Wang, W. Huang, L. Chi, M. Al-Hashimi, T. J. Marks and A. Facchetti. High- k Gate Dielectrics for Emerging Flexible and Stretchable Electronics, *Chem. Rev.*, 2018, **118**, 5690–5754.

38 C. E. Diesendruck, N. R. Sottos, J. S. Moore and S. R. White. Biomimetic Self-Healing, *Angew. Chemie - Int. Ed.*, 2015, **54**, 10428–10447.

39 D. Y. Wu, S. Meure and D. Solomon. Self-healing polymeric materials: A review of recent developments, *Prog. Polym. Sci.*, 2008, **33**, 479–522.

40 Y. J. Tan, J. Wu, H. Li and B. C. K. Tee. Self-Healing Electronic Materials for a Smart and Sustainable Future, *ACS Appl. Mater. Interfaces*, 2018, **10**, 15331–15345.

41 F. W. Went. Cladistics Linked references are available on JSTOR for this article :, *Int. Assoc. Plant Taxon.*, 1971, **20**, 197–226.

42 B. Blaiszik, S. L. B. Kramer, J. S. Moore, N. R. Sottos, B. J. Blaiszik, S. L. B. Kramer, S. C. Olugebefola, J. S. Moore, N. R. Sottos and S. R. White. Self-Healing Polymers and Composites Second Sandia Fracture Challenge View project Shock Wave Energy Dissipation by Mechanochemically-active Materials View project Self-Healing Polymers and Composites, *Annu. Rev. Mater. Res*, 2010, **40**, 179–211.

43 F. Herbst, D. Döhler, P. Michael and W. H. Binder. Self-healing polymers via supramolecular forces, *Macromol. Rapid Commun.*, 2013, **34**, 203–220.

44 B. Zhang, Z. A. Digby, J. A. Flum, E. M. Foster, J. L. Sparks and D. Konkolewicz. Self-healing, malleable and creep limiting materials using both supramolecular and reversible covalent linkages, *Polym. Chem.*, 2015, **6**, 7368–7372.

45 C. De Nardi, S. Bullo, L. Ferrara, L. Ronchin and A. Vavasori. Effectiveness of crystalline admixtures and lime/cement coated granules in engineered self-healing capacity of lime mortars, *Mater. Struct. Constr.*, 2017, **50**, 1–12.

46 M. N. Tahir, M. U. Ocheje, K. Wojtkiewicz and S. Rondeau-gagné. 3 Self-Healing Materials : Design and Applications, .

47 S. R. White, N. R. Sottos, P. H. Geubelle, J. S. Moore, M. R. Kessler, S. R. Sriram, E. N. Brown and S. Viswanathan. Autonomic healing of polymer composites, *Nature*, 2001, **409**, 794–797.

48 J. Yang, M. W. Keller, J. S. Moore, S. R. White, N. R. Sottos, J. Yang, M. W. Keller, J. S. Moore, S. R. White and N. R. Sottos. Microencapsulation of Isocyanates for Self-Healing Polymers Microencapsulation of Isocyanates for Self-Healing Polymers, 2008, **41**, 9650–9655.

49 S. H. Cho, H. M. Andersson, S. R. White, N. R. Sottos and P. V. Braun. Polydiniethylsiloxane-based self-healing materials, *Adv. Mater.*, 2006, **18**, 997–1000.

50 A. Nasresfahani and P. M. Zelisko. Synthesis of a self-hea(1) Nasresfahani, A.; Zelisko, P. M. Synthesis of a Self-Healing Siloxane-Based Elastomer Cross-Linked via a Furan-Modified Polyhedral Oligomeric Silsesquioxane Investigation of a Thermally Reversible Silicon-Based Cross-Link. Polym, *Polym. Chem.*, 2017, **8**, 2942–2952.

51 C. C. Deng, W. L. A. Brooks, K. A. Abboud and B. S. Sumerlin. Boronic acid-based hydrogels undergo self-healing at neutral and acidic pH, *ACS Macro Lett.*, 2015, **4**, 220–224.

52 W. Li, C. Zhang, S. Qi, X. Deng, W. Wang, B. Yang, J. Liu and Z. Dong. Polymer Chemistry, .

53 B. D. Fairbanks, S. P. Singh, C. N. Bowman and K. S. Anseth. Photodegradable, photoadaptable hydrogels via radical-mediated disulfide fragmentation reaction, *Macromolecules*, 2011, **44**, 2444–2450.

54 G. Zhao, C. Yang, L. Guo, H. Sun, C. Chen and W. Xia. Visible light-induced oxidative coupling reaction: Easy access to Mannich-type products, *Chem. Commun.*, 2012, **48**, 2337–2339.

55 P. M. Imbesi, C. Fidge, J. E. Raymond, S. I. Cauët and K. L. Wooley. Model Diels-Alder studies for the creation of amphiphilic cross-linked networks as healable, antibiofouling coatings, *ACS Macro Lett.*, 2012, **1**, 473–477.

56 F. Yu, X. Cao, J. Du, G. Wang and X. Chen. Multifunctional Hydrogel with Good Structure Integrity, Self-Healing, and Tissue-Adhesive Property Formed by Combining

Diels-Alder Click Reaction and Acylhydrazone Bond, *ACS Appl. Mater. Interfaces*, 2015, **7**, 24023–24031.

57 A. Chao, I. Negulescu and D. Zhang. Dynamic Covalent Polymer Networks Based on Degenerative Imine Bond Exchange: Tuning the Malleability and Self-Healing Properties by Solvent, *Macromolecules*, 2016, **49**, 6277–6284.

58 M. Pepels, I. Filot, B. Klumperman and H. Goossens. Self-healing systems based on disulfide-thiol exchange reactions, *Polym. Chem.*, 2013, **4**, 4955–4965.

59 G. Deng, F. Li, H. Yu, F. Liu, C. Liu, W. Sun, H. Jiang and Y. Chen. Dynamic hydrogels with an environmental adaptive self-healing ability and dual responsive Sol-Gel transitions, *ACS Macro Lett.*, 2012, **1**, 275–279.

60 Z. P. Zhang, M. Z. Rong, M. Q. Zhang and C. Yuan. Alkoxyamine with reduced homolysis temperature and its application in repeated autonomous self-healing of stiff polymers, *Polym. Chem.*, 2013, **4**, 4648–4654.

61 C. Yuan, M. Z. Rong, M. Q. Zhang, Z. P. Zhang and Y. C. Yuan. Self-healing of polymers via synchronous covalent bond fission/radical recombination, *Chem. Mater.*, 2011, **23**, 5076–5081.

62 H. Li, R. Wang, H. Hu and W. Liu. Surface modification of self-healing poly(urea-formaldehyde) microcapsules using silane-coupling agent, *Appl. Surf. Sci.*, 2008, **255**, 1894–1900.

63 C. Wang, H. Wu, Z. Chen, M. T. Mcdowell, Y. Cui and Z. Bao. Self-healing chemistry enables the stable operation of silicon microparticle anodes for high-energy lithium-ion batteries, *Nat. Chem.*, 2013, **5**, 1042–1048.

64 C. Wang, N. Liu, R. Allen, J. B. H. Tok, Y. Wu, F. Zhang, Y. Chen and Z. Bao. A rapid and efficient self-healing thermo-reversible elastomer crosslinked with graphene oxide, *Adv. Mater.*, 2013, **25**, 5785–5790.

65 Y. Chen, A. M. Kushner, G. A. Williams and Z. Guan. Multiphase design of autonomic self-healing thermoplastic elastomers, *Nat. Chem.*, 2012, **4**, 467–472.

66 R. P. Sijbesma, F. H. Beijer, L. Brunsveld, B. J. B. Folmer, J. H. K. K. Hirschberg, R. F. M. Lange, J. K. L. Lowe and E. W. Meijer. Reversible polymers formed from self-complementary monomers using quadruple hydrogen bonding, *Science (80-.).*, 1997, **278**, 1601–1604.

67 D. Mozhdehi, S. Ayala, O. R. Cromwell and Z. Guan. Self-healing multiphase polymers via dynamic metal-ligand interactions, *J. Am. Chem. Soc.*, 2014, **136**, 16128–16131.

68 Z. Tang, J. Huang, B. Guo, L. Zhang and F. Liu. Bioinspired Engineering of Sacrificial Metal-Ligand Bonds into Elastomers with Supramechanical Performance and Adaptive Recovery, *Macromolecules*, 2016, **49**, 1781–1789.

69 C. H. Li, C. Wang, C. Keplinger, J. L. Zuo, L. Jin, Y. Sun, P. Zheng, Y. Cao, F. Lissel, C. Linder, X. Z. You and Z. Bao. A highly stretchable autonomous self-healing elastomer, *Nat. Chem.*, 2016, **8**, 618–624.

70 B. Sandmann, B. Happ, S. Kupfer, F. H. Schacher, M. D. Hager and U. S. Schubert. The self-healing potential of triazole-pyridine-based metallopolymers, *Macromol. Rapid Commun.*, 2015, **36**, 604–609.

71 N. et al. Holten-Andersen. Metal-coordination: using one of nature's tricks to control soft material mechanics., *J. Mater. Chem. B 2, 2467*, 2013, 5791–5797.

72 F. Dumitru, A. van der Lee and M. Barboiu. Chiral superstructures from homochiral Zn2+, Co2+, Fe2+-2,6-bis (aryl ethylimine)pyridine complexes, *Chirality*, 2019, **31**, 763–775.

73 S. Schmatloch, M. F. González and U. S. Schubert. Metallo-supramolecular diethylene glycol: Water-soluble reversible polymers, *Macromol. Rapid Commun.*, 2002, **23**, 957–961.

74 T. S. Thakur, R. Dubey and G. R. Desiraju. Crystal Structure and Prediction, *Annu. Rev. Phys. Chem.*, 2015, **66**, 21–42.

75 P. Blue, P. Blue and W. W. Ii. Coordination polymers design, analysis and application, in *Royal Society of Chemistry*, 2009, pp. 1–18Coordination polymers design, analysis and application.

76 M. L. Tong and X. M. Chen. Synthesis of Coordination Compounds and Coordination Polymers, *Synthesis of Coordination Compounds and Coordination Polymers*, Elsevier B.V., 2017.

77 W. Jacob and R. Mukherjee. Synthesis, structure, and properties of monomeric Fe(II), Co(II), and Ni(II) complexes of neutral N-(aryl)-2-pyridinecarboxamides, *Inorganica Chim. Acta*, 2006, **359**, 4565–4573.

78 Y. L. Rao, A. Chortos, R. Pfattner, F. Lissel, Y. C. Chiu, V. Feig, J. Xu, T. Kurosawa, X.

Gu, C. Wang, M. He, J. W. Chung and Z. Bao. Stretchable self-healing polymeric dielectrics cross-linked through metal-ligand coordination, *J. Am. Chem. Soc.*, 2016, **138**, 6020–6027.

79 Y. Cao, T. G. Morrissey, E. Acome, S. I. Allec, B. M. Wong, C. Keplinger and C. Wang. A Transparent, Self-Healing, Highly Stretchable Ionic Conductor, *Adv. Mater.*, 2017, **29**, 1–9.

80 J. 6b08220. pd. Ko, Y. J. Kim and Y. S. Kim. Self-Healing Polymer Dielectric for a High Capacitance Gate Insulator, *ACS Appl. Mater. Interfaces*, 2016, **8**, 23854–23861.

81 X. Y. Jia, J. F. Mei, J. C. Lai, C. H. Li and X. Z. You. A Highly Stretchable Polymer that Can Be Thermally Healed at Mild Temperature, *Macromol. Rapid Commun.*, 2016, **37**, 952–956.

82 W. H. Binder. The Past 40 Years of Macromolecular Sciences: Reflections on Challenges in Synthetic Polymer and Material Science, *Macromol. Rapid Commun.*, 2019, **40**, 1–7.

83 I. L. Hia, V. Vahedi and P. Pasbakhsh. Self-Healing Polymer Composites: Prospects, Challenges, and Applications, *Polym. Rev.*, 2016, **56**, 225–261.

84 K. Imato, M. Nishihara, T. Kanehara, Y. Amamoto, A. Takahara and H. Otsuka. Self-healing of chemical gels cross-linked by diarylbibenzofuranone-based trigger-free dynamic covalent bonds at room temperature, *Angew. Chemie - Int. Ed.*, 2012, **51**, 1138–1142.

85 Y. Yang, X. Ding and M. W. Urban. Chemical and physical aspects of self-healing materials, *Prog. Polym. Sci.*, 2015, **49**–**50**, 34–59.

86 S.-M. Kim, H. Jeon, S.-H. Shin, S.-A. Park, J. Jegal, S. Y. Hwang, D. X. Oh and J. Park. Self-Healing Materials: Superior Toughness and Fast Self-Healing at Room Temperature Engineered by Transparent Elastomers (Adv. Mater. 1/2018), *Adv. Mater.*, 2018, **30**, 1870001.

87 R. R. L. De, D. A. C. Albuquerque, T. G. S. Cruz, F. M. Yamaji and F. L. Leite. Measurement of the Nanoscale Roughness by Atomic Force Microscopy: Basic Principles and Applications, *At. Force Microsc. - Imaging, Meas. Manip. Surfaces At. Scale*, , DOI:10.5772/37583.

88 Y. Yang and M. W. Urban. Self-healing polymeric materials, *Chem. Soc. Rev.*, 2013, **42**, 7446–7467.

89 T. Aida, E. W. Meijer and S. I. Stupp. Functional Supramolecular Polymers, *Science (80-.).*, 2012, **335**, 813–817.

90 A. B. W. Brochu, S. L. Craig and W. M. Reichert. Self-healing biomaterials, *J. Biomed. Mater. Res. - Part A*, 2011, **96 A**, 492–506.

91 J. Y. Oh, S. Rondeau-Gagné, Y. C. Chiu, A. Chortos, F. Lissel, G. J. N. Wang, B. C. Schroeder, T. Kurosawa, J. Lopez, T. Katsumata, J. Xu, C. Zhu, X. Gu, W. G. Bae, Y. Kim, L. Jin, J. W. Chung, J. B. H. Tok and Z. Bao. Intrinsically stretchable and healable semiconducting polymer for organic transistors, *Nature*, 2016, **539**, 411–415.

92 S. Zhang and F. Cicoira. Water-Enabled Healing of Conducting Polymer Films, *Adv. Mater.*, 2017, 29, 1703098.

93 Y. L. Rao, A. Chortos, R. Pfattner, F. Lissel, Y. C. Chiu, V. Feig, J. Xu, T. Kurosawa, X. Gu, C. Wang, M. He, J. W. Chung and Z. Bao. Stretchable self-healing polymeric dielectrics cross-linked through metal-ligand coordination, *J. Am. Chem. Soc.*, 2016, **138**, 6020–6027.

94 M. L. Hammock, A. Chortos, B. C. K. Tee, J. B. H. Tok and Z. Bao. 25th anniversary article: The evolution of electronic skin (E-Skin): A brief history, design considerations, and recent progress, *Adv. Mater.*, 2013, **25**, 5997–6038.

95 W. H. Binder. The Past 40 Years of Macromolecular Sciences: Reflections on Challenges in Synthetic Polymer and Material Science, *Macromol. Rapid Commun.*, 2019, **40**, 1–7.

96 R. P. Wool. Self-healing materials: A review, *Soft Matter*, 2008, **4**, 400–418.

97 J. A. Syrett, C. R. Becer and D. M. Haddleton. Self-healing and self-mendable polymers, *Polym. Chem.*, 2010, **1**, 978–987.

98 N. Holten-Andersen, A. Jaishankar, M. J. Harrington, D. E. Fullenkamp, G. DiMarco, L. He, G. H. McKinley, P. B. Messersmith and K. Y. C. Lee. Metal-coordination: using one of nature's tricks to control soft material mechanics, *J. Mater. Chem. B*, 2014, **2**, 2467.

99 H. Ying, Y. Zhang and J. Cheng. Dynamic urea bond for the design of reversible and self-healing polymers, *Nat. Commun.*, 2014, **5**, 1–9.

100 S. M. Kim, H. Jeon, S. H. Shin, S. A. Park, J. Jegal, S. Y. Hwang, D. X. Oh and J. Park. Superior Toughness and Fast Self-Healing at Room Temperature Engineered by Transparent Elastomers, *Adv. Mater.*, 2018, **30**, 1–8.

101 Z. Xu. Mechanics of metal-catecholate complexes: The roles of coordination state and

metal types, *Sci. Rep.*, 2013, **3**, 7–9.

102 J. Zhao, R. Xu, G. Luo, J. Wu and H. Xia. Self-healing poly(siloxane-urethane) elastomers with remoldability, shape memory and biocompatibility, *Polym. Chem.*, 2016, **7**, 7278–7286.

103 B. S. Cash, J. J.; Kubo, T.; Bapat, A. P.; Sumerlin. Room-Temperature Self-Healing Polymers Based on Dynamic- Covalent Boronic Esters, *Macromolecules*, 2015, 2098.

104 Y. Zhao, W. Zhang, L. P. Liao, H. M. Wang and W. J. Li. The self-healing composite anticorrosion coating, *Phys. Procedia*, 2011, **18**, 216–221.

105 Y. L. Liu and T. W. Chuo. Self-healing polymers based on thermally reversible Diels-Alder chemistry, *Polym. Chem.*, 2013, **4**, 2194–2205.

106 R. Hoogenboom. Hard autonomous self-healing supramolecular materials-A contradiction in terms?, *Angew. Chemie - Int. Ed.*, 2012, **51**, 11942–11944.

107 D. Y. Zhu, M. Z. Rong and M. Q. Zhang. Self-healing polymeric materials based on microencapsulated healing agents: From design to preparation, *Prog. Polym. Sci.*, 2015, **49**–**50**, 175–220.

108 J. A. Syrett, G. Mantovani, W. R. S. Barton, D. Price and D. M. Haddleton. Self-healing polymers prepared via living radical polymerisation, *Polym. Chem.*, 2010, **1**, 102–106.

109 J. Pignanelli, B. Billet, M. Straeten, M. Prado, K. Schlingman, M. J. Ahamed and S. Rondeau-Gagné. Imine and metal–ligand dynamic bonds in soft polymers for autonomous self-healing capacitive-based pressure sensors, *Soft Matter*, 2019, **15**, 7654–7662.

110 Y. L. Rao, V. Feig, X. Gu, G. J. Nathan Wang and Z. Bao. The effects of counter anions on the dynamic mechanical response in polymer networks crosslinked by metal–ligand coordination, *J. Polym. Sci. Part A Polym. Chem.*, 2017, **55**, 3110–3116.

111 S. Bode, M. Enke, R. K. Bose, F. H. Schacher, S. J. Garcia, S. van der Zwaag, M. D. Hager and U. S. Schubert. Correlation between scratch healing and rheological behavior for terpyridine complex based metallopolymers, *J. Mater. Chem. A*, 2015, **3**, 22145–22153.

112 J. M. Sirrine, S. A. Schexnayder, J. M. Dennis and T. E. Long. Urea as a monomer for isocyanate-free synthesis of segmented poly(dimethyl siloxane) polyureas, *Polymer (Guildf).*, 2018, **154**, 225–232.

113 D. D. Zhang, Y. B. Ruan, B. Q. Zhang, X. Qiao, G. Deng, Y. Chen and C. Y. Liu. A self-

healing PDMS elastomer based on acylhydrazone groups and the role of hydrogen bonds, *Polymer (Guildf).*, 2017, **120**, 189–196.

114 B. Zhang, P. Zhang, H. Zhang, C. Yan, Z. Zheng, B. Wu and Y. Yu. A Transparent, Highly Stretchable, Autonomous Self-Healing Poly(dimethyl siloxane) Elastomer, *Macromol. Rapid Commun.*, 2017, **38**, 1–9.

115 L. Liu, S. Liang, Y. Huang, C. Hu and J. Yang. A stretchable polysiloxane elastomer with self-healing capacity at room temperature and solvatochromic properties, *Chem. Commun.*, 2017, **53**, 12088–12091.

116 F. García, J. Pelss, H. Zuilhof and M. M. J. Smulders. Multi-responsive coordination polymers utilising metal-stabilised, dynamic covalent imine bonds, *Chem. Commun.*, 2016, **52**, 9059–9062.

117 H. Liu, H. Zhang, H. Wang, X. Huang, G. Huang and J. Wu. Weldable, malleable and programmable epoxy vitrimers with high mechanical properties and water insensitivity, *Chem. Eng. J.*, 2019, **368**, 61–70.

118 A. F. Wells. Structural Inorganic Chemistry, 5th Edition, Clarendon Press, Oxford, 1984, p. 1288Structural Inorganic Chemistry, 5th Edition.

119 R. D. Shannon. Revised Effective Ionic Radii and Systematic Studies of Interatomie Distances in Halides and Chalcogenides, *Acta Crystallogr.*, 1976, **A32**, 751–767.

120 J. Cui, F. M. Nie, J. X. Yang, L. Pan, Z. Ma and Y. S. Li. Novel imidazolium-based poly(ionic liquid)s with different counterions for self-healing, *J. Mater. Chem. A*, 2017, **5**, 25220–25229.

121 J. Pignanelli, K. Schlingman, T. B. Carmichael, S. Rondeau-Gagné and M. J. Ahamed. A Comparative Analysis of Capacitive-Based Flexible PDMS Pressure Sensors, *Sensors Actuators A. Phys.*, 2019, **285**, 427–436.

122 Y. Wang, J. He, S. Aktas, S. A. Sukhishvili and D. M. Kalyon. Rheological behavior and self-healing of hydrogen-bonded complexes of a triblock Pluronic® copolymer with a weak polyacid, *J. Rheol. (N. Y. N. Y).*, 2017, **61**, 1103–1119.

123 E. Archives. Engineering Archives, Engineering Archives, http://www.engineeringarchives.com/img/les_mom_necking_1.png.

124 Malvern Instruments Worldwide. Malvern Instruments White Paper - A Basic Introduction to Rheology Shear Flow, 2016, 1–20.

CHAPTER 5: CONCLUSIONS, FUTURE WORK AND PERSPECTIVES

5.1. Conclusion

In summary, a dynamic, self-healing and tunable PDMS based elastomer was established based on a simple, cost effective and large-scalable method of metal-ligand crosslinking of pyridine-capped elastomeric chains. Through the rational design of soft siloxane-based oligomers with imine and metal-coordination moieties, a unique combination of dynamic bonds was enabled through a simple condensation reaction of amino-terminated siloxane chains with pyridine carboxaldehyde. Cross linking of the resulting oligomers with Fe(BF4)2 with varying metal to ligand ratios demonstrated the tunability of the system through simply controlling the amount of coordination sites. As the amount of coordination sites increased relative to the end termini ligands of the oligomer, the greater the stretchability of the cross-linked elastomer, with results reaching up to an 800% strain before failure. Samples prepared through coordination with a 1:3 metal to ligand ratio proved to have autonomous intrinsic self-healing up to 88% of its original mechanical strength after a 48-hour healing period at room temperature. The dynamic versatility of the coordinate bonds was further demonstrated through the degradability of the material at mild conditions. Due to the dielectric nature of PDMS, the self-healing material was used as a dielectric layer of a capacitance-based pressure sensor using a previously reported design.(Cite) The dynamic response of the sensor before and after a damage-heal cycle showed a good response time and accuracy. The device functioned with a sensitivity of 0.33 kPa-1 at low pressures tested (0-5 kPa) with no significant deviations after a 48 hours damage-heal cycle of the dielectric layer, further enhancing the promise of our system.

The PDMS based system was also crosslinked using various other metal sources including Co(BF4)2 Zn(BF4)2, Zn(Otf)2 and Zn(ClO4)2, which demonstrated the wide range of mechanical properties possible based on altering the ratio of metal to ligand, the metal identity as well as the counterion effects of the metal salt used. Young's modulus of the system ranged from 0.23 to 10.2 MPa depending on the metal salt used to cross link the oligomeric chains. Therefore, in order to fine-tune the thermomechanical properties of soft elastomers has been developed through dynamic metal-ligand interactions. The various metal centers used in this study all demonstrated rapid, autonomous, intrinsic self-healing at room temperature within two hours. The strength of the metal-ligand interaction had a direct effect on the mechanical properties of the resulting crosslinked materials. The samples cross linked through Zn(II), Fe(II) and Co(II) demonstrated a maximum strain before fracture of 525%, 75% and 25%, and a self-healing efficiency of 88%, 71% and 61%

respectively. The smaller the bond length, the stronger the crosslinks and therefore the less strain endured before fracture, and the higher the modulus attained. Comparing Fe(II), Co(II) and Zn(II) metal-ligand coordination using tetrafluoroborate based salts resulted in Young's Modulus of 1.8 MPa, 8.10 MPa and 0.26 MPa, respectively. The counter-ion used also demonstrated a prominent effect on the thermomechanical and self-healing efficiency of the materials. The effect of the counterion is evident through analysis of the tensile strain analysis where the Young's modulus ranged from 0.23 MPa to 10.2 MPa through alteration of the counterion from a larger trimethyl sulfonate anion to a smaller chlorate anion. It was concluded that the larger counterions induce a plasticizing effect resulting in an increased maximum strain before failure and lower Young's modulus. As a result of this high tunability, low cost and facile preparation, this new dynamic polymer system is promising for the creation of the next generation of stretchable materials for electronics that require simple processing, high mechanical robustness, degradability, conformability and durability in order to enhance the performance and lifespan of electronics.

5.2 Future Work and Perspectives

The next steps of this research are to study the dielectric constant of the material to determine if the metal-ligand interactions effect on the dielectric constant of PDMS. The characterization of the self-healing capabilities of thin films is also an important characteristic to study in order to determine the limitations of the system at the microscale. Additionally, the use of the materials for large scale printing of dielectric layers for various applications such as solar cells, field-effect transistors and capacitors in order to optimize the processing methods for the next generation of flexible electronics. Due to the ease of preparation of the dynamically crosslinked material at the gram scale, as well as its solubility in low boiling point solvents, the system shows high potential for slot-coat die printing. It is anticipated that as the field of flexible and stretchable electronics continues to grow, new materials that possess mechanical durability, self-healing capabilities and tunable properties that can be produced in a large scale through printing technologies. As a result of the ability to produce materials into functional inks with the capability to be printed onto a variety of substrates at low cost with conformable opportunities for industrial production.

With the results highlighted within this thesis, it is believed that our system will contribute to the next generation of soft, flexible, self-healing materials for large scale, cost effective applications that will ultimately enhance the robustness of flexible electronics for use in our daily lives.

APPENDICES

APPENDIX A. CHAPTER 3 SUPPORTING INFORMATION

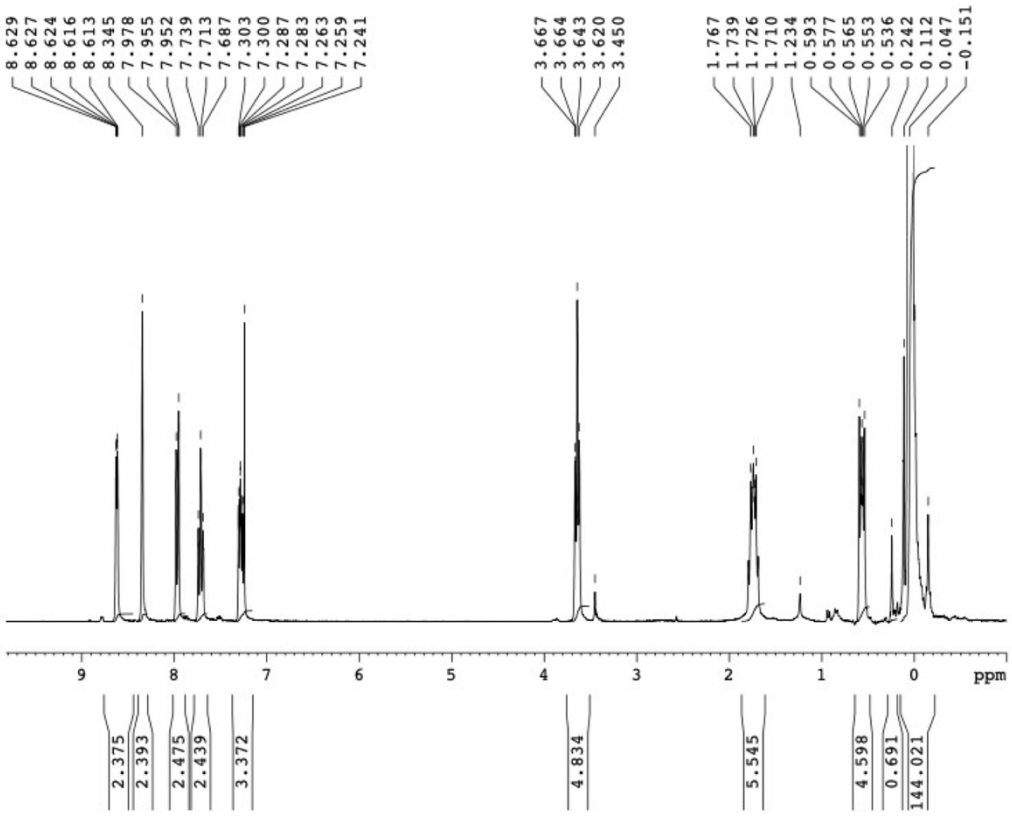

Figure A1. ^{1}H NMR spectrum of pre-polymer 1 in $CDCl_3$ after washing with hexanes/MeCN.

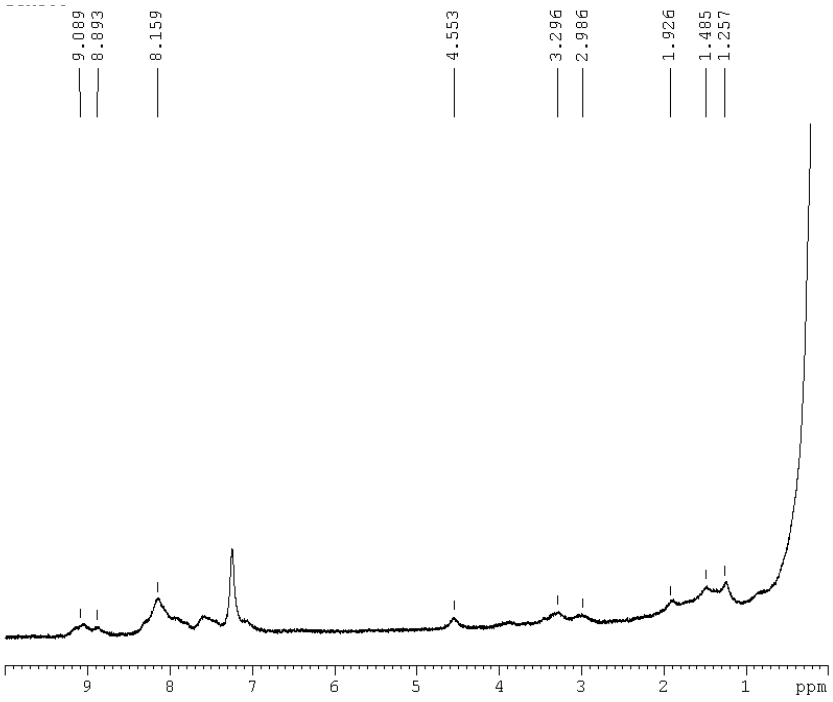

Figure A2. ^{1}H NMR spectrum of pre-polymer 1 crosslinked with Fe(II) in $CDCl_3$

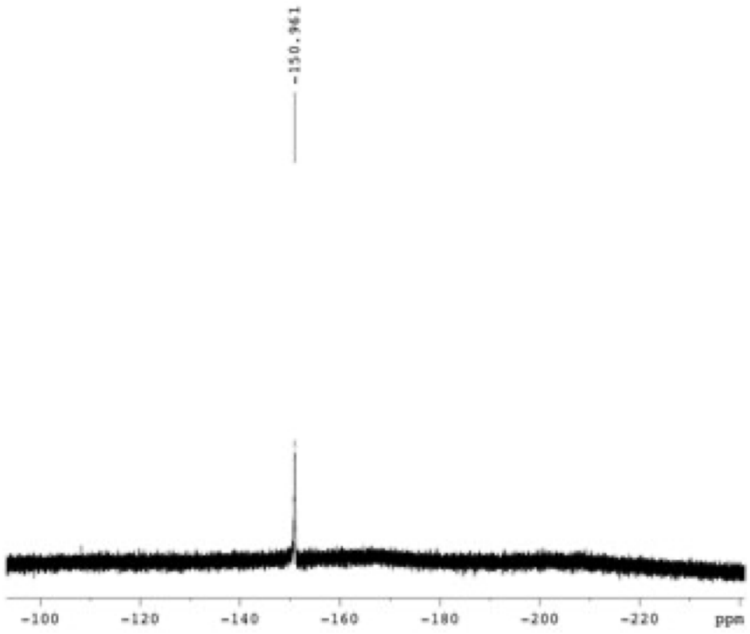

Figure A.3. ^{19}F NMR spectrum of pre-polymer 1 crosslinked with Fe(II) in $CDCl_3$.

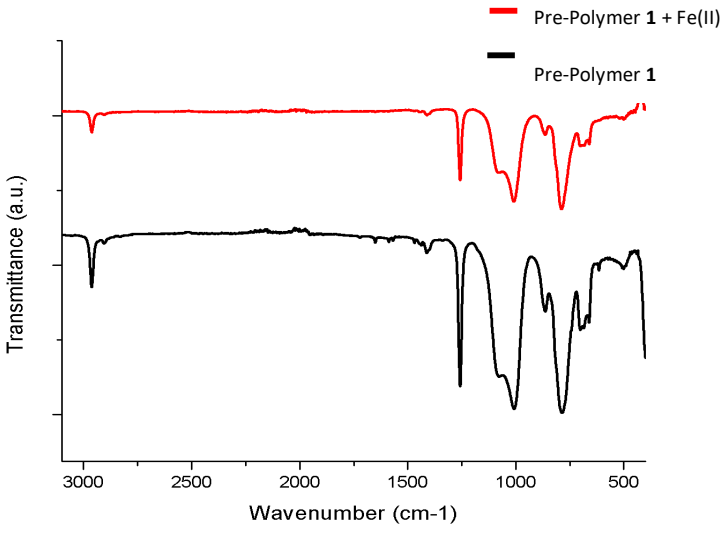

Figure A4. FT-IR spectra of pre-polymer 1 before and after crosslinking with 0.25 eq. of $Fe(BF_4)_2$.

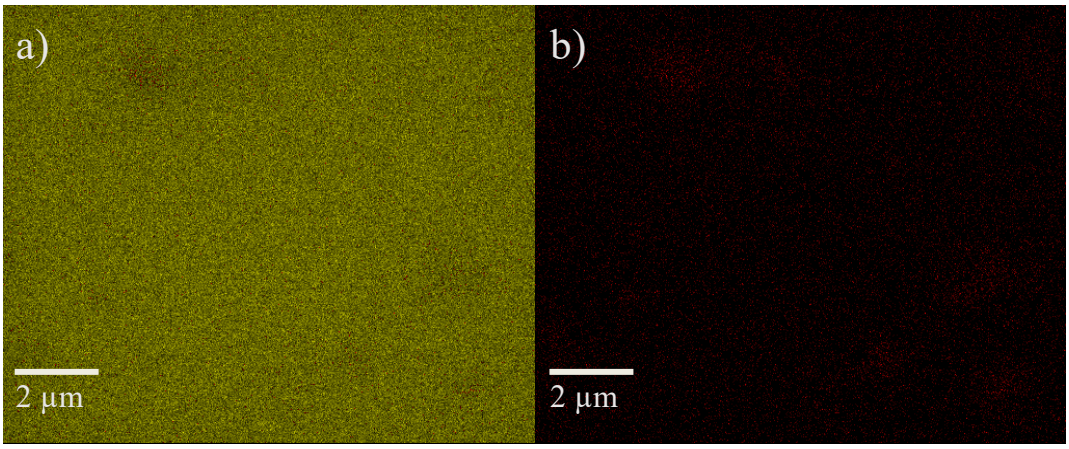

Figure A5. Energy-dispersive x-ray spectroscopy (EDX) analysis map; a) scanning electron Micrograph of EDX scanning area cumulative elemental overlay (yellow = Si, red = Fe), and b) independent elemental overlay of Fe atoms. Scale bar is 2 µm.

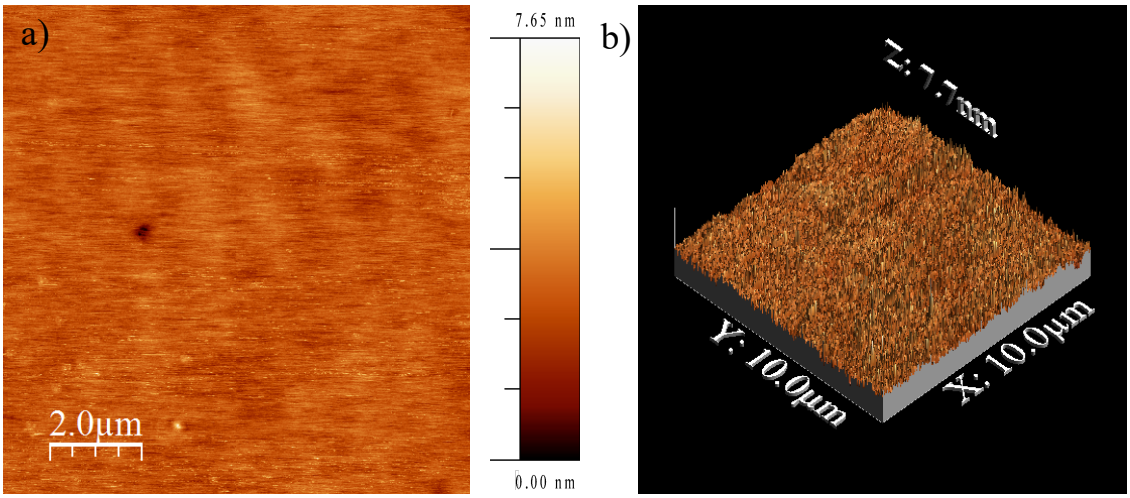

Figure A6. Atomic force microscopy (AFM) a) height image, and b) 3d image of pre-polymer 1 after Fe(II) coordination. Scale bar is 2.0 µm.

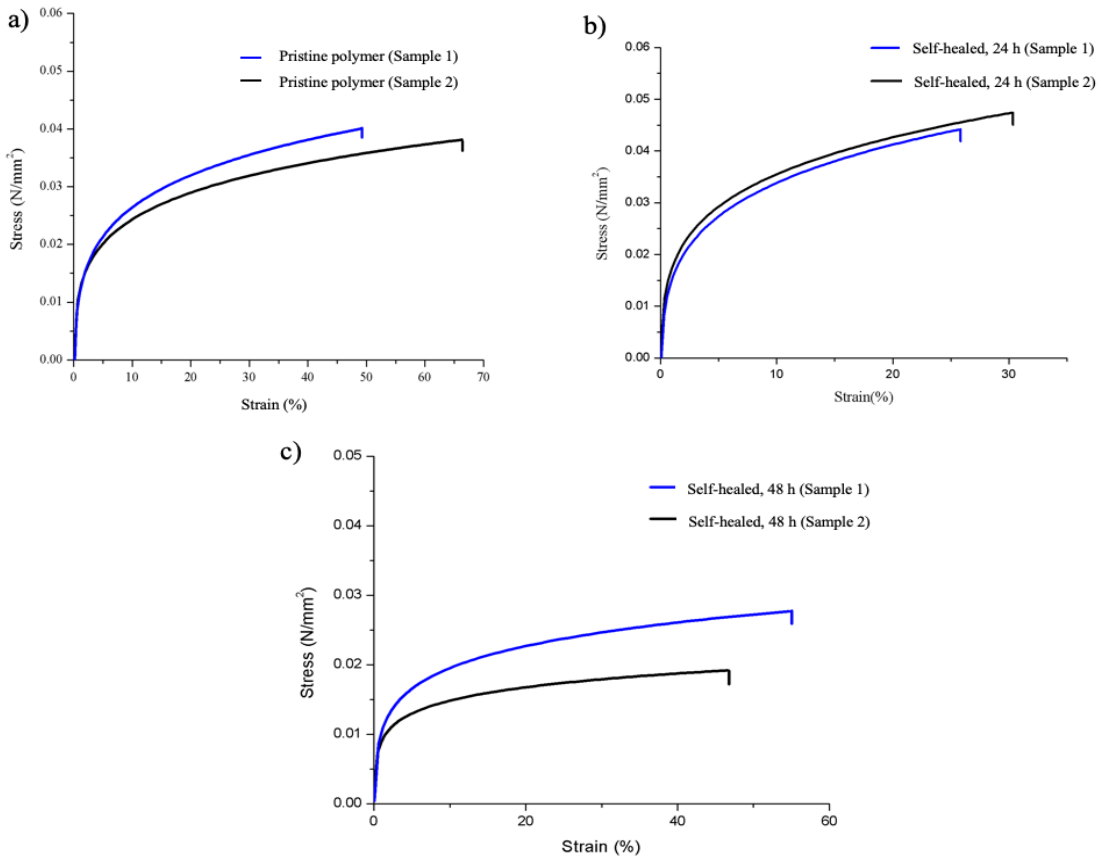

Figure A7. Stress-strain curves of pre-polymer 1 crosslinked with 0.33 equivalent of $Fe(BF_4)_2$ a) before; b) after self-healing for 24 hours, and c) after self-healing for 48 hours at room temperature. Measurements were recorded on two samples from two different batches of materials.

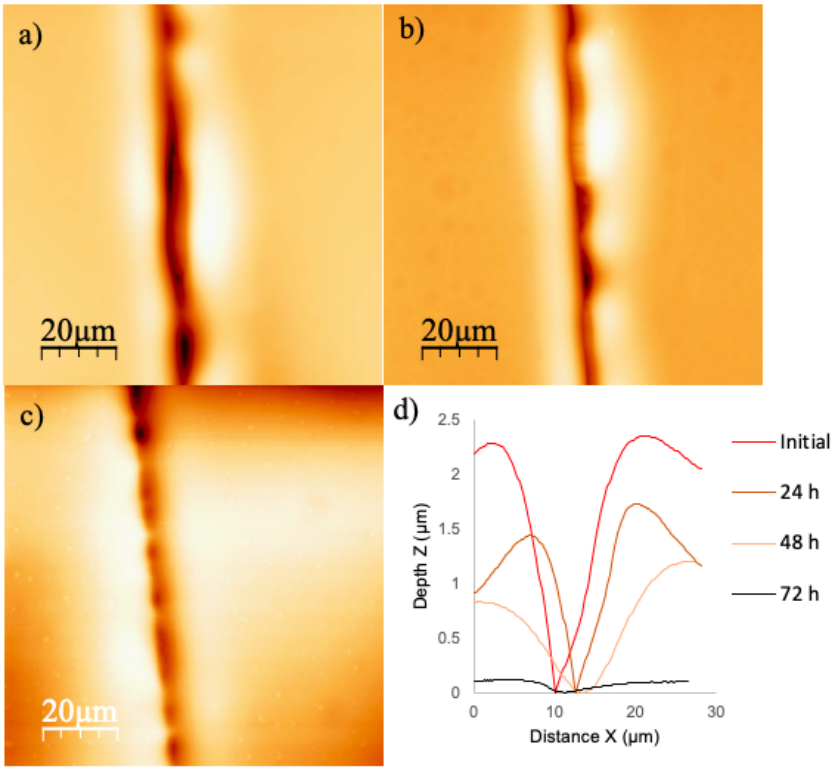

Figure A.8. Atomic force microscopy (AFM) height images of pre-polymer 1 after Fe(II) coordination a) after being cut with a razor blade; b) after 24 hours of self-healing; c) after 72 hours of self-healing, and d) depth profile of the damaged zone and its evolution upon self-healing. Scale bar is 20 µm. No more cut at the nanoscale was observed by AFM after more than 72 hours.

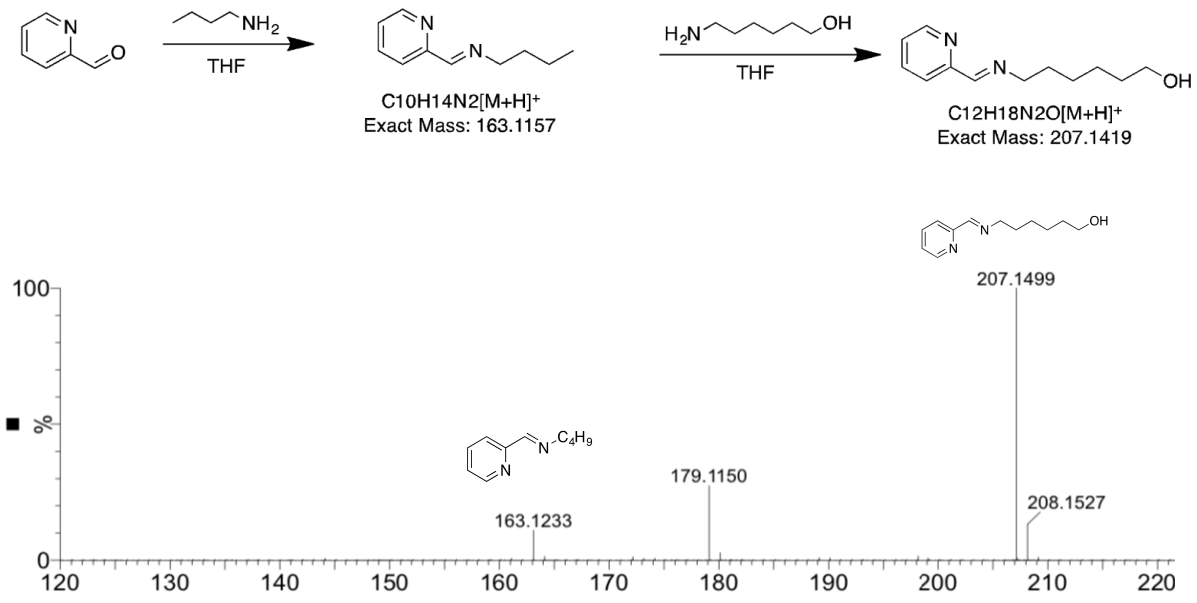

Figure A9. Preparation of compound (*E*)-*N*-butyl-1-(pyridin-2-yl)methenamine and investigation of the dynamic behavior of the imine bond by mass spectrometry. Measurements were completed in ASAP(+) sensitivity mode using the crude samples.

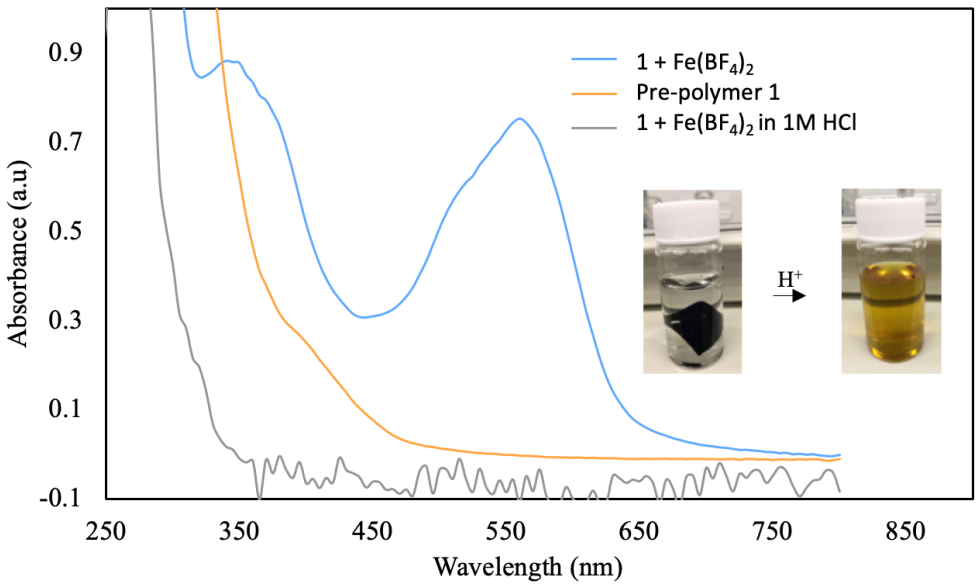

Figure A10. UV-Vis spectra of pre-polymer 1 pristine, after Fe(II) coordination, and after being stirred in a 1.0 M solution of hydrochloric acid for 4 hours.

a)

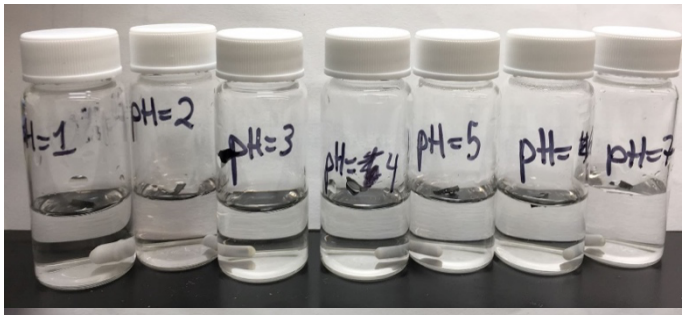

b)

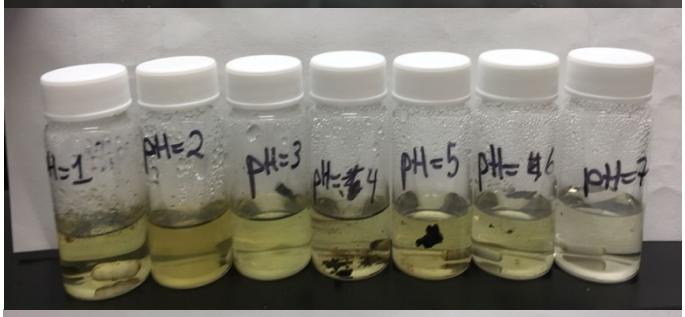

c)

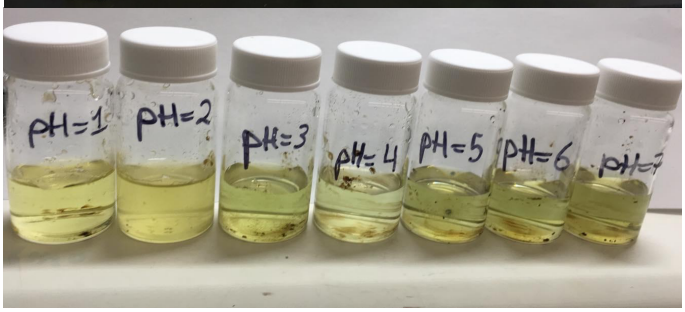

Figure A11. Degradation of Fe(II)-crosslinked soft polymer at various pH (aqueous HCl solutions) upon a) initial time; b) 24 hours, and c) 72 hours of stirring.

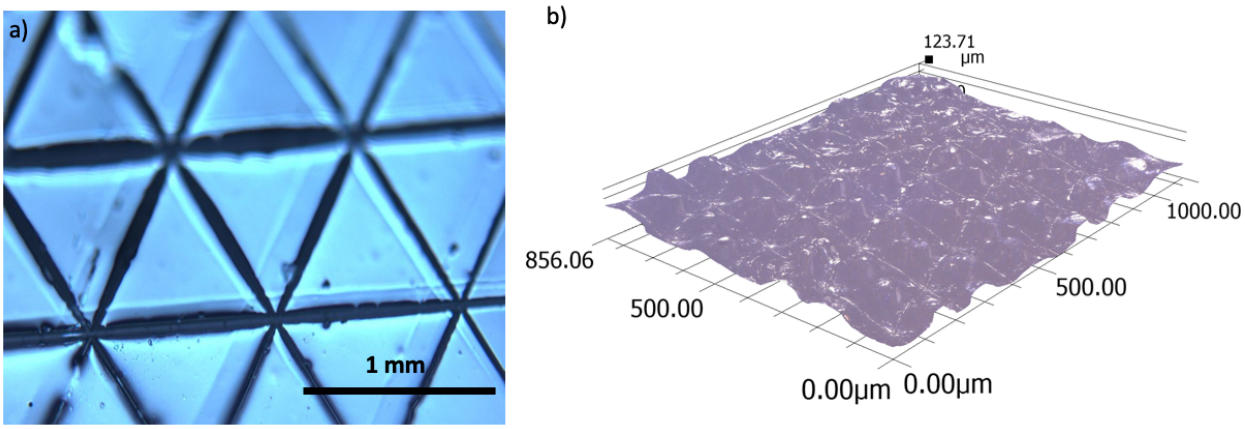

Figure A12. a) 2-D Optical Microscope image of dielectric structures and b) 3D image of dielectric structures.

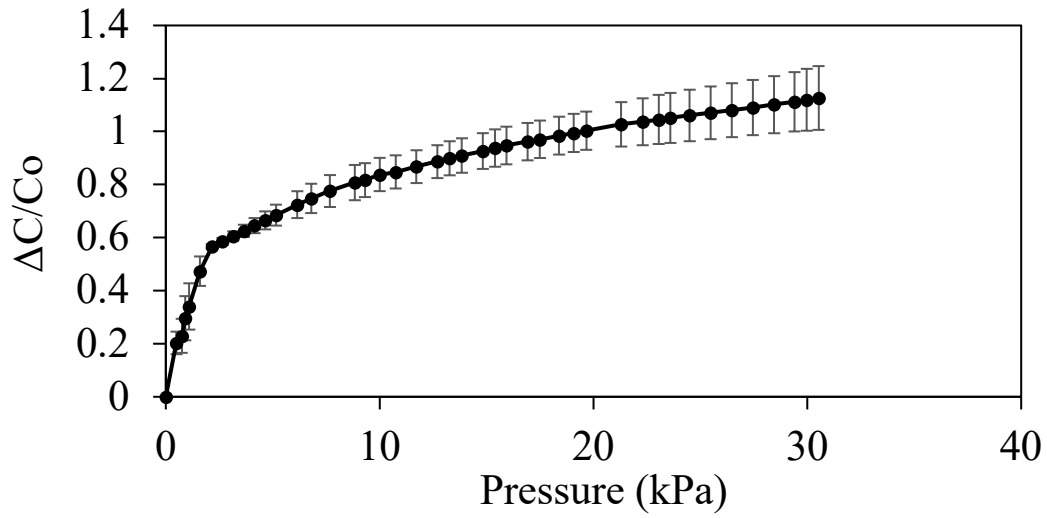

Figure A13. a) Standard deviation between devices sensitivity: Pristine,100 cycles at 30% strain, healed for 24 hours, and healed after 100 cycles at 30% strain. Sensitivity averaged over 4 devices.

APPENDIX B. CHAPTER 4 SUPPORTING INFORMATION

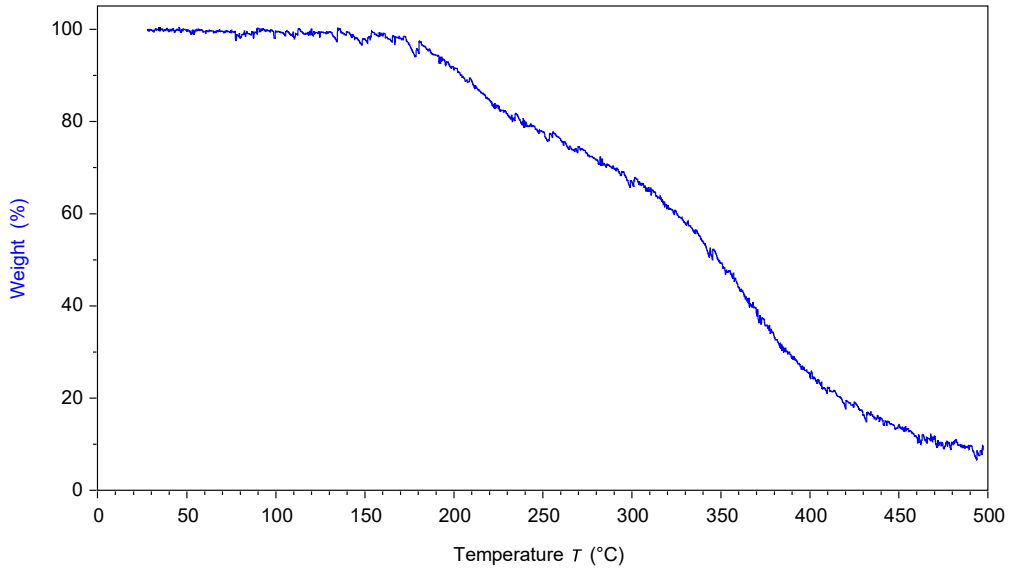

Figure B1. Thermogravimetric analysis of pre-polymer P1 crosslinked with $Co(BF_4)_2$

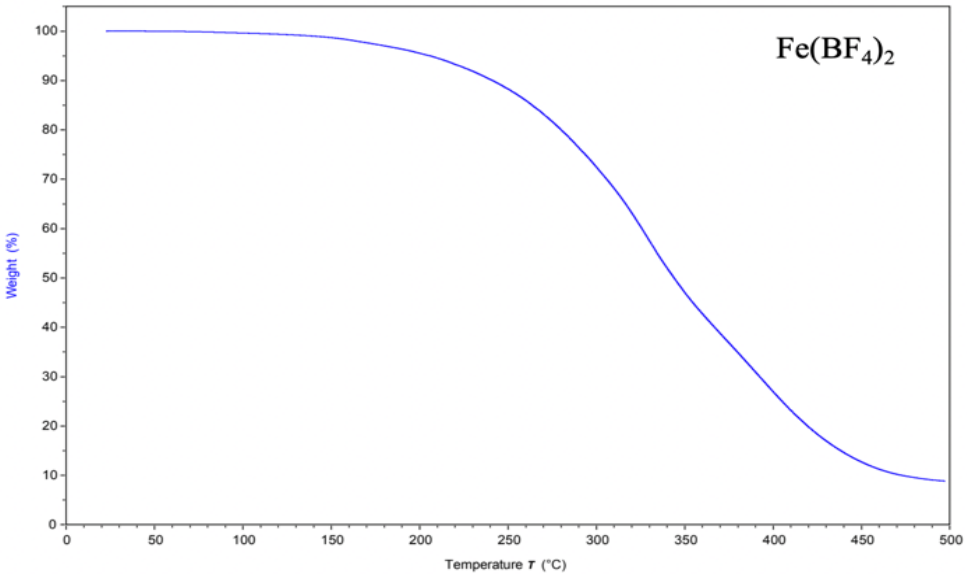

Figure B2. Thermogravimetric analysis of pre-polymer P1 crosslinked with $Fe(BF_4)_2$.

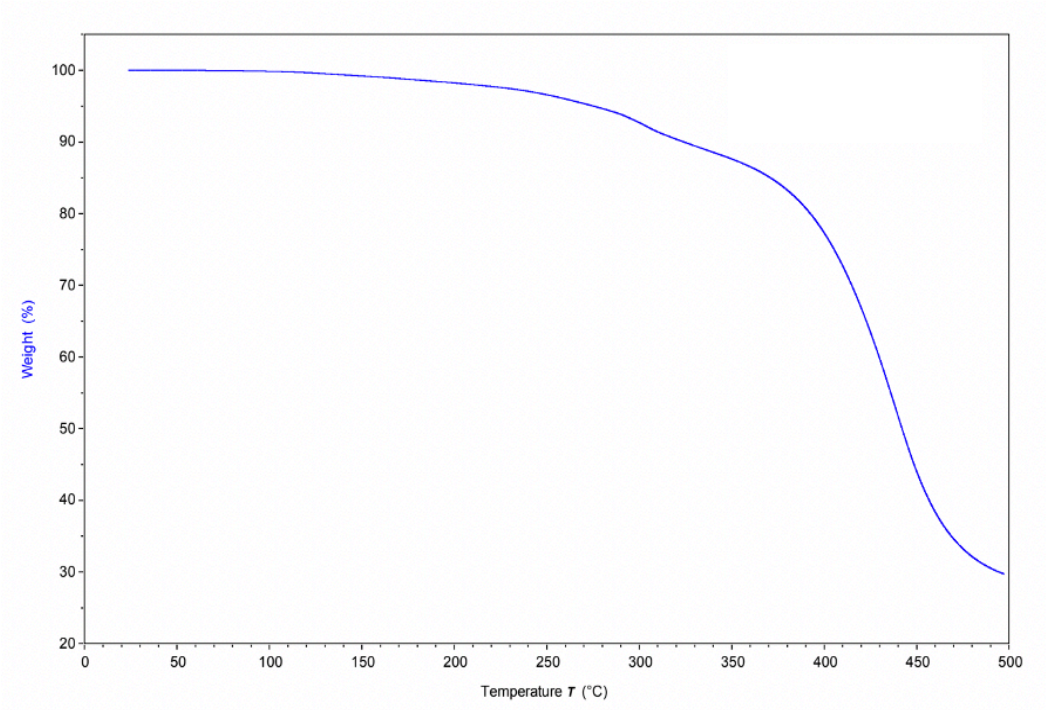

Figure B3. Thermogravimetric analysis of pre-polymer P1 crosslinked with $Zn(OTf)_2$

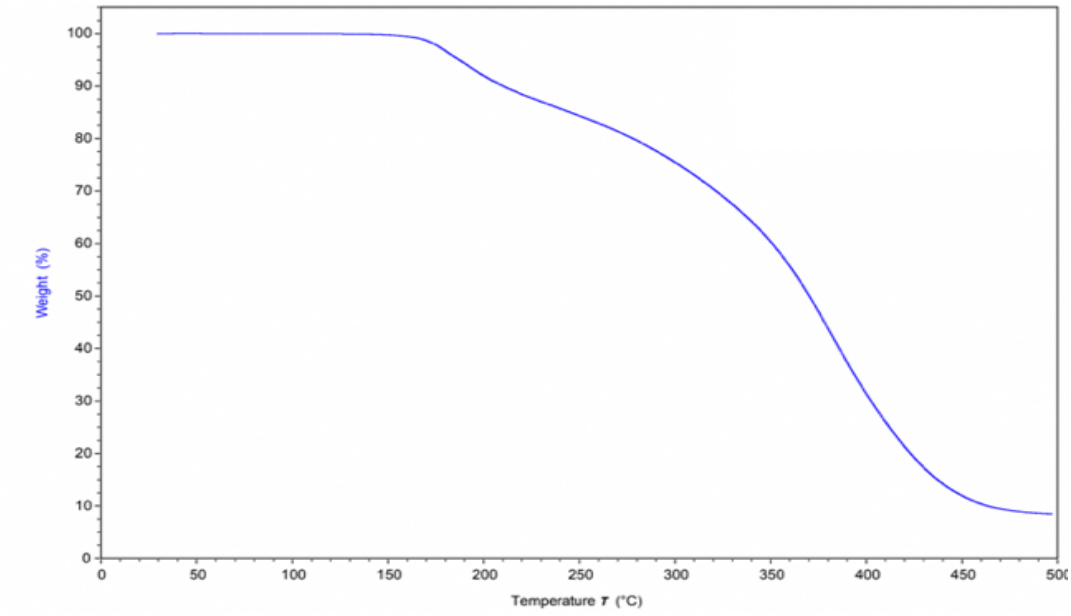

Figure B4. Thermogravimetric analysis of pre-polymer P1 crosslinked with $Zn(BF_4)_2$

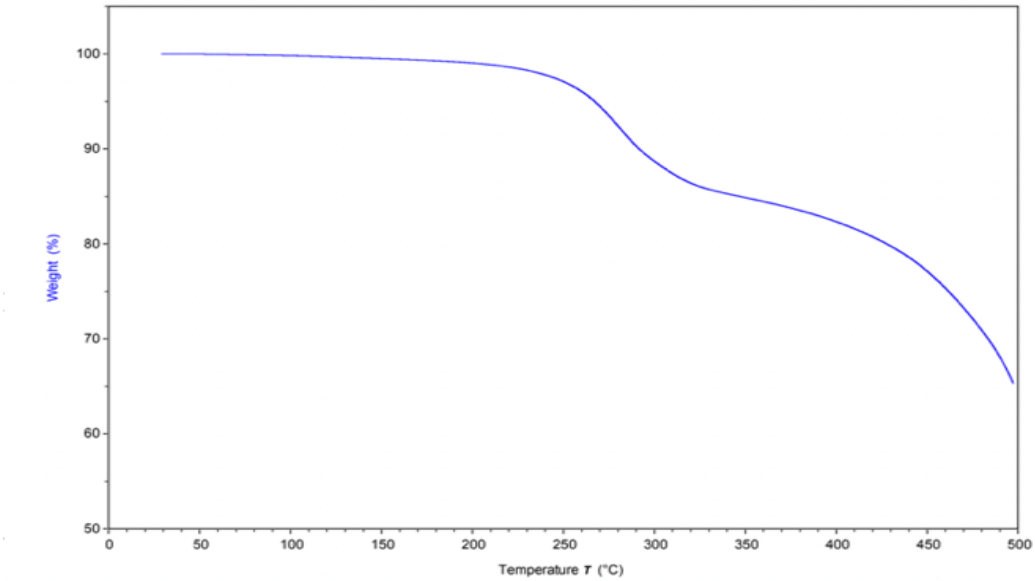

Figure B5. Thermogravimetric analysis of pre-polymer P1 crosslinked with $Zn(ClO_4)_2$

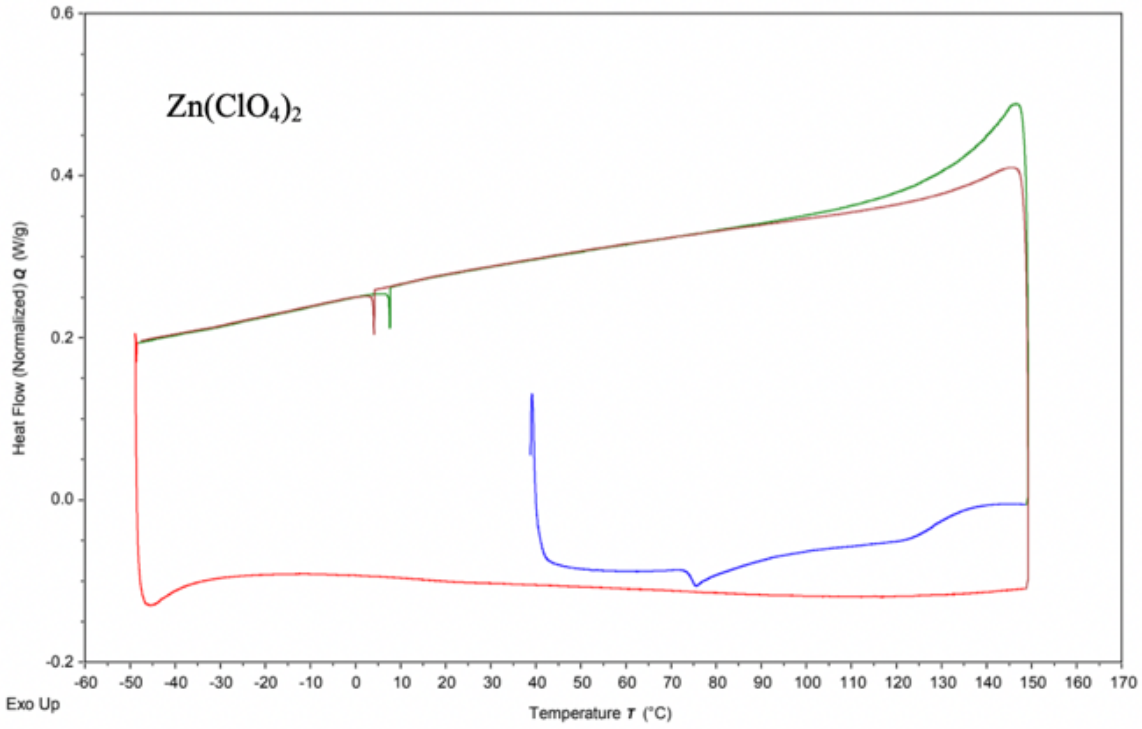

Figure B6. Differential scanning calorimetry curve for pre-polymer P1 crosslinked with $Zn(ClO_4)_2$

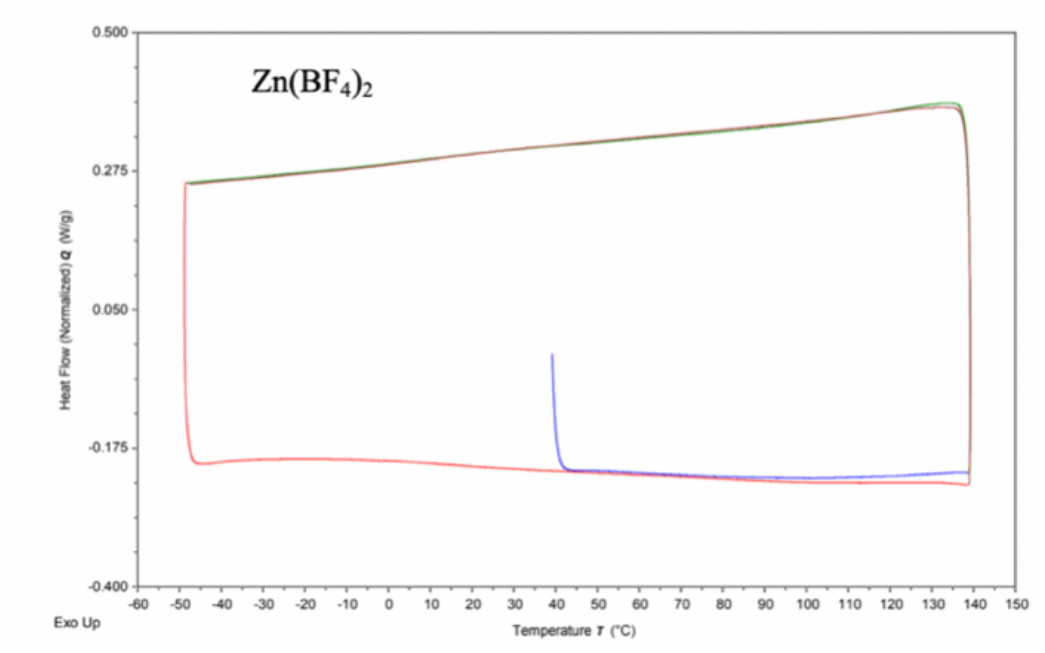

Figure B7. Differential scanning calorimetry curve for pre-polymer P1 crosslinked with $Zn(BF_4)_2$

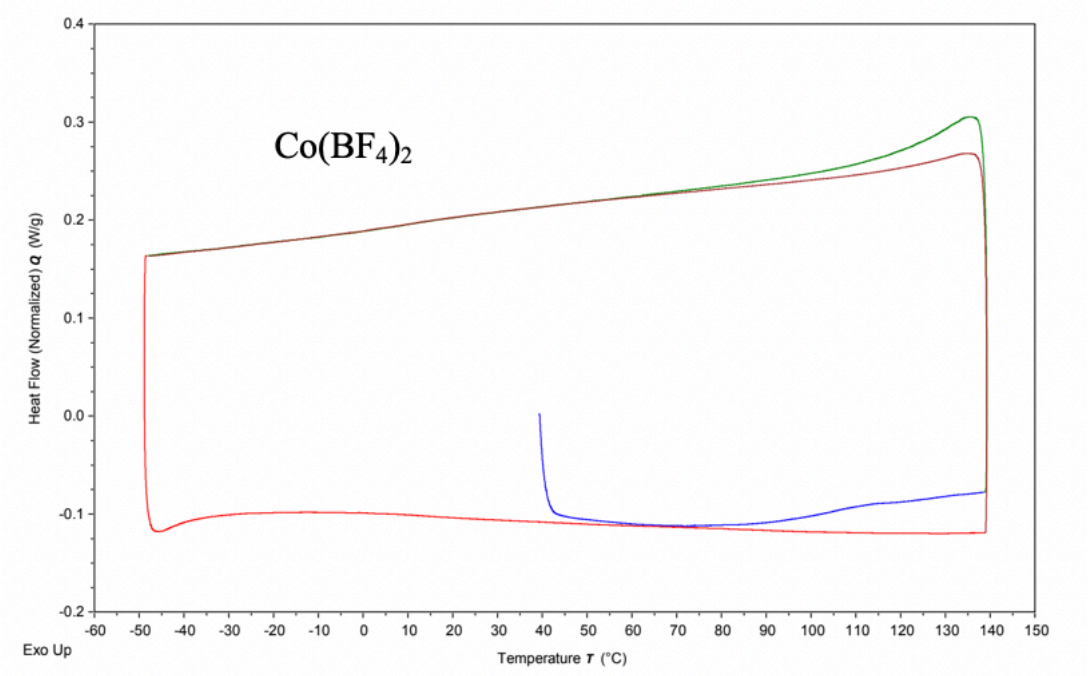

Figure B8. Differential scanning calorimetry curve for pre-polymer P1 crosslinked with $Co(BF_4)_2$

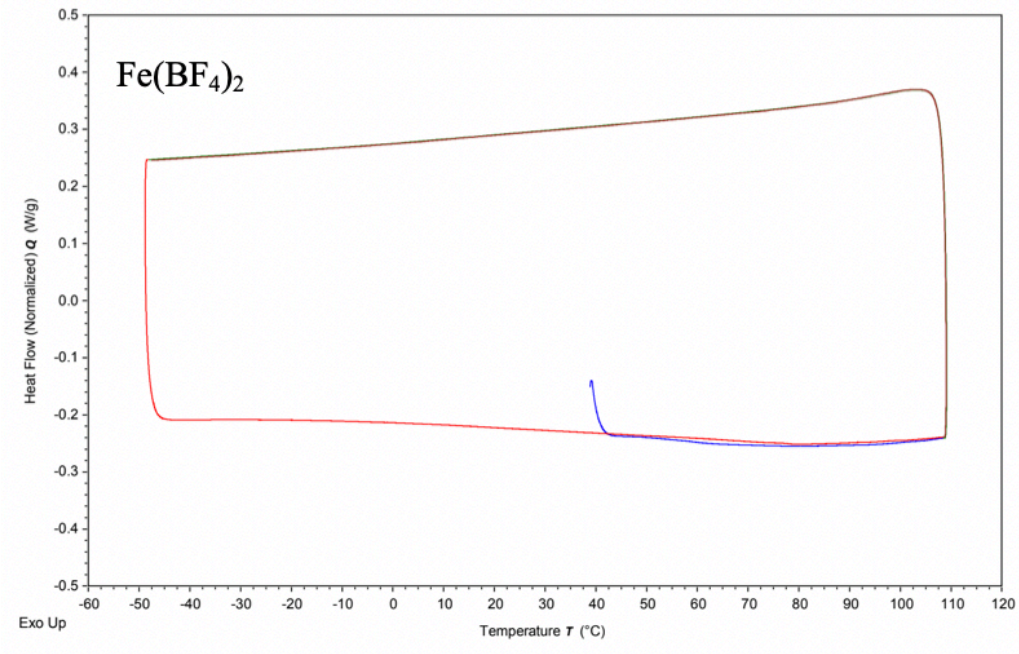

Figure B9. Differential scanning calorimetry curve for pre-polymer P1 crosslinked with $Fe(BF_4)_2$

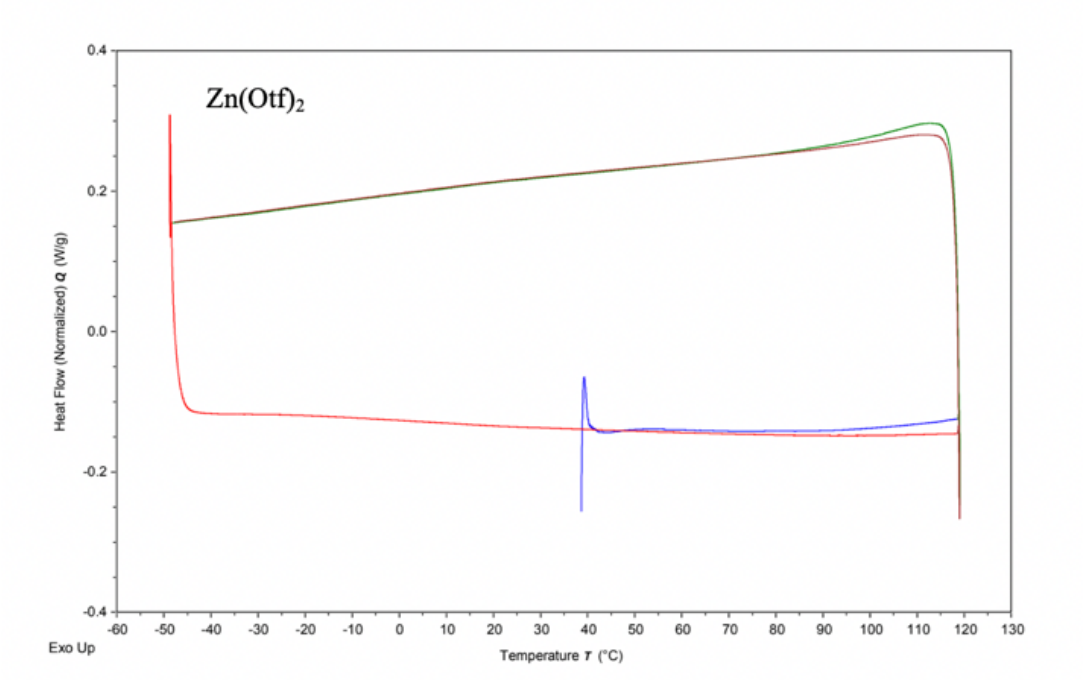

Figure B10. Differential scanning calorimetry curve for pre-polymer P1 crosslinked with Zn(OTf)

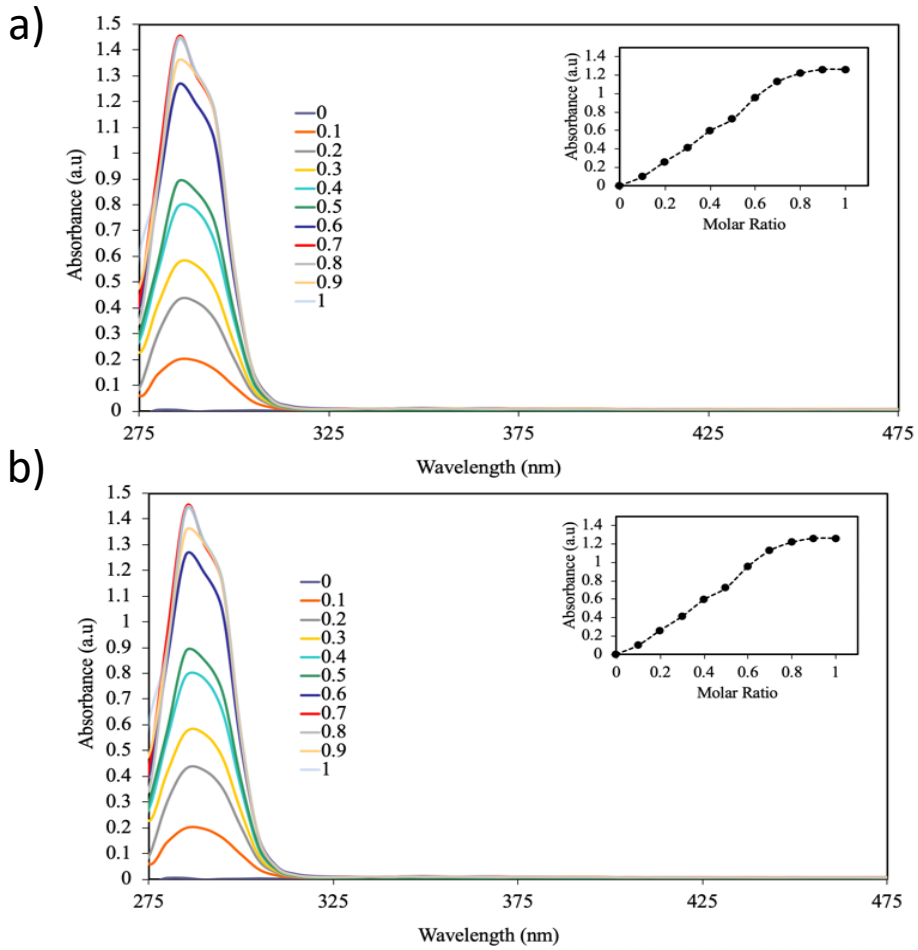

Figure B11. a) UV-vis absorption spectra of P1 in CH2Cl2 with Zn(OTf)2; b) UV-vis absorption spectra of P1 in CH2Cl2 with Zn(ClO4)2; insets plot molar ratio of each Zn(II) salt versus absorbance at 290 nm. Each titration included 0.1 molar equivalents of the respective metal salt per N-ligand in P1.

VITA AUCTORIS

Name: Julia Pignanelli

Place of Birth: Windsor, Ontario

Year of Birth: 1996

Education: Univeristy of Windsor, Windsor, Ontario

B.Sc. (2014-2018)

University of Windsor, Windsor, Ontario M.Sc. (2017-2019)